

Oropharyngeal microbiota clusters in children with asthma/wheeze associate with allergy, blood transcriptomic immune pathways and exacerbations risk

Mahmoud I. Abdel-Aziz, PhD^{1,2,3,4}; Jonathan Thorsen, MD, PhD^{5,6}; Simone Hashimoto, MD, PhD^{1,2,3,7}; Susanne J. H. Vijverberg, PhD^{1,2,3}; Anne H. Neerincx, PhD^{1,2,3}; Paul Brinkman, PhD^{1,2,3}; Wim van Aalderen, MD, PhD⁷; Jakob Stokholm, MD, PhD^{5,8}; Morten Arendt Rasmussen, MD, PhD^{5,8}; Michael Roggenbuck-Wedemeyer, MD, PhD^{9,10}; Nadja H. Vissing, MD, PhD⁵; Martin Steen Mortensen, PhD⁹; Asker Daniel Brejnrod, PhD¹¹; Louise J. Fleming, MD¹²; Clare S. Murray, MD¹³; Stephen J. Fowler, MD, PhD¹³; Urs Frey, MD, PhD¹⁴; Andrew Bush, MD, FRCP, FRCPC¹²; Florian Singer, MD, PhD¹⁵; Gunilla Hedlin, MD, PhD¹⁶; Björn Nordlund, RN, PhD¹⁶; Dominick E. Shaw, PhD¹⁷; Kian Fan Chung, MD, DSc¹²; Ian M. Adcock, PhD¹²; Ratko Djukanovic, MD, PhD¹⁸; Charles Auffray, PhD¹⁹; Aruna T. Bansal, PhD²⁰; Ana R. Sousa, PhD²¹; Scott S. Wagers, MD, PhD²²; Bo Lund Chawes, MD, PhD⁶; Klaus Bønnelykke, MD, PhD⁶; Søren Johannes Sørensen, PhD⁹; Aletta D. Kraneveld PhD²³; Peter J. Sterk, MD, PhD^{1,2}; Graham Roberts, DM¹⁸; Hans Bisgaard, MD, PhD⁵; Anke H. Maitland-van der Zee, PharmD, PhD^{1,2,3,7}; on behalf of the U-BIOPRED Study Group.

1 Department of Pulmonary Medicine, Amsterdam UMC, University of Amsterdam, 1105 AZ Amsterdam, the Netherlands.

2 Amsterdam Institute for Infection and Immunity, Amsterdam, the Netherlands.

3 Amsterdam Public Health, Amsterdam, the Netherlands.

4 Department of Clinical Pharmacy, Faculty of Pharmacy, Assiut University, 71526 Assiut, Egypt.

5 COPSAC, Copenhagen Prospective Studies on Asthma in Childhood, Herlev and Gentofte Hospital, University of Copenhagen, Copenhagen, Denmark.

6 Novo Nordisk Foundation Center for Basic Metabolic Research, Faculty of Health and Medical Sciences, University of Copenhagen, Copenhagen, Denmark.

7 Department of Paediatric Pulmonary Medicine, Emma Children's Hospital, Amsterdam UMC, University of Amsterdam, 1105 AZ Amsterdam, the Netherlands.

26 8 Department of Food Science, University of Copenhagen, Frederiksberg, Denmark.

27 9 Section of Microbiology, Department of Biology, University of Copenhagen, Copenhagen, Denmark.

28 10 Novozymes, Bagsvaerd, Denmark.

29 11 Section of Bioinformatics, Department of Health Technology, Technical University of Denmark, Lyngby,

30 Denmark.

31 12 National Heart and Lung Institute, Imperial College London, and Royal Brompton and Harefield NHS Trust,

32 London, United Kingdom.

33 13 Division of Infection, Immunity and Respiratory Medicine, School of Biological Sciences, Faculty of Biology,

34 Medicine and Health, University of Manchester, and Manchester Academic Health Science Centre and NIHR

35 Biomedical Research Centre, Manchester University Hospitals NHS Foundation Trust, Manchester, United Kingdom.

36 14 University Children's Hospital Basel, University of Basel, Basel, Switzerland.

37 15 Division of Paediatric Pulmonology and Allergology, Department of Paediatrics and Adolescent Medicine,

38 Medical University of Graz, Austria & Division of Paediatric Respiratory Medicine and Allergology, Department of

39 Paediatrics, Inselspital, Bern University Hospital, University of Bern, Switzerland.

40 16 Astrid Lindgren Children's Hospital, Karolinska University Hospital, and Department of Women's and Children's

41 Health, Karolinska Institutet, Stockholm, Sweden.

42 17 NIHR Respiratory Biomedical Research Unit, University of Nottingham, Nottingham, United Kingdom.

43 18 NIHR Southampton Biomedical Research Centre, University Hospital Southampton NHS Foundation Trust and

44 Clinical and Experimental Sciences and Human Development and Health, University of Southampton, Southampton,

45 United Kingdom.

46 19 European Institute for Systems Biology and Medicine, CIRI UMR5308, CNRS-ENS-UCBL-INSERM, Lyon, France.

47 20 Acclarogen Ltd, St John's Innovation Centre, Cambridge, United Kingdom.

48 21 Respiratory Therapeutic Unit, GlaxoSmithKline, Stockley Park, United Kingdom.

49 22 BioSci Consulting, Maasmechelen, Belgium.

50 23 Division of Pharmacology, Utrecht Institute for Pharmaceutical Sciences, Faculty of Science, Utrecht University,

51 Utrecht, the Netherlands.

52

Corresponding author details:

Prof. Dr. Anke-Hilse Maitland-van der Zee

Department of Pulmonary Medicine, Amsterdam UMC, University of Amsterdam, 1105 AZ Amsterdam, the Netherlands.

e-mail: a.h.maitland@amsterdamumc.nl, Telephone: +31 (0) 20 5668137

Authorship contribution:

MIA has performed the analysis and drafted the initial version of the manuscript. MIA, AHM, JT, GR and PJS have contributed to the design of the analysis plan. All co-authors have contributed to the acquisition of data, interpretation of the analysis, revision, drafting, critical appraisal and ensuring accuracy and integrity of the analysis. All co-authors have provided final approval of the version to be published. AHM is the corresponding author.

Funding:

U-BIOPRED has received funding from the Innovative Medicines Initiative (IMI) Joint Undertaking under grant agreement no. 115010, resources of which are composed of financial contributions from the European Union's Seventh Framework Programme (FP7/2007–2013) and European Federation of Pharmaceutical Industries and Associations (EFPIA) companies' in-kind contributions (www.imi.europa.eu). The researcher MIA has received a full scholarship from the Ministry of Higher Education of the Arab Republic of Egypt.

73 **Short running head: “Bacterial asthma/wheezing subtypes in children”**

74 **Manuscript Subject descriptor:** PEDIATRICS 14.1 Clinical Studies: Asthma

75 **Article type:** Original article

76 **Word count:** 4,000 without abstract, references, tables, figures, and disclosures

77 **References number:** 60

78 **Tables:** 4 in the main manuscript + 7 supplementary

79 **Figures:** 3 in the main manuscript + 17 supplementary

80 **Online Repository:** This article has an online data supplement, which is accessible from this issue’s table
81 of content online at www.atsjournals.org.

82 **At a Glance Commentary**

83 **Scientific Knowledge on the Subject**

84 Children with asthma or wheezing were reported to have airway microbial imbalances. However, it is not
85 yet clear whether characterizing the microbiota in oropharyngeal swabs, as a non-invasive sampling
86 compartment, could help identifying clinically relevant phenotypes in children with asthma or wheezing.

87 **What This Study Adds to the Field**

88 In this study, we show that the oropharyngeal microbiota could identify 4 distinct clusters that were
89 different in allergic status and spirometry and that exhibited differential expression of TGF- β and Wnt/ β -
90 catenin signaling pathways in blood. These clusters were independent predictors of future exacerbation
91 events in children with severe disease, within 12-18 months of follow-up.

Abstract

Rationale:

Children with preschool wheezing or school-age asthma are reported to have airway microbial imbalances.

Objective:

To identify clusters in children with asthma or wheezing using oropharyngeal microbiota profiles.

Methods:

Oropharyngeal swabs, from the Unbiased BIOmarkers for the Prediction of REspiratory Disease outcomes pediatric asthma/wheezing cohort, were characterized by 16S rRNA gene sequencing and unsupervised hierarchical clustering was performed on the Bray-Curtis β -diversity. Enrichment scores (ESs) of the MSigDB Hallmark gene sets were computed from the blood transcriptome using gene set variation analysis. Children with severe asthma or severe wheezing were followed up for 12-18 months, with assessing the frequency of exacerbations.

Measurements and Main Results:

Oropharyngeal samples of 241 children (age range: 1-17 years, 40% female) revealed 4 taxa-driven clusters dominated by *Streptococcus*, *Veillonella*, *Rothia* and *Haemophilus*, respectively. The clusters showed significant differences in atopic dermatitis, grass pollen sensitization, FEV₁ % predicted post-salbutamol, and the annual asthma exacerbation frequency during follow-up. The *Veillonella*-cluster was the most allergic and included highest percentage of children with ≥ 2 exacerbations/year during follow-up. The oropharyngeal clusters were different in the ESs of transforming growth factor β (highest in *Veillonella*-cluster) and Wnt/ β -Catenin signaling (highest in *Haemophilus*-cluster) transcriptomic pathways in blood (all q -values < 0.05).

115 **Conclusion:**

116 The analysis of the oropharyngeal microbiota of children with asthma/wheezing identified four clusters
117 with distinct clinical characteristics (phenotypes) that associate with exacerbations' risk and
118 transcriptomic pathways involved in airway remodeling. This suggests that further exploration of the
119 oropharyngeal microbiota may lead to novel pathophysiological insights and potentially new treatment
120 approaches.

121

122 **Abstract word count:** 250

123 **Keywords (Mesh):** Asthma; Wheezing; Phenotype; Microbiota; Precision Medicine

124

125

126

127

128

Introduction

Asthma is the most common chronic disease affecting children. Childhood asthma is a multi-faceted disease that presents with varied clinical manifestations and treatment responses. In addition, childhood asthma-like symptoms were reported to increase risk of COPD in adulthood [1]. The underlying mechanisms of childhood asthma or preschool wheezing are not completely understood and thought to originate from multiple interacting factors, including genetic susceptibility, environmental exposures, and microbiota [2]. The host-residing microbiota regulates and works in an alliance with the immune system and is thought to partly mediate the link between environmental exposures and asthma pathophysiology [3, 4]. Therefore, assessing the microbiota profiles in children with wheezing or asthma may reveal distinct host, microbiome, and disease links that could play a role in disease development.

Omics-guided asthma characterization approaches have been utilized recently to delineate groups (i.e. clusters) of patients with asthma that share similar molecular profiles and exhibit distinct phenotypic asthma characteristics [5]. Underpinning these asthma phenotypes with specific molecular fingerprints may lead to tailoring diagnostic and/or therapeutic decisions. This may result in better patient care, reduce the risk of severe complications, and prevent inappropriate medication use. In adults, the Unbiased BIOmarkers for the Prediction of REspiratory Disease outcomes (U-BIOPRED) revealed sputum taxa-driven clusters linked to asthma severity and underlying inflammatory status, particularly sputum neutrophilia [6]. Similar findings in adults with asthma have been reported elsewhere [7], suggesting that the sputum microbiota may help refine the neutrophilic asthma phenotype in adult patients with severe asthma. Combining other omics, including transcriptomics, delineates associated molecular mechanisms characterizing the taxa-driven clusters and may improve our understanding of the pathophysiology [8]. In children, obtaining samples representing the lower airways (e.g. induced sputum, bronchoalveolar lavage fluid, or endobronchial biopsies samples) is challenging. Evidence suggests the ecological

continuity of the microbiota structure within the respiratory tract [9-11], advocating the need to investigate the value of non-invasive microbiota sampling in the assessment of children with wheeze or asthma. Studies have shown changes in pharyngeal microbiota are associated with the risk of later developing asthma in young children [12-15] or associated with different asthma characteristics [16, 17]. However, attempts to assess the value of airways microbiota in stratifying children with wheezing or asthma into clinically meaningful groups are scarce.

To clarify the role of the oropharyngeal microbiota in pediatric preschool-age wheeze and school-age asthma, we examined oropharyngeal swabs by 16S rRNA gene sequencing in the European U-BIOPRED pediatric cohort [18]. In a previous report from this dataset, we found limited differences in diversity and differential abundances between children with severe and mild-to-moderate asthma or wheeze, but a significant association with age [19]. Building on these results, we hypothesized that oropharyngeal microbiota profiles may reveal distinct clusters in children with preschool-age wheezing or asthma during school-age. This study specifically aims to 1) perform unsupervised unbiased clustering of oropharyngeal microbiota profiles of children and assess whether these clusters are linked with distinct asthma characteristics (phenotypes), 2) elucidate the possible underlying biological pathways of the revealed phenotypic clusters using the peripheral blood transcriptome, and 3) to reveal whether the baseline clusters are associated with future exacerbations during 12-18 months of follow-up in children with severe school-age asthma and severe preschool-age wheezing.

Methods

Study design

The U-BIOPRED study is a multicenter European observational cohort study including children with physician-diagnosed mild-to-moderate and severe school-age asthma and preschool wheezing aged 1-17 years old as previously described [18]. Children were recruited from 7 study centers encompassing 5 European countries (United Kingdom, Denmark, Sweden, the Netherlands, and Switzerland) and were mainly of a Caucasian ethnic origin. Children were allocated into four cohorts comprising A) severe school-age asthma, B) mild-to-moderate school-age asthma, C) severe preschool-age wheeze or D) mild-to-moderate preschool-age wheeze. All study centers obtained ethics committees approval and parents/caregivers gave written informed consent. Children gave assent where age-appropriate. The study was registered at ClinicalTrials.gov (identifier number: NCT01982162). All study centers followed uniform Standard Operating Procedures (SOPs) in all study procedures as described [18].

Participants

A total of 131 preschool-aged children with wheeze (n=77 severe, n=54 mild-moderate) and 140 school-aged children with asthma (n=97 severe, n=43 mild-moderate) were recruited to the U-BIOPRED pediatric cohorts. The flow diagram of patient inclusion is shown in Figure E1. Asthma/wheeze severity was defined according to the Global Initiative for Asthma (GINA) and the Innovative Medicines Initiative guidelines [20, 21] and fully described elsewhere [18]. Body mass index (BMI) was converted into z-scores according to the World Health Organization growth charts [22]. Participants were assessed for atopy [23, 24] (details in the online supplement) and environmental tobacco smoke exposure by measuring urinary cotinine levels [18]. In addition, they underwent spirometry and fractional exhaled nitric oxide (FE_{NO}) testing (for older capable children) as described [18]. Quality of life was evaluated using the standard Pediatric Asthma (Caregiver's) Quality of Life Questionnaire (PA(C)QLQ) [25, 26] and

asthma control was evaluated using the (childhood) Asthma Control Test ((c)ACT) [27, 28]. A (c)ACT score >19 indicates well-controlled asthma. Other family and medical histories were collected from the children or caregivers and the physicians as appropriate.

Children with severe asthma or severe wheezing (n= 125/151, 82.8%) were followed up prospectively in time (12-18 months after the baseline visit), during which the frequency of asthma exacerbation (as defined [29]) per year was documented (i.e. future exacerbations).

Samples collection and omics analysis

Full details for samples collection and omics analysis are described previously [19] and in the online supplement.

Oropharyngeal swabs and 16S gene V4 microbiome sequencing

Briefly, oropharyngeal (throat) swabs for microbiota processing were taken from the posterior pharyngeal wall, behind the uvula. The 16S ribosomal RNA (rRNA) gene in the collected samples was amplified for the hypervariable V4 region and sequencing was performed using the Illumina MiSeq Desktop Sequencer. The microbiome sequencing data can be found in the European Nucleotide Archive database (accession number: PRJEB47973). Paired-end reads (250 bp x 2) from amplicon sequencing were quality checked using FastQC [30] and MultiQC [31], and then cleaned by removing V4 region primers using Cutadapt [32]. Further processing was performed using the DADA2 pipeline as described [33]. Briefly, the pipeline works by performing quality filtering and trimming, dereplicating sequences, learning dataset-specific error rates, denoising by removing potentially containing errors sequences, merging paired-end reads while removing mismatches to reduce errors, constructing amplicon sequence variants (ASVs), removing chimera by implementing “bimera” method. Finally, taxonomic classification of ASVs was done by the Silva database version 132 [34].

Blood collection and transcriptomics analysis

Peripheral blood was isolated and gene expression was assessed by Affymetrix HT HG-U133+ PM arrays (Affymetrix, Santa Clara, CA). The microarray data are deposited in the Gene Expression Omnibus database (accession number: GSE123750). Raw microarray data were quality assessed and pre-processed by robust multi-array average normalization (RMA) method [35] as implemented in the affy R package. Transcriptomic pathway enrichment analysis was performed by an unsupervised approach using the gene set variation analysis (GSVA) R package against gene sets from the Molecular Signatures Database (MSigDB) release version 7.4 [36].

Data and statistical analysis

The general data analysis workflow is shown in Figure E2 and is further described previously [6] and in detail in the online supplement.

Briefly, a clustering benchmarking strategy using hierarchical ward2, partition around the medoids, and topological data analysis (TDA) was implemented to subtype children with asthma or wheezing according to their microbiota profiles. The clusters were checked for differences in microbial profiles by Shannon α -diversity (using a Kruskal-Wallis H test followed by a Dunn's post-hoc test) and by Linear discriminant analysis Effect Size (LEfSe) for differentially abundant bacteria at phylum and species levels (using an LDA score > 2 and an FDR q -value < 0.01). Furthermore, the taxa-driven clusters were tested for differences in certain demographic and clinical characteristic (such as allergic status, atopy, and spirometry) and the frequency of future exacerbations/year using Kruskal-Wallis H or Pearson Chi-Square tests as appropriate. Clinical characteristics that were statistically significant after univariate analysis, were adjusted for several potential confounders using logistic or linear multiple regression models as appropriate. Potential confounders (covariates) to adjust for in the regression models were determined using a directed acyclic graph [37] (DAG, Figure E3). A simple mediation analysis was conducted to

239 investigate whether microbiota Cluster 2 is an independent predictor of future asthma exacerbations
240 (≥ 2) or if this is mediated by the atopic dermatitis status.

241 The GSVA enrichment scores (ES) of the tested gene sets (i.e. transcriptomic pathways) were compared
242 between the clusters by Kruskal-Wallis H-test and multiple testing was corrected by FDR, followed by
243 permutation analysis (10000 times). Linear regression models were used to investigate whether the
244 enrichment scores of the significant gene sets are dependent on the participants' clusters assignments
245 after adjusting for multiple covariates (as defined in the DAG).

246 All analyses were performed using R studio (version 1.1.453) with R software (version 3.6.1).

247

Results

Baseline characteristics of study participants

A total of 241 participants provided baseline oropharyngeal swabs that have been sequenced to a read depth of at least 1000 that passed the quality control. The baseline characteristics of the subjected are shown in Table 1. The median age of the included participants was 6 years, 40% were females, 80% were White and 70% were atopic.

Four main taxa-driven clusters were generated

The median sequencing reads number passing the quality control was 11,975 (IQR= 7,613-21,098) per sample. Negative extraction controls showed different microbial composition and significantly lower Shannon α -diversity compared with oropharyngeal swabs, while correct classification of all bacterial genera was achieved in the mock community (Figure E4). The main bacterial genera detected in the oropharyngeal swab samples were; *Streptococcus*, *Veillonella*, *Haemophilus*, *Prevotella*, and *Rothia* (Figure E5).

Clustering performed on Bray-Curtis beta-diversity suggested 4 optimum clusters as evaluated by the majority vote of multiple indices (Figure E6), resulting in 4 children groups by hierarchical ward2 (Figure 1A) and partition around medoids (PAM, Figure 1B) clustering. Quantitative assessment of similarity in participants' assignment between the hierarchical ward and PAM clustering was performed by means of Rand index (RI= 0.85) and Pearson Chi-Square test ($\chi^2= 498.1$, $p < 1 \times 10^{-4}$) suggesting high similarity in the two clustering assignments. Visual representation by topological data analysis (TDA) shows that the 4 microbiota clusters are enriched (according to SAFE scores) into 4 distinct regions of the TDA network (Figure E7A and Figure E7B). The 4 clusters were also visualized by the PCoA plot on the Bray-Curtis distance with depicting the 95% ellipses (Figure E8).

The hierarchical clusters had significantly different microbial Shannon α -diversity (Figure E9), showing a decreasing order of median diversity as follows: Cluster 4>Cluster 2>Cluster3=Cluster1. The mean relative abundances of most abundant bacterial genera and the individual samples' compositions were stratified according to the clusters' assignments (Figure E10 and Figure E11, respectively). Analysis by the LEfSe method revealed the differential abundance of the most abundant bacterial phyla and species between the clusters (Figure 2). Cluster 1 showed main enrichment of bacterial genus *Streptococcus* and phylum *Firmicutes*, Cluster 2 of genus *Veillonella* and phylum *Patescibacteria*, Cluster 3 of genus *Rothia* and phylum *Actinobacteria*, and Cluster 4 of genera *Haemophilus* and *Neisseria*, as well as phylum *Proteobacteria*. The TDA was consistent with the LEfSe method, in which the same regions of the TDA network enriched with the cluster's assignment, showed increased relative abundances of the above-mentioned bacterial genera (Figure E12 and Figure E13). Of note, *Moraxella* was detected in a small percentage of samples and in low abundances (5.0% of samples, 0.01% mean relative abundance). It was relatively higher in abundance in Cluster 1 compared with the other clusters, although the results were not statistically significant after FDR correction. Decision tree analysis showed that the relative abundances of only 3 bacterial genera (*Streptococcus*, *Veillonella*, and *Haemophilus*) (Figure E14) could be used to classify the children into the corresponding clusters with an accuracy of 0.86 (95% CI: 0.75-0.94, P -value = 8.24×10^{-15}) using a holdout validation set.

There were no statistically significant associations between the participants' clusters assignments and the 7 study centers from which samples were collected or the season of sample collection (p -values were 0.390 and 0.526, respectively).

Taxa-driven clusters show distinct clinical characteristics

Table 2 shows the demographic and clinical characteristics of the 4 taxa-driven clusters. The clusters showed statistically significant differences in atopic dermatitis diagnosis, and FEV₁ % predicted values post-salbutamol (the latter also shown in Figure E15). These differences remained significant after adjusting for several covariates (Table E2, and Table E3, *q*-values <0.05). Table 3 shows characteristics of the atopic sensitization of the clusters. The clusters showed statistically significant differences in (aeroallergen) atopic sensitization specifically to grass pollens and the number of aeroallergen sensitizations (the latter also shown in Figure E16). After adjusting for covariates, grass aeroallergen sensitization (but not overall sensitization) was statistically significantly associated with the clusters (Table E4).

Differential peripheral blood transcriptomic pathways in the taxa-driven clusters

A total of 188/241 (78%) participants provided peripheral blood samples for transcriptomic analysis. Figure 3 shows the statistically significant transcriptomic pathways between the taxa-driven clusters. A total of 3 hallmark pathways were statistically different between the taxa-driven clusters, of which the Wnt/ β -Catenin and the Transforming growth factor β (TGF- β) signaling transcriptomic pathways remained significant after multiple testing corrections. Cluster 4 had the highest median ESs for the Wnt/ β -Catenin signaling pathway, while cluster 2 had the highest median ESs for the TGF- β signaling pathway. The permutation analysis *p*-values were 9.9×10^{-5} and 0.001 for the Wnt/ β -Catenin and the TGF- β signaling, respectively. The pathways showed statistically significant associations with the clusters after adjusting for different covariates (Table E5).

Baseline microbiota clusters were associated with future exacerbations in children with severe asthma or wheezing

The baseline microbiota clusters were significantly associated with the exacerbations risk during a follow-up period of 12-18 months (Table 4). Logistic regression analysis showed that microbiota clusters are a significant predictor of having ≥ 2 future exacerbations/year after adjusting for several covariates (Table E5). In particular, Cluster 3 And Cluster 4 had statistically significantly lower odds ratio (OR) of having ≥ 2 future exacerbations/year relative to cluster 2, (OR = 0.06, 95% CI: 0.01-0.43, and OR = 0.11, 95% CI: 0.03-0.34, q -values < 0.05, respectively, Table E6). Other covariates that were associated with frequency of ≥ 2 exacerbations/year including atopic dermatitis diagnosis, center of inclusion and recent prescription of antibiotics at baseline visit (all q -values<0.05, Table E6). Notably, the transcriptomic (Wnt/ β -Catenin, and TGF- β signaling) pathways ESs were not selected by the stepwise regression model as significant predictors of having ≥ 2 future exacerbations. Mediation analysis (Table E7) showed that microbiota Cluster 2 is an independent predictor of having ≥ 2 future exacerbations and this association was not mediated by the atopic dermatitis status, whether this was not adjusted or adjusted for the different covariates.

A summary overview of clinical features associated with the taxa-driven clusters is described in Box 1 and Figure E17.

Discussion

Using unsupervised clustering of oropharyngeal microbiota profiles, we found that children with school-age asthma and preschool-age wheezing could be stratified into 4 clusters which differed significantly by 1) atopic dermatitis diagnosis, grass pollen sensitization, and post-bronchodilator FEV₁ % predicted, 2) the Wnt/ β -Catenin and TGF- β signaling peripheral blood transcriptomic pathways and 3) frequency of future exacerbations among children with severe disease.

Age has been reported a significant contributor to the variability in the microbiome compositions, while the largest influence of age on microbial profiles was observed very early in life during which microbial maturation is achieved [38, 39]. In this study, the clustering strategy performed only showed a trend of non-statistically significant differences between the clusters concerning age, with cluster 2 being more likely to include older school-age children compared to the other clusters. In addition, in this study, no clear separation of the oropharyngeal microbiota clusters between children with school-age asthma and children with preschool wheezing stratified by disease severity was found, showing an overlapping oropharyngeal microbiome composition in this studied cohort (aged 1-17 years old). These findings are in line with previous U-BIOPRED study [19], suggesting that classical clinical labelling of asthma or wheezing severity cannot be fully explained by the underlying microbiota composition, and attempts to reclassify/rephenotype children with asthma or wheezing should be sought. In this regard, clustering children by underlying microbiota composition may offer new insight in disease pathophysiology, particularly if this could be linked with objective measures of disease burden, such as future exacerbations.

The taxa-driven clusters were significantly different in atopic dermatitis diagnosis and grass pollen sensitization. Particularly, Cluster 2 included the highest percentage of children with atopic dermatitis, grass pollen sensitization, and school-aged children with severe asthma. In addition, severe

asthma/wheezing children within this cluster had the highest percentage of those who experienced ≥ 2 exacerbations in the following year. Atopic sensitization and co-morbid allergy are amongst the main characteristics that shape childhood asthma phenotypes [40, 41]. Our findings are partly in line with other studies, for example; in one study it was found that concomitant atopic dermatitis might be one of the factors associated with severe asthma [42]. Moreover, reports have shown that atopic sensitization to inhalant allergens increases the risk of acute exacerbations and asthma-related hospital admissions in childhood asthma [43]. In a study conducted in children with asthma aged 3-17 years old, it was found that viral infections and allergen sensitization synergistically increased risk of asthma-related hospital admissions [44]. In our study, both the taxa-driven clusters additionally with atopic dermatitis diagnosis were found to be significantly associated with the frequency of future exacerbations confirming previous observations. This suggest that microbiota-allergen interaction may play a role in the pathogenesis of childhood asthma [45] and this interaction needs further investigations in future childhood asthma studies.

Cluster 2 (*Veillonella*-dominant and the second-highest cluster in Shannon α -diversity) and Cluster 4 (*Haemophilus*- and *Neisseria*-dominant and the highest cluster in Shannon α -diversity) included the highest percentage of children with severe asthma/wheezing who experienced episodes of future exacerbations (≥ 2 and 1 exacerbations, respectively) compared with the other clusters. In addition, Cluster 2 children had lower FEV₁ % predicted post-salbutamol compared with the other clusters. These results are partly in line with findings from another study which showed that increased bacterial Shannon α -diversity and increased *Veillonella* and *Neisseria* abundances in hypopharyngeal aspirates were associated with increased duration of asthma-like episodes in preschoolers [46]. In the same study, an augmented effect of azithromycin in decreasing the asthma-like episodes was particularly seen in children with elevated bacterial relative abundances of *Veillonella* and *Neisseria* genera [46]. In other microbiome studies in which the oropharynx was sampled, preschool wheezers had partly increased

376 levels of *Neisseria* genus compared with non-wheezers [47], while children with school-age asthma (6-12
377 years old) had increased abundances of *Haemophilus* genus compared with healthy controls [48]. These
378 findings suggest that the pharyngeal relative compositions of the above-mentioned bacterial genera may
379 play a role in childhood asthma pathogenesis and may be useful in the phenotypic assessment of
380 children with asthma/wheezing.

381 Interestingly, Cluster 3 (*Rothia*-dominant) included the highest percentage of children who did not
382 experience any future exacerbations during the follow-up period. This is in line with findings from the U-
383 BIOPRED adult cohort, in which high abundance *Rothia mucilaginosa* in sputum was associated with a
384 less severe asthma phenotype [6]. Moreover, *Rothia mucilaginosa* was found to be negatively correlated
385 with matrix metalloproteinases (MMP-1, MMP-8, and MMP-9) and pro-inflammatory markers (IL-8, IL-
386 1 β) in sputum of adults with bronchiectasis [49]. In vivo/in vitro mechanistic investigation in the same
387 study revealed that *Rothia mucilaginosa* potentially mitigates inflammation via inhibiting the NF- κ B
388 pathway activation, which may influence the severity and development of chronic airway diseases [49].
389 These findings suggest that *Rothia* species may have protective effect in adults and children with severe
390 asthma or wheezing.

391 The peripheral blood transcriptome showed statistically significant differences between the clusters in
392 two main pathways: the TGF- β and the Wnt/ β -Catenin signaling pathways. The TGF- β pathway was
393 relatively up-regulated in Cluster 2 (the most atopic) and, to a lesser extent, Cluster 4 compared with
394 Cluster 1. The TGF- β signaling pathway has been reported to be involved in airway remodeling in atopic
395 asthma following exposure to an allergen [50] and may play a role in asthma severity [51]. The TGF- β
396 pathway has been reported to regulate the immune system in response to bacterial infections [52]. On
397 the other hand, the Wnt/ β -Catenin signaling pathway was relatively up-regulated in the
398 *Haemophilus/Neisseria* predominant-Cluster 4 compared with the other clusters. Similarly, the Wnt/ β -

catenin pathway has been reported to regulate remodeling in asthmatic airways and may play a role in asthma pathogenesis [53-55]. In addition, Wnt signaling is believed to be one of the key pathways involved in host-bacterial pathogen interactions [56]. The Canonical Wnt/ β -Catenin signaling pathway was found to be activated after infection with virulent strains of *Haemophilus* species leading to disruption of the epithelial barrier in pigs [57]. In addition, it was recently found that WNT/ β -catenin signaling is a key regulator of macrophage phagocytosis after exposing COPD airway epithelium to non-typeable *Haemophilus influenzae* [58]. In light of the findings of this study and evidence of involvement of these pathways in airway remodeling and pathogenesis, further research is needed to explore the interaction of the oropharyngeal microbiota with these pathways in childhood asthma.

In this study, we showed that clustering on the oropharyngeal microbiota revealed subtypes of asthma/wheezing children with distinct clinical characteristics (phenotypes). A decision tree based on the relative abundances of only 3 main bacterial genera showed that we can classify the children with an 86% accuracy as estimated from a hold-out validation set. These bacterial genera were among the most abundant and prevalent bacterial taxa found in other pediatric cohorts in which the pharynx was sampled for microbiota analysis [46-48]. This suggests that the taxa-driven clustering strategy in this study may be generalizable to other asthma/wheezing cohorts and settings. Phenotyping in children with asthma/wheezing remains challenging particularly due to the difficulty of obtaining invasive samples representing the lower airways and their inflammatory status. The oropharyngeal (throat) swabs are relatively easy to obtain and 16S sequencing is likely to be an affordable option to sequence the bacterial profiles within these samples. Hence, using the oropharyngeal taxa-driven clustering may help clinicians to non-invasively define subgroups among children with asthma/wheezing who may benefit from personalized monitoring and/or treatment options. Yet, validation of findings in external cohorts and different populations remains necessary before findings can be rendered translatable to clinical practice,

and to assess whether the airway microbiome can be therapeutically targeted in children with asthma or wheezing [59].

Our study has many strengths. First, the adopted analysis strategy is unsupervised and is not driven by a priori hypothesis. Second, the prospective international multi-center design of this study, the relatively large sample size, and the wide age range of the included cohort make the results likely more generalizable and valid than previously reported single-center studies with lower sample sizes. Third, the oropharyngeal samples are easy to collect and convenient for patients and healthcare professionals, making the phenotypic assessment based on oropharyngeal microbiota feasible. Finally, internally validating the findings by using different clustering algorithms makes the statistical analysis more robust.

However, there are also limitations. First, the 16S amplicon sequencing technique used is limited in identifying bacterial taxa up to species level and this imposes some hindrance in identifying the pathogenicity of the differentially abundant bacterial genera between the clusters. More sophisticated techniques, such as shotgun metagenomics that enable species or strain level identification of bacteria, may therefore provide a better insight in this regard. However, in another U-BIOPRED study conducted in adult patients with severe asthma, clustering based on 16S amplicon sequencing revealed similar patient clusters to shotgun metagenomics, and this suggests that the affordable 16S amplicon sequencing is potentially applicable in clinical settings where metagenomics cannot be performed [6]. Second, we sampled only one compartment for bacterial sequencing (oropharyngeal swabs). Whether other sampling compartments and detecting other microorganisms (e.g. viruses/fungi) will provide additional information needs to be determined. Third, although patients were followed up clinically for 12 to 18 months, no additional biological samples were collected to assess the longitudinal shifts in microbial profiles with time. Although the taxa-driven clusters were found to be relatively stable after 12-18 months in adults with severe asthma [6], further longitudinal investigations are still needed in

children with asthma. Forth, we did not collect some parameters in the U-BIOPRED pediatric cohort, such as birth weight and antenatal (in utero) and perinatal antibiotic treatment history, therefore; we were not able to investigate whether they are associated with oropharyngeal microbiota profiles. Further research is needed to investigate whether these characteristics could influence the oropharyngeal microbiota composition. Fifth, assessing the peripheral blood gene expression may not reflect the airway-centric asthma pathobiology, and therefore; further research is needed to investigate whether the microbiota composition is directly linked to pathophysiologic biological pathways underlying the diseases airways. Sixth, corticosteroids have been reported to influence the composition of the airway microbiome [60]. Although we have adjusted for corticosteroids intake in all regression analysis performed, this may not reflect the systemic levels of corticosteroids and this could influence the oropharyngeal microbiota composition. Finally, using an external cohort for validation is still needed to confirm the present findings.

In conclusion, we have shown that oropharyngeal taxa-driven clustering can be used as an unsupervised method of detecting subtypes in children with preschool wheezing and school-aged asthma. These subtypes exhibited differences in allergic status, lung function, blood transcriptomic pathways involved in airway remodeling, and frequency of future exacerbations. These findings suggest that the oropharyngeal microbiota can be used as a non-invasive approach to phenotype children with asthma or wheezing.

Acknowledgements

The authors would like to thank all the participating children and their families. In addition, the U-BIOPRED is a consortium effort and we wish to acknowledge the help and expertise of the individuals and groups whose names are mentioned in the U-BIOPRED study group list available in the online repository.

Competing interests:

MIA, SH, SJHV, PB, JS, MAR, MRW, NHV, MSM, ADB, SJF, UF, AB, GH, DS, CA, ATB, ARS, BLC, and ADK have no conflicts of interest to disclose. **JT** reports receiving Honoria from AstraZeneca. **AHN** reports receiving a grant from ERANET Systems Medicine and ZonMW [project number: 9003035001]. **WVA** has received honoraria for participating in a medical advisory board for Boehringer Ingelheim BV and for giving lectures for OMRON Healthcare Europe BV. **G's** University received funding from EU IMI for this research. **LF** has received honoraria and Consulting fees from Astra Zeneca, Sanofi, Adherium, Novartis, Teva and Respiri, outside the submitted work. **CSM** reports grants from National Institute for Health Research, Asthma UK, Innovate UK, Moulton Charitable Foundation, North West lung Centre Charity outside the submitted work; honoraria for lecture fees from GSK and Novartis and participation in advisory boards for Sanofi and Adherium Ltd. **FS** reports financial support from Novartis Pharma Switzerland, Vertex Pharmaceuticals Switzerland, and non-financial support from Chiesi Pharmaceuticals Austria outside the submitted work. **BN** owns stocks in MediTuner AB, a company supporting remote digital management of asthma. **KFC's** institution received MRC, EPSRC and GSK grants for asthma research, and he reports receiving Honoria from Novartis & AZ and participating in advisory board meetings for Roche, Merck, Rickett- Beckinson & Shionogi on asthma, COPD and chronic cough. **IMA** received unrestricted research grants from the EU-IMI, GSK, Sanofi, MRC and EPSRC and lecture fees from AZ, Eurodrug, Sanofi and Sunovion, and he also serves on advisory boards for Chiesi, GSK, Kineset

487 and Sanofi and fees for expert testimony from Chiesi. **RD** has no specific conflicts in respect of this study
488 but wishes, nevertheless, to disclose receiving payments for participation in advisory board meetings
489 with GSK, Regeneron and Kymab, and he is also co-founder and a shareholder of Synairgen, a University
490 of Southampton spin-out company where he has shares and is a consultant. **SSW's** BioSci Consulting
491 company received consulting fees from Kings College Hospital NHS Foundation Trust, Academic Medical
492 Research, AMC Medical Research BV, Asthma UK, Athens Medical School, Boehringer Ingelheim
493 International GmbH, CHU de Toulouse, CIRO, DS Biologicals Ltd, ÉCOLE POLYTECHNIQUE FÉDÉRALE DE
494 LAUSANNE, European Respiratory Society, FISEVI, Fluidic Analytics Ltd., Fraunhofer IGB, Fraunhofer
495 ITEM, GlaxoSmithKline Research & Dev Ltd, Holland & Knight, Karolinska Institutet Fakturor, KU Leuven,
496 Longfonds, National Heart & Lung Institute, Novartis Pharma AG, Owlstone Medical Limited, PEXA AB,
497 UCB Biopharma S.P.R.L., Umeå University, Univ. Hospital Southampton NHS Foundation Trust, Università
498 Campus Bio-Medico di Roma, Università Cattolica Del Sacro Cuore, Universität Ulm, University of Bern,
499 University of Edinburgh, University of Hull, University of Leicester, University of Loughborough,
500 University of Luxembourg, University of Manchester, University of Nottingham, Vlaams Brabant, Dienst
501 Europa, Imperial College London, Boehringer Ingelheim, Breathomix, Gossamer Bio, Astrazeneca, CIBER,
502 OncoRadiomics, University of Leiden, University of Wurzburg, Chiesi Pharmaceutical, University of Liege,
503 Teva Pharmaceuticals, Sanofi, Pulmonary Fibrosis Foundation, and Three Lakes Foundation. **KB** received
504 consulting fees from Sanofi and Astra Zeneca, lecture fees from Boehringer Ingelheim and fees for
505 participant in advisory board for ALK-Abelló Nordic. **SJS's** institution received grants from Novo Nordic
506 Foundation (NNF) and Independent Research Fund Denmark's (DFF). **PJS** is scientific advisor and has an
507 officially non-substantial interest in the SME Breathomix BV that produces electronic noses and the
508 accompanying analysis algorithms. **GR's** University received funding from EU IMI for this research. **HB**
509 reports receiving grants from The Lundbeck Foundation, The Ministry of Health, Danish Council for
510 Strategic Research, and The Capital Region Research Foundation. **AHM** has received grants from Health

511 Holland and she is the PI of a P4O2 (Precision Medicine for more Oxygen) public private partnership
512 sponsored by Health Holland involving many private partners that contribute in cash and/or in kind
513 (Boehringer Ingelheim, Breathomix, Fluida, Ortec Logiqcare, Philips, Quantib-U, Smartfish, SODAQ,
514 Thirona, TopMD and Novartis), and received unrestricted research grants from GSK, Boehringer
515 Ingelheim and Vertex, and received consulting fees paid to her institution from Boehringer Ingelheim
516 and Astra Zeneca, and received honoraria for lectures paid to her institution from GlaxosmithKline;
517 outside the submitted work.

518 Besides the above mentioned, authors declare no potential, perceived, or real conflict of interest
519 regarding the content of this manuscript.

520

521

522 **References**

- 523 1. Bisgaard H, Nørgaard S, Sevelsted A, et al. Asthma-like symptoms in young children increase the
524 risk of COPD. *J Allergy Clin Immunol.* 2021;147(2):569-76.e9.
- 525 2. Pijnenburg MW, Frey U, De Jongste JC, et al. Childhood asthma: pathogenesis and phenotypes.
526 *Eur Respir J.* 2022;59(6).
- 527 3. Belkaid Y, Hand TW. Role of the microbiota in immunity and inflammation. *Cell.*
528 2014;157(1):121-41.
- 529 4. Abdel-Aziz MI, Vijverberg SJH, Neerincx AH, et al. The crosstalk between microbiome and
530 asthma: Exploring associations and challenges. *Clin Exp Allergy.* 2019;49(8):1067-86.
- 531 5. Abdel-Aziz MI, Neerincx AH, Vijverberg SJ, et al. Omics for the future in asthma. *Semin*
532 *Immunopathol.* 2020;42(1):111-26.
- 533 6. Abdel-Aziz MI, Brinkman P, Vijverberg SJH, et al. Sputum microbiome profiles identify severe
534 asthma phenotypes of relative stability at 12 to 18 months. *J Allergy Clin Immunol.* 2021;147(1):123-34.
- 535 7. Diver S, Richardson M, Haldar K, et al. Sputum microbiomic clustering in asthma and chronic
536 obstructive pulmonary disease reveals a *Haemophilus*-predominant subgroup. *Allergy.* 2020;75(4):808-
537 17.
- 538 8. Abdel-Aziz MI, Vijverberg SJH, Neerincx AH, et al. A multi-omics approach to delineate sputum
539 microbiome-associated asthma inflammatory phenotypes. *Eur Respir J.* 2022;59(1).
- 540 9. Charlson ES, Bittinger K, Haas AR, et al. Topographical continuity of bacterial populations in the
541 healthy human respiratory tract. *Am J Respir Crit Care Med.* 2011;184(8):957-63.
- 542 10. Dickson RP, Erb-Downward JR, Freeman CM, et al. Spatial Variation in the Healthy Human Lung
543 Microbiome and the Adapted Island Model of Lung Biogeography. *Ann Am Thorac Soc.* 2015;12(6):821-
544 30.
- 545 11. Ahmed B, Cox MJ, Cuthbertson L, et al. Comparison of the upper and lower airway microbiota in
546 children with chronic lung diseases. *PLoS One.* 2018;13(8):e0201156.
- 547 12. Bisgaard H, Hermansen MN, Buchvald F, et al. Childhood asthma after bacterial colonization of
548 the airway in neonates. *N Engl J Med.* 2007;357(15):1487-95.
- 549 13. Thorsen J, Rasmussen MA, Waage J, et al. Infant airway microbiota and topical immune
550 perturbations in the origins of childhood asthma. *Nat Commun.* 2019;10(1):5001.
- 551 14. Raita Y, Camargo CA, Jr., Bochkov YA, et al. Integrated-omics endotyping of infants with
552 rhinovirus bronchiolitis and risk of childhood asthma. *J Allergy Clin Immunol.* 2021;147(6):2108-17.
- 553 15. Raita Y, Perez-Losada M, Freishtat RJ, et al. Nasopharyngeal metatranscriptome profiles of
554 infants with bronchiolitis and risk of childhood asthma: a multicentre prospective study. *Eur Respir J.*
555 2022;60(1).
- 556 16. Chiu CY, Chan YL, Tsai MH, et al. Cross-talk between airway and gut microbiome links to IgE
557 responses to house dust mites in childhood airway allergies. *Sci Rep.* 2020;10(1):13449.
- 558 17. Perez-Losada M, Authalet KJ, Hoptay CE, et al. Pediatric asthma comprises different phenotypic
559 clusters with unique nasal microbiotas. *Microbiome.* 2018;6(1):179.
- 560 18. Fleming L, Murray C, Bansal AT, et al. The burden of severe asthma in childhood and
561 adolescence: results from the paediatric U-BIOPRED cohorts. *Eur Respir J.* 2015;46(5):1322-33.
- 562 19. Thorsen J, Stokholm J, Rasmussen MA, et al. Asthma and Wheeze Severity and the
563 Oropharyngeal Microbiota in Children and Adolescents. *Ann Am Thorac Soc.* 2022.
- 564 20. Bel EH, Sousa A, Fleming L, et al. Diagnosis and definition of severe refractory asthma: an
565 international consensus statement from the Innovative Medicine Initiative (IMI). *Thorax.*
566 2011;66(10):910-7.

21. Bousquet J. Global initiative for asthma (GINA) and its objectives. *Clin Exp Allergy*. 2000;30 Suppl 1(s1):2-5.
22. de Onis M, Onyango AW, Borghi E, et al. Development of a WHO growth reference for school-aged children and adolescents. *Bull World Health Organ*. 2007;85(9):660-7.
23. Siles RI, Hsieh FH. Allergy blood testing: A practical guide for clinicians. *Cleve Clin J Med*. 2011;78(9):585-92.
24. Abdel-Aziz MI, Brinkman P, Vijverberg SJH, et al. eNose breath prints as a surrogate biomarker for classifying patients with asthma by atopy. *J Allergy Clin Immunol*. 2020;146(5):1045-55.
25. Juniper EF, Guyatt GH, Feeny DH, et al. Measuring quality of life in children with asthma. *Qual Life Res*. 1996;5(1):35-46.
26. Juniper EF, Guyatt GH, Feeny DH, et al. Measuring quality of life in the parents of children with asthma. *Qual Life Res*. 1996;5(1):27-34.
27. Nathan RA, Sorkness CA, Kosinski M, et al. Development of the asthma control test: a survey for assessing asthma control. *J Allergy Clin Immunol*. 2004;113(1):59-65.
28. Liu AH, Zeiger R, Sorkness C, et al. Development and cross-sectional validation of the Childhood Asthma Control Test. *J Allergy Clin Immunol*. 2007;119(4):817-25.
29. Reddel HK, Taylor DR, Bateman ED, et al. An official American Thoracic Society/European Respiratory Society statement: asthma control and exacerbations: standardizing endpoints for clinical asthma trials and clinical practice. *Am J Respir Crit Care Med*. 2009;180(1):59-99.
30. Andrews S. FastQC: A Quality Control Tool for High Throughput Sequence Data 2010 [Available from: <http://www.bioinformatics.babraham.ac.uk/projects/fastqc/>].
31. Ewels P, Magnusson M, Lundin S, et al. MultiQC: summarize analysis results for multiple tools and samples in a single report. *Bioinformatics*. 2016;32(19):3047-8.
32. Martin M. Cutadapt removes adapter sequences from high-throughput sequencing reads. *EMBnetjournal*. 2011;17(1):3.
33. Callahan BJ, McMurdie PJ, Rosen MJ, et al. DADA2: High-resolution sample inference from Illumina amplicon data. *Nat Methods*. 2016;13(7):581-3.
34. Quast C, Pruesse E, Yilmaz P, et al. The SILVA ribosomal RNA gene database project: improved data processing and web-based tools. *Nucleic Acids Res*. 2013;41(Database issue):D590-6.
35. Irizarry RA, Bolstad BM, Collin F, et al. Summaries of Affymetrix GeneChip probe level data. *Nucleic Acids Res*. 2003;31(4):e15.
36. Liberzon A, Birger C, Thorvaldsdottir H, et al. The Molecular Signatures Database (MSigDB) hallmark gene set collection. *Cell Syst*. 2015;1(6):417-25.
37. Textor J, van der Zander B, Gilthorpe MS, et al. Robust causal inference using directed acyclic graphs: the R package 'dagitty'. *Int J Epidemiol*. 2016;45(6):1887-94.
38. Mortensen MS, Brejnrod AD, Roggenbuck M, et al. The developing hypopharyngeal microbiota in early life. *Microbiome*. 2016;4(1):70.
39. Stokholm J, Blaser MJ, Thorsen J, et al. Maturation of the gut microbiome and risk of asthma in childhood. *Nat Commun*. 2018;9(1):141.
40. Bel EH. Clinical phenotypes of asthma. *Curr Opin Pulm Med*. 2004;10(1):44-50.
41. Howrylak JA, Fuhlbrigge AL, Strunk RC, et al. Classification of childhood asthma phenotypes and long-term clinical responses to inhaled anti-inflammatory medications. *J Allergy Clin Immunol*. 2014;133(5):1289-300, 300 e1-12.
42. Lee JK, Han D. Atopic dermatitis is an important comorbidity in severe asthma. *Ann Allergy Asthma Immunol*. 2018;120(6):661-2.
43. Jackson DJ, Sykes A, Mallia P, et al. Asthma exacerbations: origin, effect, and prevention. *J Allergy Clin Immunol*. 2011;128(6):1165-74.

44. Murray CS, Poletti G, Keadze T, et al. Study of modifiable risk factors for asthma exacerbations: virus infection and allergen exposure increase the risk of asthma hospital admissions in children. *Thorax*. 2006;61(5):376-82.
45. Jackson DJ, Busse WW, Bacharier LB, et al. Association of respiratory allergy, asthma, and expression of the SARS-CoV-2 receptor ACE2. *J Allergy Clin Immunol*. 2020;146(1):203-6 e3.
46. Thorsen J, Stokholm J, Rasmussen MA, et al. The Airway Microbiota Modulates Effect of Azithromycin Treatment for Episodes of Recurrent Asthma-like Symptoms in Preschool Children: A Randomized Clinical Trial. *Am J Respir Crit Care Med*. 2021;204(2):149-58.
47. Powell EA, Fontanella S, Boakes E, et al. Temporal association of the development of oropharyngeal microbiota with early life wheeze in a population-based birth cohort. *EBioMedicine*. 2019;46:486-98.
48. Boutin S, Depner M, Stahl M, et al. Comparison of Oropharyngeal Microbiota from Children with Asthma and Cystic Fibrosis. *Mediators Inflamm*. 2017;2017:5047403.
49. Rigauts C, Aizawa J, Taylor SL, et al. *Rothia mucilaginosa* is an anti-inflammatory bacterium in the respiratory tract of patients with chronic lung disease. *Eur Respir J*. 2022;59(5).
50. Torrego A, Hew M, Oates T, et al. Expression and activation of TGF-beta isoforms in acute allergen-induced remodelling in asthma. *Thorax*. 2007;62(4):307-13.
51. Al-Alawi M, Hassan T, Chotirmall SH. Transforming growth factor beta and severe asthma: a perfect storm. *Respir Med*. 2014;108(10):1409-23.
52. Sanjabi S, Oh SA, Li MO. Regulation of the Immune Response by TGF-beta: From Conception to Autoimmunity and Infection. *Cold Spring Harb Perspect Biol*. 2017;9(6).
53. Kwak HJ, Park DW, Seo JY, et al. The Wnt/beta-catenin signaling pathway regulates the development of airway remodeling in patients with asthma. *Exp Mol Med*. 2015;47(12):e198.
54. Jia XX, Zhu TT, Huang Y, et al. Wnt/beta-catenin signaling pathway regulates asthma airway remodeling by influencing the expression of c-Myc and cyclin D1 via the p38 MAPK-dependent pathway. *Exp Ther Med*. 2019;18(5):3431-8.
55. Sharma S, Tantisira K, Carey V, et al. A role for Wnt signaling genes in the pathogenesis of impaired lung function in asthma. *Am J Respir Crit Care Med*. 2010;181(4):328-36.
56. Rogan MR, Patterson LL, Wang JY, et al. Bacterial Manipulation of Wnt Signaling: A Host-Pathogen Tug-of-War. *Front Immunol*. 2019;10:2390.
57. Hua K, Li Y, Zhou H, et al. *Haemophilus parasuis* Infection Disrupts Adherens Junctions and Initializes EMT Dependent on Canonical Wnt/beta-Catenin Signaling Pathway. *Front Cell Infect Microbiol*. 2018;8:324.
58. Skronska-Wasek W, Durlanik S, Le HQ, et al. The antimicrobial peptide S100A8/A9 produced by airway epithelium functions as a potent and direct regulator of macrophage phenotype and function. *Eur Respir J*. 2022;59(4).
59. Chotirmall SH, Bogaert D, Chalmers JD, et al. Therapeutic Targeting of the Respiratory Microbiome. *Am J Respir Crit Care Med*. 2022;206(5):535-44.
60. Leitao Filho FS, Takiguchi H, Akata K, et al. Effects of Inhaled Corticosteroid/Long-Acting $\beta(2)$ -Agonist Combination on the Airway Microbiome of Patients with Chronic Obstructive Pulmonary Disease: A Randomized Controlled Clinical Trial (DISARM). *Am J Respir Crit Care Med*. 2021;204(10):1143-52.

659 **Tables:**

660 **Table 1:** Baseline characteristics for the recruited children with asthma or wheezing.

Characteristic	All children with microbiota profiles (n = 241)
Age in years, median (IQR)	6.0 (4.0, 13.0)
Female, n (%)	96/241 (40%)
Ethnicity, n (%) <ul style="list-style-type: none"> Caucasian (white) Black African Central Asian East Asian South Asian Arabic North Heritage Multiple Races Other 	192/241 (80%) 11/241 (5%) 6/241 (2%) 2/241 (1%) 2/241 (1%) 6/241 (2%) 18/241 (7%) 4/241 (2%)
Body mass index (BMI) z-score, median (IQR)	0.61 (0.01, 1.42) (n=240)
Asthma/wheezing cohort, n (%) <ul style="list-style-type: none"> Cohort A (severe school-age asthma) Cohort B (mild-to-moderate school-age asthma) Cohort C (severe preschool wheezing) Cohort D (mild-to-moderate preschool wheezing) 	86/241 (36%) 39/241 (16%) 65/241 (27%) 51/241 (21%)
Overall atopic sensitization [¶] , n (%)	159/226 (70%)
Asthma control (well-controlled) [#] , n (%)	72/181 (40%)
Quality of life (QOL) score-average, median (IQR)	5.30 (3.70, 6.47) (n=238)
Lung function test, median (IQR) <ul style="list-style-type: none"> FEV₁ % predicted pre-salbutamol FEV₁ % predicted post-salbutamol FE_{NO} (in ppb) 	92.9 (81.6, 106.7) (n=135) 103.5 (92.6, 113.0) (n=143) 30.0 (15.6, 57.0) (n=117)
Asthma medications, n (%) <ul style="list-style-type: none"> ICS SABA 	212/241 (88%) 227/241 (94%)

<ul style="list-style-type: none"> • LABA • OCS (maintenance) • SAMA • LAMA • LTRA • Nasal steroids 	137/241 (57%) 40/241 (17%) 15/241 (6%) 3/241 (1%) 143/241 (59%) 18/241 (7%)
Antibiotics intake, n (%)	
<ul style="list-style-type: none"> • Antibiotics (recent) • Antibiotics (recent & previous) 	30/241 (12%) 36/241 (15%)

Categorical variables are described as n (% of n), and continuous variables as median (interquartile range, (IQR)). BMI: body mass index, FEV₁: forced expiratory volume in 1 second, FE_{NO}: fractional exhaled nitric oxide, ICS: inhaled corticosteroids, LTRA: leukotriene antagonist, SABA: short-acting beta-agonist, SAMA: short-acting muscarinic antagonists, LABA: long-acting beta-agonist, LAMA: long-acting muscarinic antagonists, OCS: oral corticosteroids, ppb: part per billion, QOL: quality of life. For continuous measures (variables), the number of samples (n=) available for a specific measure is only provided when missing data were present. ¶ Overall atopic sensitization refers to atopic sensitization to aero- or food-allergens by either a positive skin prick test (wheal diameter ≥3mm) and/or a positive allergen-specific IgE (≥0.35kU/L) # A (childhood) asthma control test score >19 indicates well-controlled school-age asthma or preschool-age wheezing.

671 **Table 2:** Demographic and clinical characteristics of the oropharyngeal taxa-driven clusters.

Characteristic	Cluster 1 (n = 50)	Cluster 2 (n = 88)	Cluster 3 (n = 21)	Cluster 4 (n = 82)	P-value
Demographics					
Age in years, median (IQR)	5.0 (3.3-13.0)	9.5 (4.8-13.0)	5.0 (3.0-12.0)	5.0 (3.3-12.0)	0.144
Female, n (%)	21/50 (42%)	38/88 (43%)	5/21 (24%)	32/82 (39%)	0.430
Ethnicity, n (%)					0.427
• Caucasian (white)	44/50 (88%)	64/88 (73%)	19/21 (90%)	65/82 (79%)	
• Black African	0/50 (0%)	4/88 (5%)	1/21 (5%)	6/82 (7%)	
• Central Asian	2/50 (4%)	3/88 (3%)	0/21 (0%)	1/82 (1%)	
• East Asian	1/50 (2%)	0/88 (0%)	0/21 (0%)	1/82 (1%)	
• South Asian	0/50 (0%)	0/88 (0%)	0/21 (0%)	2/82 (2%)	
• Arabic North Heritage	1/50 (2%)	4/88 (5%)	0/21 (0%)	1/82 (1%)	
• Multiple Races	2/50 (4%)	11/88 (12%)	1/21 (5%)	4/82 (5%)	
• Other	0/50 (0%)	2/88 (2%)	0/21 (0%)	2/82 (2%)	
Body mass index (BMI) z-score, median (IQR)	0.59 (-0.12-1.01) (n=49)	0.77 (0.05-1.77) (n=88)	0.27 (0.10-1.08) (n=21)	0.61 (0.02-1.15) (n=82)	0.544
Delivery mode (C-section), n (%)	12/50 (24%)	25/88 (28%)	3/21 (14%)	18/82 (22%)	0.335
Smoking history, n (%)					
• Maternal smoking during pregnancy	5/50 (10%)	13/86 (15%)	2/20 (10%)	6/82 (7%)	0.453
• Second hand smoking	12/50 (24%)	18/85 (21%)	4/21 (19%)	11/79 (14%)	0.494
• Cotinine present (in urine)	4/43 (9%)	10/74 (14%)	2/20 (10%)	8/74 (11%)	0.911
Clinical characteristics					
Asthma/wheezing cohort, n (%)					0.057
• Cohort A (severe school-age asthma)	13/50 (26%)	39/88 (44%)	5/21 (24%)	29/82 (35%)	

<ul style="list-style-type: none"> • Cohort B (mild-to-moderate school-age asthma) • Cohort C (severe preschool wheezing) • Cohort D (mild-to-moderate preschool wheezing) 	10/50 (20%)	16/88 (18%)	4/21 (19%)	9/82 (11%)	
	15/50 (30%)	20/88 (23%)	10/21 (48%)	20/82 (24%)	
	12/50 (24%)	13/88 (15%)	2/21 (10%)	24/82 (29%)	
History of diagnosed allergic disorders (ever), n (%)					
<ul style="list-style-type: none"> • Atopic dermatitis (ever), n (%) • Allergic rhinitis (ever), n (%) 	24/50 (48%) 23/46 (50%)	68/87 (78%) 42/82 (51%)	13/21 (62%) 12/21 (57%)	55/81 (68%) 34/78 (44%)	0.003 0.633
Asthma control (well-controlled) [#] , n (%)	18/38 (47%)	24/72 (33%)	8/13 (62%)	22/58 (38%)	0.188
Quality of life (QOL) score-average, median (IQR)	5.4 (4.1-6.7) (n=50)	5.3 (3.3-6.4) (n=86)	5.3 (4.6-6.4) (n=21)	5.2 (3.7-6.5) (n=81)	0.853
Lung function test, median (IQR)					
<ul style="list-style-type: none"> • FEV₁ % predicted pre-salbutamol • FEV₁ % predicted post-salbutamol • FE_{NO} (in ppb) 	97.5 (86.6-108.1) (n=28) 108.7 (95.9-117.5) (n=29) 43.0 (13.5-58.3) (n=20)	88.9 (74.3-99.31) (n=55) 98.3 (88.8-107.7) (n=59) 29.0 (16.0-50.0) (n=53)	96.3 (87.7-108.8) (n=11) 107.2 (104.2-118.3) (n=10) 35.0 (14.0-97.0) (n=9)	95.5 (87.0-106.9) (n=41) 102.9 (94.1-109.9) (n=45) 27.0 (14.5-58.0) (n=35)	0.108 0.047 0.954
Asthma/other mediations, n (%)					
<ul style="list-style-type: none"> • ICS • SABA • LABA • OCS (maintenance) • SAMA • LAMA • LTRA 	43/50 (86%) 48/50 (96%) 25/50 (50%) 6/50 (12%) 4/50 (8%) 1/50 (2%) 24/50 (48%)	80/88 (91%) 85/88 (97%) 56/88 (64%) 14/88 (16%) 6/88 (7%) 0/88 (0%) 58/88 (66%)	20/21 (95%) 19/21 (90%) 11/21 (52%) 5/21 (24%) 0/21 (0%) 0/21 (0%) 13/21 (62%)	69/82 (84%) 75/82 (91%) 45/82 (55%) 15/82 (18%) 5/82 (6%) 2/82 (2%) 48/82 (59%)	0.390 0.422 0.406 0.623 0.670 0.503 0.235

• Nasal steroids	3/50 (6%)	9/88 (10%)	0/21 (0%)	6/82 (7%)	0.415
Antibiotics intake, n (%)					
• Antibiotics (recent)	7/50 (14%)	9/88 (10%)	2/21 (10%)	12/82 (15%)	0.803
• Antibiotics (recent & previous)	7/50 (14%)	10/88 (11%)	4/21 (19%)	15/82 (18%)	0.600

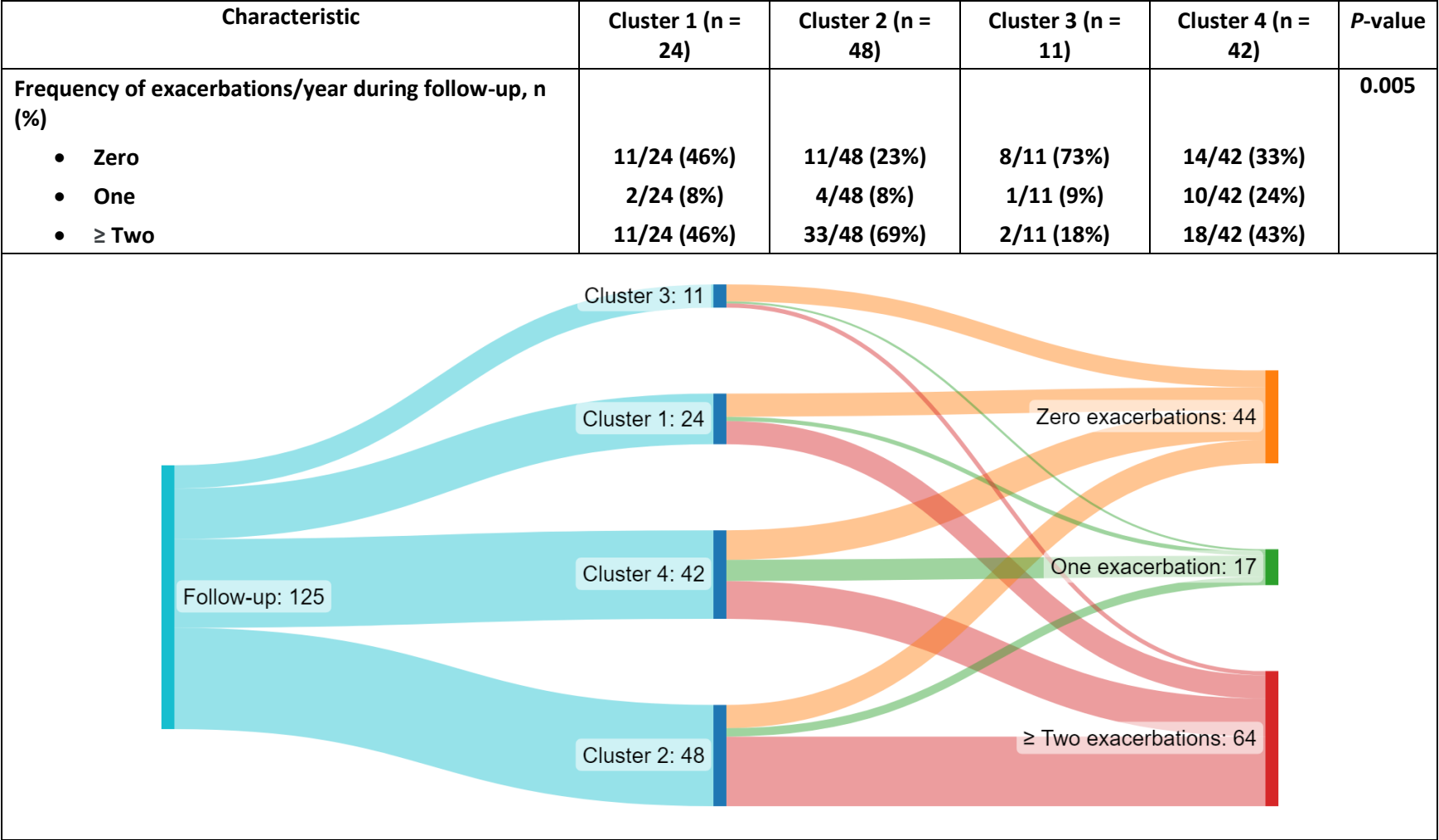
Categorical variables are described as n (% of n), and continuous variables as median (interquartile range, (IQR)). BMI: body mass index, FEV₁: forced expiratory volume in 1 second, FE_{NO}: fractional exhaled nitric oxide, ICS: inhaled corticosteroids, LTRA: leukotriene antagonist, SABA: short-acting beta-agonist, SAMA: short-acting muscarinic antagonists, LABA: long-acting beta-agonist, LAMA: long-acting muscarinic antagonists, OCS: oral corticosteroids, ppb: part per billion, QOL: quality of life. For continuous measures (variables), the number of samples (n=) available for a specific measure is only provided when missing data were present. P-values were calculated by a Pearson's Chi-square test with Monte Carlo simulation (10000 permutations) or by a Kruskal-Wallis h test as appropriate. # A (childhood) asthma control test score >19 indicates well-controlled school-age asthma or preschool-age wheezing.

682 **Table 3:** Characteristics of atopic sensitization among the 4 taxa-driven clusters.

Characteristic	Cluster 1 (n = 50)	Cluster 2 (n = 88)	Cluster 3 (n = 21)	Cluster 4 (n = 82)	P-value
Overall atopic sensitization[¶], n (%)	25/47 (53%)	65/83 (78%)	13/18 (72%)	56/78 (72%)	0.022
Common aeroallergens sensitization, n (%)	25/47 (53%)	62/83 (75%)	13/18 (72%)	46/78 (59%)	0.045
Common aeroallergens, n (%)					
• House dust mites	19/46 (41%)	46/81 (57%)	11/17 (65%)	31/77 (40%)	0.068
• Tree	17/46 (37%)	33/79 (42%)	6/16 (38%)	21/70 (30%)	0.522
• Mold	6/43 (14%)	27/78 (35%)	4/16 (25%)	19/71 (27%)	0.111
• Grass	13/46 (28%)	45/81 (56%)	8/18 (44%)	29/74 (39%)	0.021
• Pet animal (cat/dog)	22/46 (48%)	52/81 (64%)	7/18 (39%)	36/75 (48%)	0.079
Number of aeroallergen classes, median (IQR)	0.0 (0.0-3.0) (n=47)	3.0 (1.0-4.00) (n=83)	1.5 (0.0-3.8) (n=18)	1.0 (0.0-3.0) (n=78)	0.021
Total IgE (in kU/L), median (IQR)	292.6 (54.7-924.7) (n=38)	245.1 (95.8-1,002.5) (n=76)	105.0 (52.8-310.0) (n=17)	150.0 (38.9-682.3) (n=68)	0.240

683 Categorical variables are described as n (% of n), and continuous variables as median (interquartile range, (IQR)). ¶ Overall atopic sensitization
684 refers to sensitization to either aero- and/or food-allergens by either a positive skin prick test (wheal diameter ≥3mm) and/or a positive allergen-
685 specific IgE (≥0.35kU/L). P-values were calculated by a Pearson's Chi-square test with Monte Carlo simulation (10000 permutations) or by a
686 Kruskal-Wallis H test as appropriate.

687 **Table 4:** Baseline microbiota cluster assignments and the frequency of exacerbations per year during follow-up (12-18 months after baseline
688 visit).



689 Lower panel shows Sankey diagram for Baseline microbiota cluster assignments and frequency of exacerbations/year during follow-up.

Box 1: Summary overview of the clinical characteristics of the taxa-driven clusters.

Cluster 1

Cluster 1 included 50 (20.7%) patients. Cluster 1 had the least children with atopic dermatitis diagnosis ($n=24/50$, 48%, post-hoc $p = 0.001$), the least children with atopic sensitization ($n=25/47$, 53%, post-hoc $p = 0.003$) particularly to grass pollens ($n=13/46$, 28%, post-hoc $p = 0.020$), and had the lowest median number of the aeroallergens sensitizations (median = 0, IQR (0-3)) compared with the other clusters (all $ps < 0.05$). Generally, patients within Cluster 1 showed the lowest median ESs of blood transcriptomic signatures related to the Wnt/ β -Catenin ($p < 0.001$, $q < 0.01$), the TGF- β signaling ($p < 0.01$, $q < 0.05$) and the myogenesis ($p < 0.05$, $q > 0.05$) MSigDB hallmark pathways.

Cluster 2

Cluster 2 was the largest cluster and included 88 patients (36.5%). Cluster 2 included older school-aged asthmatics (median age=9.5, IQR (4.8-13.0)), and exhibited the highest percentage of school-age severe asthmatics ($n=39/88$, 44%, post-hoc $p = 0.034$) compared with the other clusters (median age = 5), however; neither differences were statistically significant at overall clusters' level ($p = 0.144$ and 0.057 , respectively). Cluster 2 showed the highest percentage of atopic dermatitis diagnosis ($n=68/87$, 78%, post-hoc $p = 0.005$), the highest percentage of atopic sensitization to aeroallergens particularly grass pollens ($n=45/81$, 56%, post-hoc $p = 0.005$), and had highest median number of the aeroallergens sensitizations (median = 3, IQR (1-4)) compared with the other clusters. In addition, Cluster 2 had the lowest median values of FEV₁ % predicted values post-bronchodilator (median=98.3, IQR (88.8-107.7)) and had the highest percentage of children with severe symptoms who experienced future exacerbations ($n=37/48$, 77%), particularly ≥ 2 future exacerbations/year ($n=33/48$, 69%, post-hoc $p = 0.002$) during the follow-up period (all $ps < 0.05$). This Cluster showed the relatively highest median ESs of TGF- β signaling MSigDB hallmark pathway ($p < 0.01$, $q < 0.05$).

Cluster 3

Cluster 3 was the smallest cluster and included 21 patients (8.7%). This cluster had the highest percentage of preschoolers with severe wheezing ($n=10/21$, 48%, post-hoc $p = 0.026$) compared with the other clusters, however; this difference was not statically significant at the overall clusters' level ($p = 0.057$). This cluster had a significantly higher median values of FEV₁ % predicted post-bronchodilator compared with Cluster 2 (median 107.2, IQR (104.2-118.3), and 98.3 IQR (88.8-107.7), respectively, $p < 0.05$), and had the highest percentage of children with severe symptoms ($n=8/11$, 73%, post-hoc $p = 0.006$) who did not experience any future exacerbations during the follow-up period.

Cluster 4

Cluster 4 was the second-largest cluster and included 82 patients (34%). This cluster included the second-highest percentage of children with severe symptoms ($n=28/42$, 67%) who experienced future exacerbations and particularly included the highest percentage of children with severe symptoms who experienced one exacerbation/year ($n=18/42$, 24%, post-hoc $p = 0.018$) during the follow-up period compared with the other clusters ($p < 0.05$). This cluster showed the relatively highest median ESs of the Wnt/ β -Catenin signaling and second-highest median ESs of the TGF- β signaling MSigDB hallmark pathways (all $ps < 0.01$, $q < 0.05$).

690

691

Figure Legends:

Figure 1: A; Hierarchical agglomerative cluster dendrogram of the Bray-Curtis dissimilarities showing the 4 main children groups. **B;** Principal component plot of the clustering by partition around the medoids (PAM) shows 4 relatively detached 95% reference intervals ellipses of 4 children groups. The similarity in participants' assignment between the two clustering algorithms was assessed by Rand index (RI= 0.85) and Pearson Chi-Square test ($\chi^2= 498.1$, $p < 1 \times 10^{-4}$) showing high similarity in the clustering assignments. For assessing clusters stability, replacement of points by noise schemes (1000 iterations) resulted in mean Jaccard similarity indices ranging from 0.74-1 for the 4 clusters by either hierarchical clustering or PAM suggesting relatively stable clusters.

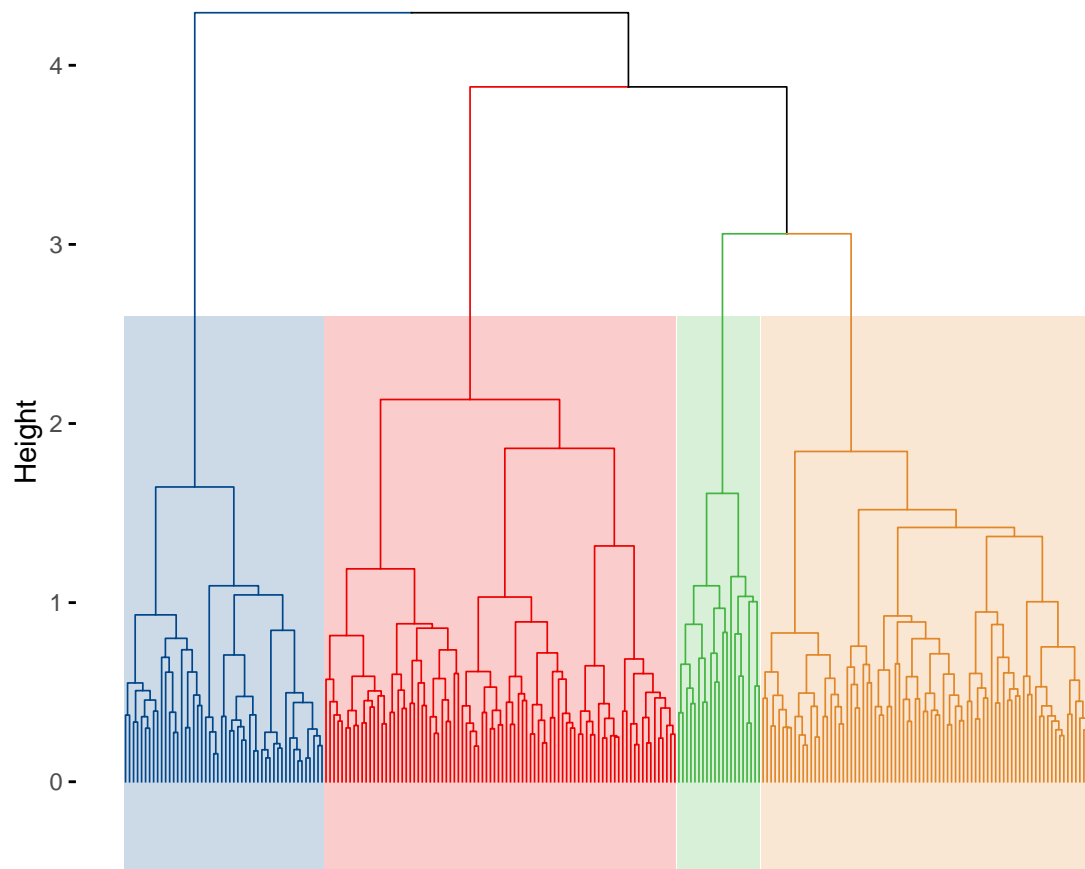
Figure 2: Differentially abundant bacterial taxa between the taxa-driven clusters using the Linear discriminant analysis Effect Size (LEfSe) statistical method. The highest enriched bacterial taxa related to each cluster are shown at phylum (**A**) and species (**B**) levels. Only differentially abundant bacterial species with an FDR q -value < 0.01 and an absolute LDA score > 2 are depicted.

Figure 3: Box-and-whisker plots showing the enrichment scores of the Molecular Signatures Database (MSigDB) gene sets between the taxa-driven clusters. Only the statistically significant gene sets are shown, and those passing the multiple testing threshold (q -value < 0.05) are shown in bold-face. Overall P -values were generated by the Kruskal-Wallis H test and pairwise P -values were generated by Dunn's post-hoc test.

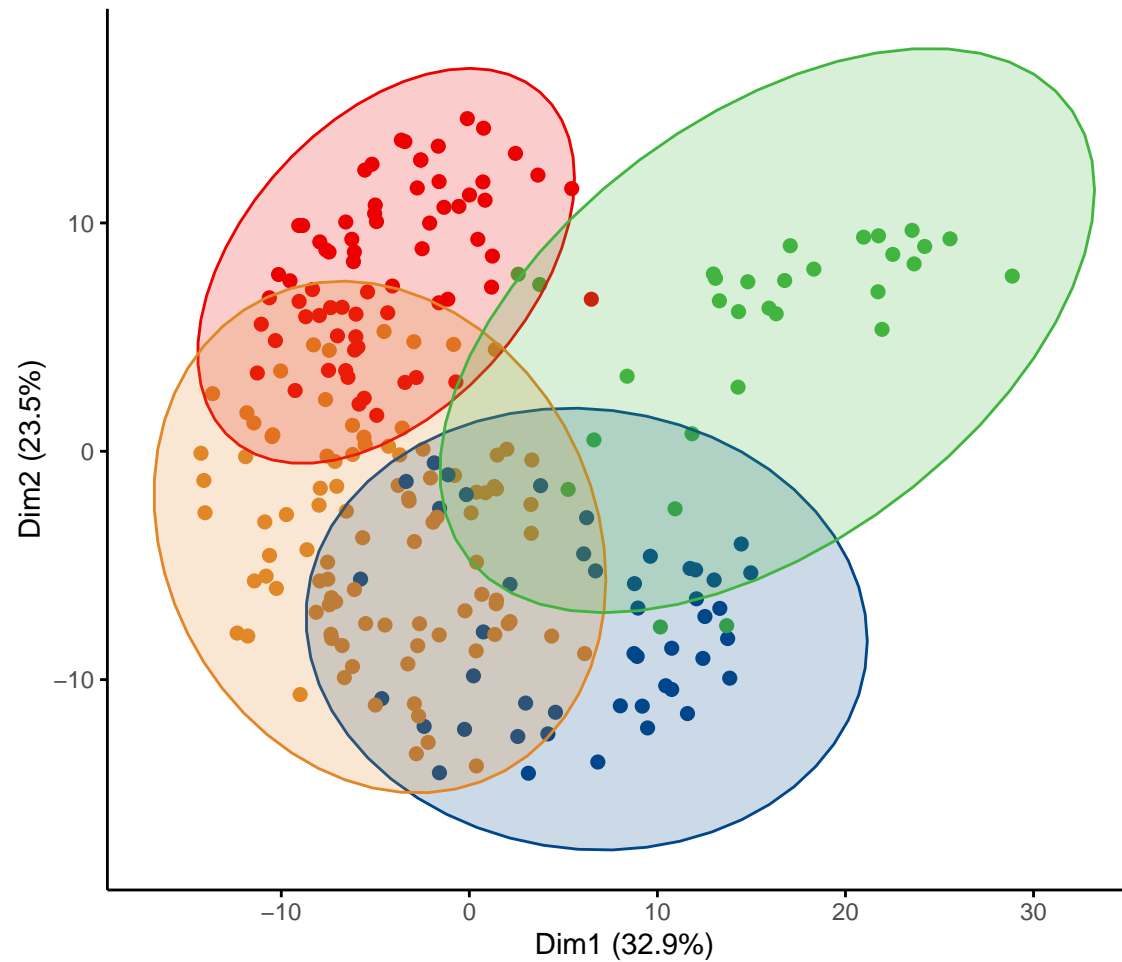
Figure 1

Clusters ■ Cluster 1 ■ Cluster 2 ■ Cluster 3 ■ Cluster 4

(A)



(B)



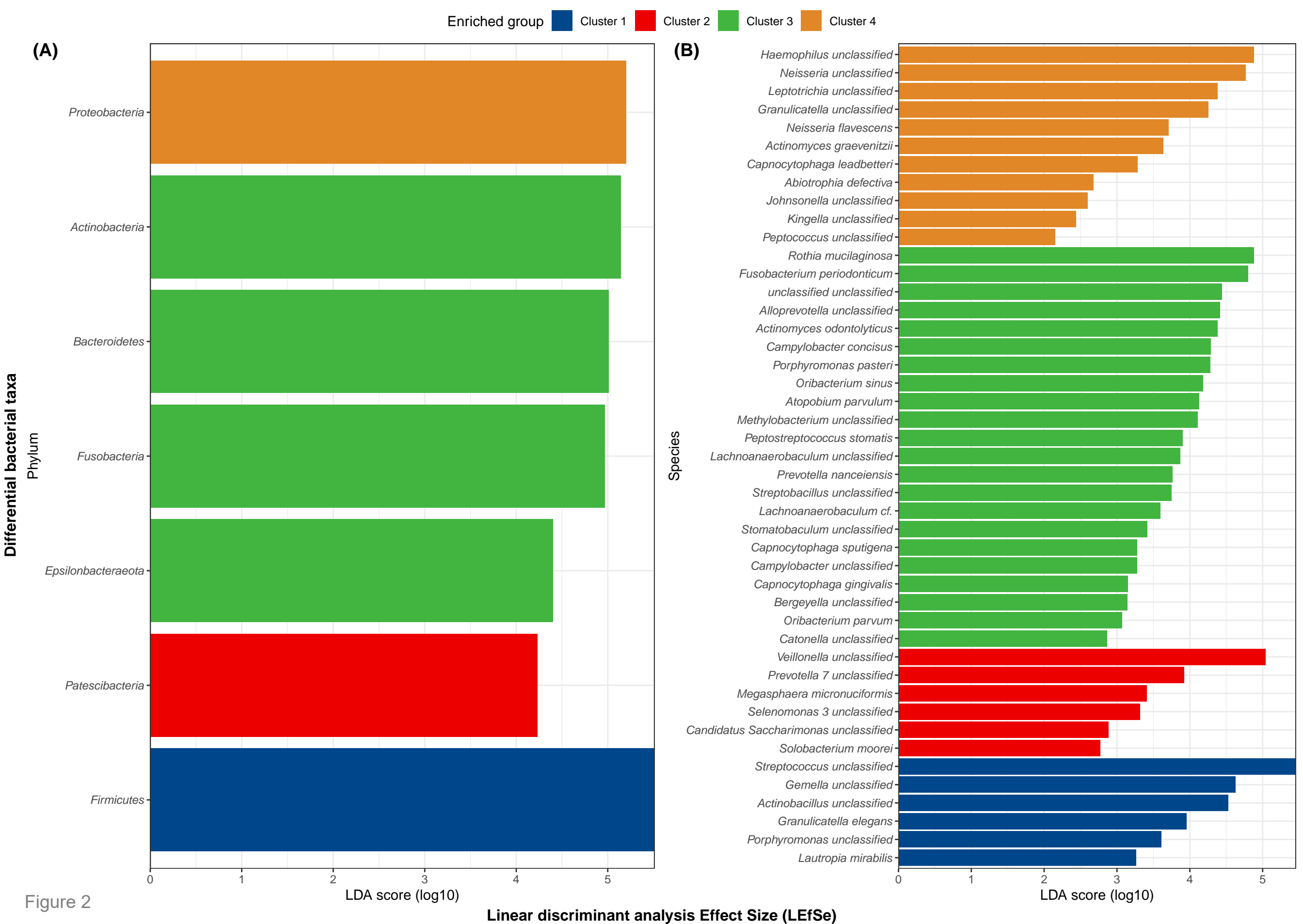




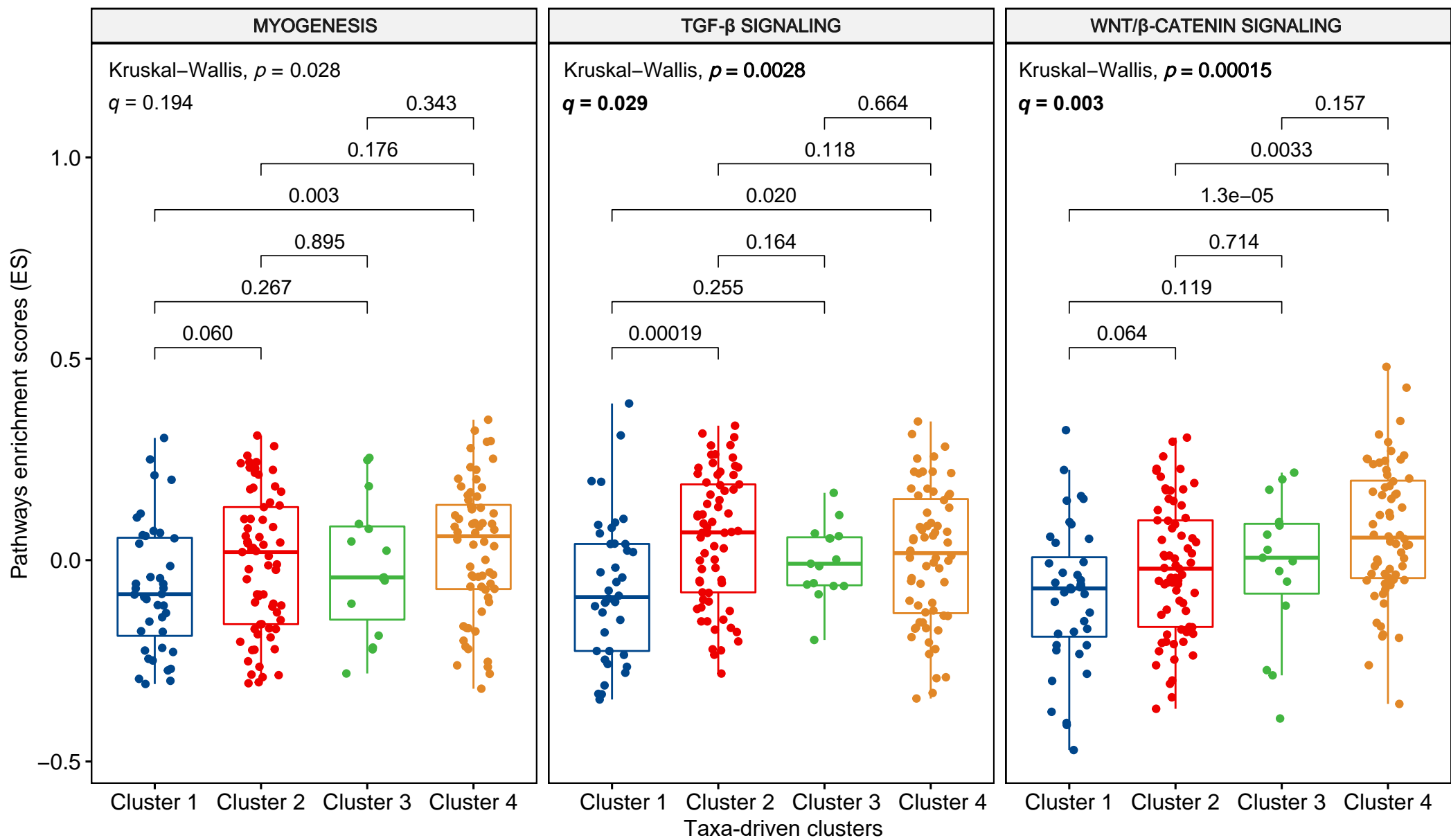


Figure 3

Clusters  Cluster 1  Cluster 2  Cluster 3  Cluster 4



Online data supplement

Oropharyngeal microbiota clusters in children with asthma/wheeze associate with allergy, blood transcriptomic immune pathways and exacerbations risk

Mahmoud I. Abdel-Aziz, PhD^{1,2,3,4}; Jonathan Thorsen, MD, PhD^{5,6}; Simone Hashimoto, MD, PhD^{1,2,3,7}; Susanne J. H. Vijverberg, PhD^{1,2,3}; Anne H. Neerincx, PhD^{1,2,3}; Paul Brinkman, PhD^{1,2,3}; Wim van Aalderen, MD, PhD⁷; Jakob Stokholm, MD, PhD^{5,8}; Morten Arendt Rasmussen, MD, PhD^{5,8}; Michael Roggenbuck-Wedemeyer, MD, PhD^{9,10}; Nadja H. Vissing, MD, PhD⁵; Martin Steen Mortensen, PhD⁹; Asker Daniel Brejnrod, PhD¹¹; Louise J. Fleming, MD¹²; Clare S. Murray, MD¹³; Stephen J. Fowler, MD, PhD¹³; Urs Frey, MD, PhD¹⁴; Andrew Bush, MD, FRCP, FRCPC¹²; Florian Singer, MD, PhD¹⁵; Gunilla Hedlin, MD, PhD¹⁶; Björn Nordlund, RN, PhD¹⁶; Dominick E. Shaw, PhD¹⁷; Kian Fan Chung, MD, DSc¹²; Ian M. Adcock, PhD¹²; Ratko Djukanovic, MD, PhD¹⁸; Charles Auffray, PhD¹⁹; Aruna T. Bansal, PhD²⁰; Ana R. Sousa, PhD²¹; Scott S. Wagers, MD, PhD²²; Bo Lund Chawes, MD, PhD⁶; Klaus Bønnelykke, MD, PhD⁶; Søren Johannes Sørensen, PhD⁹; Aletta D. Kraneveld PhD²³; Peter J. Sterk, MD, PhD^{1,2}; Graham Roberts, DM¹⁸; Hans Bisgaard, MD, PhD⁵; Anke H. Maitland-van der Zee, PharmD, PhD^{1,2,3,7}; on behalf of the U-BIOPRED Study Group.

1 Department of Pulmonary Medicine, Amsterdam UMC, University of Amsterdam, 1105 AZ Amsterdam, the Netherlands.

2 Amsterdam Institute for Infection and Immunity, Amsterdam, the Netherlands.

3 Amsterdam Public Health, Amsterdam, the Netherlands.

4 Department of Clinical Pharmacy, Faculty of Pharmacy, Assiut University, 71526 Assiut, Egypt.

5 COPSAC, Copenhagen Prospective Studies on Asthma in Childhood, Herlev and Gentofte Hospital, University of Copenhagen, Copenhagen, Denmark.

6 Novo Nordisk Foundation Center for Basic Metabolic Research, Faculty of Health and Medical Sciences, University of Copenhagen, Copenhagen, Denmark.

24 7 Department of Paediatric Pulmonary Medicine, Emma Children's Hospital, Amsterdam UMC, University of
 25 Amsterdam, 1105 AZ Amsterdam, the Netherlands.

26 8 Department of Food Science, University of Copenhagen, Frederiksberg, Denmark.

27 9 Section of Microbiology, Department of Biology, University of Copenhagen, Copenhagen, Denmark.

28 10 Novozymes, Bagsvaerd, Denmark.

29 11 Section of Bioinformatics, Department of Health Technology, Technical University of Denmark, Lyngby,
 30 Denmark.

31 12 National Heart and Lung Institute, Imperial College London, and Royal Brompton and Harefield NHS Trust,
 32 London, United Kingdom.

33 13 Division of Infection, Immunity and Respiratory Medicine, School of Biological Sciences, Faculty of Biology,
 34 Medicine and Health, University of Manchester, and Manchester Academic Health Science Centre and NIHR
 35 Biomedical Research Centre, Manchester University Hospitals NHS Foundation Trust, Manchester, United Kingdom.

36 14 University Children's Hospital Basel, University of Basel, Basel, Switzerland.

37 15 Division of Paediatric Pulmonology and Allergology, Department of Paediatrics and Adolescent Medicine,
 38 Medical University of Graz, Austria & Division of Paediatric Respiratory Medicine and Allergology, Department of
 39 Paediatrics, Inselspital, Bern University Hospital, University of Bern, Switzerland.

40 16 Astrid Lindgren Children's Hospital, Karolinska University Hospital, and Department of Women's and Children's
 41 Health, Karolinska Institutet, Stockholm, Sweden.

42 17 NIHR Respiratory Biomedical Research Unit, University of Nottingham, Nottingham, United Kingdom. 18 NIHR
 43 Southampton Biomedical Research Centre, University Hospital Southampton NHS Foundation Trust and Clinical and
 44 Experimental Sciences and Human Development and Health, University of Southampton, Southampton, United
 45 Kingdom.

46 19 European Institute for Systems Biology and Medicine, CIRI UMR5308, CNRS-ENS-UCBL-INSERM, Lyon, France.

47 20 Acclarogen Ltd, St John's Innovation Centre, Cambridge, United Kingdom.

48 21 Respiratory Therapeutic Unit, GlaxoSmithKline, Stockley Park, United Kingdom.

49 22 BioSci Consulting, Maasmechelen, Belgium.

50 23 Division of Pharmacology, Utrecht Institute for Pharmaceutical Sciences, Faculty of Science, Utrecht University,
51 Utrecht, the Netherlands.

Atopy

Atopy was defined as a positive skin prick test (SPT) defined by a wheal diameter ≥ 3 mm and/or a positive allergen-specific IgE ≥ 0.35 kU/L to a pre-specified allergen list. Skin prick testing was done using single headed lancet and positive (histamine 10 mg/ml) and negative (saline) controls (ALK-Abello, Horsholm, Denmark) as previously described [1]. All sites tested to the most common aeroallergens, namely house dust mite (mixture of *Dermatophagoides pteronyssinus* and *Dermatophagoides farinae*), animals (cat and dog), grass pollen mixture, tree pollen mixture and mold (*aspergillus*). Up to three additional allergens, such as cockroach and *Olea europea* and *Parietaria* were performed where relevant to a specific centre. Allergen-specific IgE testing was measured for the above-listed most common aeroallergens (Thermo Fisher, Uppsala, Sweden).

Samples collection and omics analysis

Oropharyngeal swabs and 16S gene V4 microbiome sequencing

A single oropharyngeal (throat) swab was collected from the posterior pharyngeal wall, behind the uvula, of each subject by research assistants using dry flocced swabs (ESwab, BD, NJ, USA). The swabs were placed in a Liquid Amies transport medium and stored at -20°C for further processing. Genomic FastDNA™ SPIN Kit for Soil (MP Biomedicals, Santa Ana, CA, USA) was used for DNA extraction and DNA extracts were checked by gel electrophoresis for consistency and quality. A two-step PCR process was implemented to amplify the 16S ribosomal RNA (rRNA) by targeting the hypervariable V4 region by primers (515F: 5'-GTGCCAGCMGCCGCGGTAA and 806R: 5'-GGACTACHVGGGTWTCTAAT) and normalization for amplicon contents was performed before undergoing sequencing. Sequencing was done using the Illumina MiSeq Desktop Sequencer (Illumina Inc., CA, USA) as described previously [2]. Paired-end reads (250 bp x 2) were pooled for subsequent quality control and bioinformatics processing. The quality of the sequence reads were checked using FastQC [3] and MultiQC [4]. Primers were

75 removed using Cutadapt [5]. The dada2 pipeline was used to quantify the Amplicon Sequence Variants
76 (ASVs) as described in detail previously [6]. Briefly, the pipeline works by performing quality filtering and
77 trimming, dereplicating sequences, learning dataset-specific error rates, denoising by removing
78 potentially containing errors sequences, merging paired-end reads while removing mismatches to reduce
79 errors, constructing amplicon sequence variants (ASVs), removing chimera, and running taxonomic
80 classification of ASVs using different publicly available databases. During the trimming and filtering step
81 of the forward and reverse sequencing reads, quartiles of the quality score distribution of nucleotide
82 positions were inspected. Parameters for the reads filtering were used as follows; truncQ=2 (truncate
83 reads at the first instance of a quality score less than or equal to 2), maxEE=5 (reads with higher than 5
84 expected errors will be discarded), and rm.phix=TRUE (discard reads that match against the phiX genom).
85 Then, learning of the error rates was performed. The estimated error rates were in a good fit to the
86 observed rates, and the error rates dropped with increased quality as expected [6]. Afterwards, the,
87 forward and reverse reads were merged using the default parameters in dada2 (minimum length of
88 overlap=20 nucleotides, and maximum nucleotides mismatches=0). Subsequently, chimeric sequences
89 were removed by implementing the Bimera method (removeBimeraDenovo function in dada2). Fourteen
90 % of the total sequences were identified as chimera and subsequently removed from the final identified
91 ASVs table. Finally, taxonomy of the identified ASVs was annotated using the Ribosomal Database Project
92 (RDP) Naive Bayesian Classifier algorithm [7] implemented in dada2 using the default parameters
93 (minimum bootstrap confidence for assigning a taxonomic level=50) against the Silva database version
94 132 [8]. Negative extraction (sterile water) and positive (mock community, BEI Resources, NIAID, NIH)
95 controls were added to each plate (sequencing run) as previously described [2], and checked against real
96 samples by comparing Shannon α -diversity (using Mann-Whitney U test) and by relative abundance
97 plots. As a sanity check, a statistical method to remove potentially contaminant sequences (decontam R

package) [9] was used to filter the ASVs table (using the prevalence method) before downstream statistical analysis.

Blood collection and transcriptomics analysis

Peripheral blood samples were collected and RNA was isolated using the PAXgene Blood RNA kit (PreAnalytiX, Hombrechtikon, Switzerland) including on-column DNase treatment (QIAGEN, Valencia, CA) and stored for further processing. A 2100 Bioanalyzer (Agilent Technologies, Santa Clara, CA) was used to assess RNA integrity, by which samples with an RNA integrity number ≥ 6 were further processed for gene expression analysis. Microarray gene expression was done by hybridization onto Affymetrix HT HG-U133+ PM arrays according to Affymetrix technical protocols using a GeneTitan Instrument (Affymetrix, Santa Clara, CA). The microarray data are deposited in the Gene Expression Omnibus database (accession number: GSE123750).

Raw microarray data (as .CEL files) were quality assessed and pre-processed by robust multi-array average normalization (RMA) method (10) as implemented in the affy R package. Probes of low expression were filtered by robust multi-array signal analysis for values < 5 and also for batch/technical effects. The intensity of the raw probe sets were background corrected and quantile-normalized by the robust RMA (rma()) function in the affy R package, using the following parameters normalize = TRUE and background = TRUE), and log base 2 transformed, followed by z-scoring the values.

Data analysis

The general data analysis workflow is shown in Figure E2.

Clustering protocol

A benchmarking clustering strategy was performed based on the approach utilized previously [10]. The Bray-Curtis β -diversity dissimilarity measure was computed on the relative abundances of the amplicon

sequence variants (ASVs) to assess the within-participants overall variability in the microbiota profiles.

An agglomerative hierarchical Ward2 clustering algorithm was applied [11] and the optimum number of

clusters was determined based on the majority vote of 4 statistical measures, namely; average

silhouettes width [12], the total within-cluster sum of square (WCSS) [13], Calinski-Harabasz [14], and

Hubert and Levin C [15] indices. Cluster assignment of the participants was internally validated by using

partition around the medoids (PAM) [16]. Agreement in the clustering of participants' assignments

between hierarchical Ward, and PAM clustering was quantified by means of Pearson Chi-Square test

with Monte Carlo simulation (10000 permutations) and Rand index (ranges from 0 to 1, indicating no

agreement to high agreement, respectively) [17]. The clusters were visualized in two-dimensional space

by the non-metric multidimensional scaling (MDS) and principal co-ordinate analysis (PCoA) on the Bray-

Curtis dissimilarity measure, in which the 95% confidence ellipses were depicted. Clustering was further

validated using topological data analysis (TDA) mapper tmap [18]. In tmap-TDA analysis, the density-

based spatial clustering algorithm (DBSCAN) was utilized (optimum epsilon was calculated using the

optimize_dbscan_eps function in tmap, resolution was selected=20 and % overlap=65, and lenses were

computed using MDS and PCoA analysis on Bray-Curtis dissimilarity measure). The spatial analysis of

functional enrichment (SAFE) scores were calculated to quantify the enrichment level of the clusters'

assignments of samples belonging to the subnetwork centered around the node (SAFE scores were

calculated by network permutation of 5000 times) as described in detail previously [18]. The nodes in the

generated TDA network were then colored according to the SAFE scores of the clusters' assignments.

Cluster-wise stability of the hierarchical and PAM clusters was evaluated by replacement of points by

noise (1000 iterations) with subsequent calculation of the Jaccard similarity index [19].

Statistical analysis

The differential microbiota profiles shaping the revealed clusters were evaluated by looking at relative abundances plots of the microbiota. The Linear discriminant analysis Effect Size (LEfSe) was used to reveal the main differentially abundant taxa between the clusters at phylum and species levels [20] after adjusting by multiple testing by Benjamini Hochberg false discovery rate (FDR) [21], where an absolute linear discriminant analysis (LDA) score >2 and FDR q -value <0.01 were used as cut-offs for significance. Similarly, the top enriched taxa by the SAFE algorithm in TDA analysis were depicted in the TDA map to check concordance with the LEfSe method revealed top differential bacterial taxa. Finally, to reveal whether a minimal set of the differential bacterial taxa could be used to guide the participants' stratification, an inference decision tree was built on the bacterial relative abundances to predict the clusters assignment. The minimum set of taxa was determined based on the LEfSe method, by selecting the top enriched taxa in each cluster (based on highest LDA score), resulting in 4 main bacterial genera that were used as input for the inference decision tree. The data were randomly divided into 75:25%, training and validation sets, respectively. A five-fold cross-validated model (using ctree2 method) was built on the training dataset (hyper-parameters tuning was based on a grid; tuneLength=100, maxdepth=1:50, and mincriterion=0.95 and 0.99). The performance of the model was tested on the left-out validation set by calculating accuracy (95% CI).

Patient cluster distribution according to the inclusion center and season of sample collection (metrological system) and differences in participants' demographic and clinical characteristics between the revealed clusters were compared using Pearson Chi-Square test with Monte Carlo simulation (10000 permutations) or Kruskal Wallis H test tests as appropriate. Results are considered significant at alpha level < 0.05 . If the overall p-value of a Kruskal-Wallis H test was significant (<0.05), a post-hoc Dunn's test was performed. If the overall p-value of a Pearson Chi-Square test was significant (<0.05), a post-hoc

analysis based on the residuals was done as previously described [22]. In addition, logistic and linear regression models were used to investigate whether the clinical characteristics of interest are dependent on the participants' clusters assignments after adjusting for multiple covariates, including age, sex, ethnicity, BMI z-scored, center and season of inclusion, inhaled, oral and nasal corticosteroids intake, reported recent antibiotic intake and potential technical covariates (library size, extraction plate ID; 2 plates, and sequencing run; 2 runs). As a first step, all covariates were forced into the regression models and the microbiota-clusters were checked whether they are significantly associated with the clinical characteristics of interest after adjusting for all other covariates. If the microbiota clusters were found to be significantly associated with clinical characteristics of interest after adjusting for all covariates, a stepwise (backward and forward selection) variable selection process [23] was then implemented in the regression models to reduce the overall model error rate. All covariates (including microbiota-clusters) had similar chance to be selected in the stepwise process. Multiple testing correction for the covariates *P*-values was performed by FDR. Similarly, the cluster assignments of severe children with asthma or wheezing were checked against the frequency of exacerbations during follow-up (using Chi-Square test with Monte Carlo simulation, and with logistic regression after adjusting for covariates). The latter was also depicted visually using a Sankey diagram. A simple mediation analysis was conducted to investigate whether microbiota Cluster 2 is an independent predictor of future asthma exacerbations (≥ 2) or if this is mediated by the atopic dermatitis status. For the mediation analysis, the outcome variable was ≥ 2 exacerbations per year during follow-up, the predictor variable was the microbiota Cluster 2 (reference level was the other clusters), and the mediator variable was atopic dermatitis status. A logistic regression model was conducted to estimate association of the predictor variable into the mediator. A second logistic regression model was conducted to estimate the association of the mediator with the outcome variable in the presence of the predictor variable. Finally, the causal mediation was performed between the two models using the `mediate()` function from the mediation R package (using default parameters),

where the 95% CIs for the estimates were computed by Quasi-Bayesian approximation (1000 simulations). Results of the mediation analysis were reported before and after adjusting for covariates.

Transcriptomic pathway enrichment analysis of the clusters was performed by an unsupervised approach using the gene set variation analysis (GSVA) based on the genes z-scores of the participants against a list of 21 Hallmark gene sets from the Molecular Signatures Database (MSigDB) release version 7.4 [24] that were previously reported to be associated with asthma disease (Table E1). The GSVA R package was used for this analysis (gsva function was utilized using the following parameters, method="gsva", abs.ranking=FALSE, min.sz=10, max.sz=500, rnaseq=FALSE and other parameters by default). The GSVA enrichment scores (ES) of the tested gene sets were compared between the clusters by Kruskal-Wallis H-test and multiple testing was corrected by FDR. Permutation analysis of the significant gene sets (pathways) was performed, in which the gene sets were resampled (10000 times) with random genes of similar size as the initially investigated Hallmark gene sets (i.e. randomly assigning genes to gene sets of similar size n as the hallmark gene sets). Enrichment scores from the randomly generated gene sets were checked for differences among the clusters using the Kruskal Wallis H test. The permutation analysis p-values were calculated using the following equation

$$\frac{\text{sum}(\text{Kruskal-Wallis test statistic of the randomly generated gene sets} \geq \text{the test statistic of the original hallmark gene set}) + 1}{\text{number of permutations} + 1}$$

. This permutation analysis was performed to check the null hypothesis that the significance is due to the presence of non-specific/non-relevant genes randomly present in a gene set. Linear regression models were used to investigate whether the enrichment scores of the significant gene sets are dependent on the participants' clusters assignments after adjusting for multiple covariates, including age, sex, ethnicity, BMI z-scored, site and season of inclusion, atopic sensitization, inhaled, oral and nasal corticosteroids intake, reported recent antibiotic intake and potential technical covariates (library size, extraction plate ID; 2 plates, and sequencing run; 2 runs). As a first step, all covariates were forced into the regression models and the microbiota-clusters were checked whether they are significantly associated with the

213 transcriptomic pathways of interest after adjusting for all other covariates. If the microbiota clusters
214 were found to be significantly associated with the transcriptomic pathways of interest after adjusting for
215 all covariates, a stepwise (backward and forward selection) variable selection process [23] was then
216 implemented in the regression models to reduce the overall model error rate. All covariates (including
217 microbiota clusters) had similar chance to be selected in the stepwise process. Multiple testing
218 correction for the covariates *P*-values was performed by FDR. Assumptions of the linear regression
219 models were checked using the Global Validation of Linear Model Assumptions as previously described
220 [25].

221 All analyses were performed using R studio (version 1.1.453) with R software (version 3.6.1) supported
222 with the following packages: phyloseq (v1.34.0), vegan (v2.6.2), stats (v4.0.3), MASS (v7.3.53), cluster
223 (v2.1.0), factoextra (v1.0.7), fpc (v2.2.9), fossil (v0.4.0), fmsb (v0.7.3), performance (v0.9.1),
224 ResourceSelection (v0.3.5), party (v1.3.9), gvlma (v1.0.0.3), GSVA (v1.40.1), microbiomeMarker
225 (v0.0.1.9000), gtsummary (v1.5.0.9004), qwraps2 (v0.5.2), chisq.posthoc.test (v0.1.2), affy (v1.70.0),
226 mediation (v4.5.0), ggplot2 (v3.3.6), and ggpubr (v0.4.0). TDA was performed in Python (version 3.8.5)
227 using tmap-TDA (v1.2) and scikit-learn (v0.24.1). Directed acyclic graph (DAG) was created using DAGitty
228 (v3.0) web interface tool (www.dagitty.net).

References for supplementary material

1. Dreborg S, Frew A. Position paper: Allergen standardization and skin tests. The European Academy of Allergology and Clinical Immunology. Allergy. 1993;48(14 Suppl):48-82.
2. Mortensen MS, Brejnrod AD, Roggenbuck M, et al. The developing hypopharyngeal microbiota in early life. Microbiome. 2016;4(1):70.
3. Andrews S. FastQC: A Quality Control Tool for High Throughput Sequence Data 2010 [Available from: <http://www.bioinformatics.babraham.ac.uk/projects/fastqc/>].
4. Ewels P, Magnusson M, Lundin S, et al. MultiQC: summarize analysis results for multiple tools and samples in a single report. Bioinformatics. 2016;32(19):3047-8.
5. Martin M. Cutadapt removes adapter sequences from high-throughput sequencing reads. 2011. 2011;17(1):3.
6. Callahan BJ, McMurdie PJ, Rosen MJ, et al. DADA2: High-resolution sample inference from Illumina amplicon data. Nat Methods. 2016;13:581.
7. Wang Q, Garrity GM, Tiedje JM, et al. Naïve Bayesian Classifier for Rapid Assignment of rRNA Sequences into the New Bacterial Taxonomy. Appl Environ Microbiol. 2007;73(16):5261-7.
8. Quast C, Pruesse E, Yilmaz P, et al. The SILVA ribosomal RNA gene database project: improved data processing and web-based tools. Nucleic Acids Res. 2013;41(Database issue):D590-D6.
9. Davis NM, Proctor DM, Holmes SP, et al. Simple statistical identification and removal of contaminant sequences in marker-gene and metagenomics data. Microbiome. 2018;6(1):226.
10. Abdel-Aziz MI, Brinkman P, Vijverberg SJH, et al. Sputum microbiome profiles identify severe asthma phenotypes of relative stability at 12 to 18 months. J Allergy Clin Immunol. 2021;147(1):123-34.
11. Ward JH. Hierarchical Grouping to Optimize an Objective Function. J Am Stat Assoc. 1963;58(301):236-44.

252 12. Rousseeuw PJ. Silhouettes: A graphical aid to the interpretation and validation of cluster
253 analysis. J Comput Appl Math. 1987;20:53-65.

254 13. Hartigan JA. Clustering Algorithms: John Wiley & Sons, Inc.; 1975. 351 p.

255 14. Caliński T, Harabasz J. A dendrite method for cluster analysis. Commun Stat 1974;3(1):1-27.

256 15. Hubert LJ, Levin JR. A general statistical framework for assessing categorical clustering in free
257 recall. Psychological Bulletin. 1976;83(6):1072-80.

258 16. Kaufman L, Leonard Kaufman PJR, Rousseeuw PJ. Finding Groups in Data: An Introduction to
259 Cluster Analysis: Wiley; 1990.

260 17. Rand WM. Objective Criteria for the Evaluation of Clustering Methods. J Am Stat Assoc.
261 1971;66(336):846-50.

262 18. Liao T, Wei Y, Luo M, et al. tmap: an integrative framework based on topological data analysis for
263 population-scale microbiome stratification and association studies. Genome Biol. 2019;20(1):293.

264 19. Hennig C. Cluster-wise assessment of cluster stability. Comput Stat Data Anal. 2007;52(1):258-
265 71.

266 20. Segata N, Izard J, Waldron L, et al. Metagenomic biomarker discovery and explanation. Genome
267 Biol. 2011;12(6):R60.

268 21. Benjamini Y, Hochberg Y. Controlling the False Discovery Rate: A Practical and Powerful
269 Approach to Multiple Testing. J R Stat Soc Series B Stat Methodol. 1995;57(1):289-300.

270 22. Beasley TM, Schumacker RE. Multiple Regression Approach to Analyzing Contingency Tables:
271 Post Hoc and Planned Comparison Procedures. The Journal of Experimental Education. 1995;64(1):79-93.

272 23. Zhang Z. Variable selection with stepwise and best subset approaches. Ann Transl Med.
273 2016;4(7):136.

274 24. Liberzon A, Birger C, Thorvaldsdottir H, et al. The Molecular Signatures Database (MSigDB)
275 hallmark gene set collection. Cell Syst. 2015;1(6):417-25.

276 25. Peña EA, Slate EH. Global Validation of Linear Model Assumptions. J Am Stat Assoc.
277 2006;101(473):341.

278

279 **Supplementary Tables:**

280 **Table E1:** list of 21 Hallmark gene sets from the Molecular Signatures Database (MSigDB) investigated using the gene set variation analysis
 281 (GSVA).

Hallmark Name	Process Category	Description	Number of genes	Gene names
PEROXISOME	cellular component	peroxisomes	104	ABCD3, ACOT8, ACOX1, ACSL1, ECH1, ECI2, EHHADH, GSTK1, HSD17B4, MLYCD, PEX11A, RETSAT, SLC27A2, PEX13, PEX14, SCP2, HSD3B7, GNPAT, ABCD2, SLC25A17, PEX2, ACAA1, HAO2, HSD17B11, CRAT, PEX11B, LONP2, IDH1, FIS1, PEX6, ABCB4, SOD1, ABCB1, ISOC1, YWHAH, EPHX2, ABCD1, HMGCL, ACSL5, ALDH9A1, DHCR24, ELOVL5, NUDT19, PRDX5, CTPS1, IDE, SLC23A2, PEX5, BCL10, NR1I2, TSPO, CNBP, MSH2, DHRS3, DIO1, SLC25A4, PRDX1, IDI1, HRAS, MVP, ABCC8, CLN6, CAT, ACSL4, IDH2, ABCC5, SOD2, SLC35B2, FDPS, ALB, FADS1, STS, SMARCC1, ITGB1BP1, SIAH1, SLC25A19, CDK7, RXRG, ALDH1A1, UGT2B17, CADM1, SERPINA6, CLN8, RDH11, CTBP1, HSD11B2, TTR, ERCC3, ATXN1, SULT2B1, CRABP2, CRABP1, TOP2A, SCGB1A1, ERCC1, DLG4, PABPC1, FABP6, ABCB9, CACNA1B, SEMA3C, VPS4B, CEL, ESR2
MYOGENESIS	development	muscle differentiation	200	ACTA1, TNNT2, MYL1, TNNC1, TNNC2, MYH3, MYLPF, TNNT3, TNNT2, CASQ2, ACTC1, MYOM1, MYL4, MYBPH, MYH7, MYH8, ACTN2, TNNT1, CRYAB, SGCG, HRC, TNNT1, DES, MYOZ1, RYR1, CSRP3, ADAM12, ATP2A1, CKM, SVIL, MYOM2, MYL6B, TPM2, MYL2, CKMT2, BIN1, MYH1, ENO3, FLII, FXD1, TPM3, DMD, IGFBP3, CHRNA1, SPEG, FHL1, ACTN3, TCAP, MYLK, MYL3, PYGM, LDB3, COX6A2, FABP3, MYL7, ITGB5, CHRNA1, SSPN, COL3A1, KCNH1, GJA5, MYF6, MYH2, MAPK12, PGAM2, MYOG, MYH4, AEBP1, HBEGF, MEF2C, NOS1, CNN3, IGFBP7, CACNA1H, GSN, CACNG1, PPFIA4, MB, SPHK1, SCHIP1, MEF2D, SMTN, CDKN1A, GAA, TPD52L1, HSPB2, SGCA, BDKRB2, COX7A1, COL4A2, PLXNB2, CTF1, COL15A1, KCNH2, AGRN, MYO1C, SIRT2, SGCD, SORBS1, VIPR1, FGF2, FKBP1B, TEAD4, CASQ1, KLF5, PDLIM7, AK1, TAGLN, RIT1, MEF2A, ANKRD2, AKT2, LAMA2, DENND2B, IFRD1, NCAM1, SYNGR2, PICK1, COL6A3, CRAT, DMPK, MYH11, MYH9, IGF1, CKB, FST, GPX3, PVALB, PTP4A3, ITGB1, HSPB8, ACHE, CHRNA1, PKIA, NAV2, HDAC5, ATP6AP1, CLU, ACSL1, COL1A1, MRAS, PDE4DIP, AGL, ERBB3, GABARAPL2, CAV3, BHLHE40, PPP1R3C, LARGE1, LPIN1, CDH13, NQO1, PRNP, PSEN2, DAPK2, LSP1, SLC6A8, REEP1, EIF4A2, SH2B1, MYBPC3, ITGA7, SPTAN1, SORBS3, PC, SCD, GNAO1, STC2, CFD, RB1, BAG1, ABLIM1, PTGIS, MAPRE3, OCEL1, SH3BGR, NOTCH1, TSC2, TGFB1, FDPS, CAMK2B, EPHB3, GADD45B, APP, APLNR, ITGB4, SOD3, FOXO4, EFS, PFKM, COL6A2, DTNA, KIFC3, SPARC, SPDEF, SLN, WWTR1, CD36, ADCY9, APOD
COAGULATION	immune	blood coagulation cascade	138	F2, PROC, C1S, MMP14, F10, PLG, C1R, SERPINE1, SERPING1, C2, F12, CFI, MMP2, C3, F9, CTSO, TMPRSS6, MMP9, PROZ, MMP1, CFB, BMP1, VWF, FGA, F11, THBD, FURIN, MMP11, F8, LGMN, HPN, CTSB, MBL2, F13B, TIMP1, CTSV, MMP8, A2M, MMP10, MASP2, FGG, C8A, PLAUI, ADAM9, GSN, CAPN2, PLAT, FN1, CTSH, OLR1, SPARC, RGN, C8B, LAMP2, C9, PROS1, CLU, F2RL2, CD9, CFH, PREP, LTA4H, GP9, DUSP14, CTSK, GDA, CASP9,

				APOC1, CRIP2, KLK8, SERPINC1, ANXA1, ITIH1, PRSS23, FBN1, MST1, F3, KLF7, CTSE, ITGB3, CAPN5, CSRP1, KLKB1, MSRB2, TFPI2, MMP3, MEP1A, GP1BA, APOA1, SERPINA1, TF, PEF1, GNG12, SIRT2, COMP, HTRA1, MAFF, LRP1, PF4, CPQ, MMP15, RABIF, HRG, C8G, APOC2, SERPINB2, RAPGEF3, CPN1, ITGA2, RAC1, DPP4, WDR1, THBS1, FYN, PDGFB, SH2B2, PECAM1, MMP7, DUSP6, CPB2, S100A13, CFD, DCT, LEFTY2, ANG, C1QA, HMGC2, ISCU, PLEK, APOC3, P2RY1, USP11, TIMP3, ACOX2, HNF4A, S100A1, GNB2, ARF4
COMPLEMENT	immune	complement cascade	200	C2, C15, CFB, C1R, SERPINE1, MMP14, SERPING1, CTSL, F5, MMP13, F7, CTSS, LGMN, PLG, C1QA, CASP1, GZMA, ADAM9, CALM3, C1QC, TIMP1, DPP4, KLK1, KLKB1, CD59, CR2, MMP15, LAP3, SPOCK2, F10, CTSB, SERPINA1, CTSO, CD40LG, CBLB, PDP1, C4BPB, PLEK, GP9, PLAUR, C3, F2, CASP4, STX4, CTSC, USP15, CR1, DUSP6, SERPINB2, GPD2, CFH, FN1, CD36, CA2, PSMB9, APOBEC3G, FCN1, GZMK, PDGFB, CLU, CASP10, LRP1, CTSD, S100A9, WAS, BRPF3, PLAT, CDA, MT3, CASP7, PRSS36, PFN1, GZMB, RNF4, ZEB1, CASP5, IRF1, CPQ, CDK5R1, ATOX1, PIK3CA, TMPPRS6, CPM, RCE1, CALM1, DOCK9, KYNU, RASGRP1, USP14, LCP2, GP1BA, KIF2A, GNB4, LCK, OLR1, PREP, MSRB1, LTA4H, ZFPM2, LYN, ACTN2, SIRT6, APOC1, PRKCD, ITGAM, DGKH, LTF, MAFF, KCNIP2, PCLO, DOCK10, SH2B3, RABIF, SRC, HPCAL4, CD46, PRDM4, GNAI3, C9, PPP2CB, IRF2, FYN, JAK2, PLA2G4A, PRCP, USP8, RHOG, L3MBTL4, LAMP2, PIM1, CXCL1, F3, GNAI2, CASP9, XPNPEP1, PLSCR1, IRF7, CD55, HSPA5, GNB2, DYRK2, PLA2G7, S100A12, GRB2, PHEX, GNGT2, DOCK4, MMP12, KCNIP3, FDX1, TIMP2, MMP8, FCER1G, RBSN, ANXA5, CTSV, GCA, EHD1, PRSS3, COL4A2, CSRP1, PIK3R5, SERPINC1, ANG, APOBEC3F, GATA3, DUSP5, CASP3, USP16, CP, PSEN1, LIPA, PCSK9, DGKG, GNG2, ME1, GMFB, SCG3, PPP4C, CCL5, CTSB, F8, APOA4, IL6, AKAP10, ERAP2, VCIPI1, HSPA1A, RAF1, NOTCH4, ADRA2B, CEBPB, HNF4A, LGALS3, TNFAIP3, CDH13, ITIH1, TFPI2, PIK3CG, S100A13
INTERFERON_ALPHA_RESPONSE	immune	interferon alpha response	97	MX1, ISG15, OAS1, IFIT3, IFI44, IFI35, IRF7, RSAD2, IFI44L, IFITM1, IFI27, IRF9, OASL, EIF2AK2, IFIT2, CXCL10, TAP1, SP110, DDX60, UBE2L6, USP18, PSMB8, IFIH1, BST2, LGALS3BP, ADAR, ISG20, GBP2, IRF1, PLSCR1, PSMB9, HERC6, SAMD9, CMPK2, IFITM3, RTP4, STAT2, SAMD9L, LY6E, IFITM2, HELZ2, CXCL11, TRIM21, PARP14, TRIM26, PARP12, NMI, RNF31, HLA-C, CASP1, TRIM14, TDRD7, DHX58, PARP9, PNPT1, TRIM25, PSME1, WARS1, EPSTI1, UBA7, PSME2, B2M, TRIM5, C1S, LAP3, LAMP3, GBP4, NCOA7, TMEM140, CD74, GMPR, PSMA3, PROCR, IL7, IFI30, IRF2, CSF1, IL15, CNP, TENT5A, IL4R, CMTR1, CD47, LPAR6, MOV10, CASP8, TXNIP, SLC25A28, SELL, TRAFD1, BATF2, RIPK2, CCRL2, NUB1, OGFR, MVB12A, ELF1
INTERFERON_GAMMA_RESPONSE	immune	interferon gamma response	200	STAT1, ISG15, IFIT1, MX1, IFIT3, IFI35, IRF7, IFIT2, OAS2, TAP1, EIF2AK2, RSAD2, MX2, IRF1, OAS3, TNFSF10, IRF9, CXCL10, IFI44, BST2, XAF1, SP110, OASL, PSMB8, IFI44L, IFITM3, DDX60, LGALS3BP, GBP4, IRF8, PSMB9, PML, IFIH1, UBE2L6, IFI27, ADAR, LY6E, STAT2, CXCL9, IL10RA, PLA2G4A, TRIM21, USP18, PTGS2, EPSTI1, C1S, DDX58, IL15, NLRC5, NMI, IDO1, PSMB10, CXCL11, ITGB7, SAMHD1, HERC6, CMPK2, SAMD9L, RTP4, PTPN2, PARP14, TNFAIP2, IFITM2, PLSCR1, SOCS1, CASP1, ICAM1, WARS1, PSME1, ISG20, IRF2, TRIM14, FCGR1A, MARCHF1, SOCS3, JAK2, HLA-DMA, PARP12, TNFAIP6, TRIM26, VCAM1, CD274, CIITA, NAMPT, SELP, GPR18, FPR1, HELZ2, PSME2, SERPING1, CCL5, RNF31, SOD2, TRIM25, LAP3, PSMA3, RNF213, PELI1, CFB, CD86, TXNIP, HLA-DQA1, GCH1, PNP, CCL7, PTPN6, SPPL2A, IL4R, PNPT1, DHX58, BTG1, CASP8, IFI30, CCL2, FGL2, CASP7, SECTM1, IL15RA, CD40, TRAFD1, HLA-DRB1, GBP6, LCP2, HLA-G, MT2A, RIPK1, KLRK1, UPP1, PSMB2, TDRD7, HIF1A, EIF4E3, VAMP8, PFKP, CD38, ZBP1, BANK1, TOR1B, RBCK1, PDE4B, MVP, IL7, BPGM, CMTR1, AUTS2, B2M, RIPK2, CD69, MYD88, PSMA2, PIM1, NOD1, CFH, TAPBP, SLC25A28, PTPN1, TNFAIP3, SSPN, NUP93, MTHFD2, CDKN1A, IRF4, NFKB1, BATF2, HLA-B, LATS2, IRF5, SLAMF7, ISOC1, P2RY14, STAT3, NCOA3, HLA-A,

				IL6, GZMA, IFNAR2, CD74, RAPGEF6, CASP4, FAS, OGFR, ARL4A, SRI, LYSMD2, CSF2RB, ST3GAL5, C1R, CASP3, CMKLR1, NFKBIA, METTL7B, ST8SIA4, XCL1, IL2RB, VAMP5, IL18BP, ZNFX1, ARID5B, APOL6, STAT4
IL6_JAK_STAT3_SIGNALING	immune	IL6 STAT3 signaling during acute phase response	87	IL4R, IL6ST, STAT1, IL1R1, CSF2RB, SOCS3, STAT3, OSMR, IL2RG, IFNGR1, TYK2, IL13RA1, TLR2, IFNGR2, IL10RB, IL6, IL1R2, IL3RA, IFNAR1, TNFRSF1A, MYD88, ACVR1B, CSF3R, ITGB3, REG1A, CXCL1, A2M, CSF2RA, IL15RA, IRF9, PDGFC, HAX1, BAK1, EBI3, INHBE, CRLF2, TNFRSF1B, CD14, PTPN1, PTPN2, IL1B, CSF1, IL18R1, TNF, PF4, CXCL13, LTBR, FAS, IL17RA, CXCL10, IL9R, STAM2, TNFRSF12A, STAT2, HMOX1, LEPR, CBL, CD9, CXCL3, TGFB1, MAP3K8, ITGA4, CD38, JUN, SOCS1, ACVRL1, PIM1, TNFRSF21, PIK3R5, GRB2, IRF1, DNTT, CSF2, IL2RA, PTPN11, IL12RB1, CCR1, CNTFR, PLA2G2A, CXCL9, CD44, IL7, CXCL11, CCL7, LTB, IL17RB, CD36
INFLAMMATORY_RESPONSE	immune	inflammation	200	CXCL10, CCL2, CCL5, FPR1, CCL20, IL1A, CXCL8, CCL7, CCL22, CXCL11, CCR7, EDN1, CD40, CXCL9, IL6, IL1B, TLR2, IL1R1, CD69, ICAM1, CCRL2, AQP9, EREG, C3AR1, GNA15, CMKLR1, PTGER4, LIF, IL15, NAMPT, OPRK1, ITGB8, PTAFR, ADM, PLAUR, NFKB1, INHBA, OSM, TNFSF10, TNFSF15, IFNGR2, ADGRE1, IL12B, CSF1, CXCL6, TNFRSF9, LYN, ACVR2A, LDLR, BDKRB1, HRH1, F3, BST2, PTGIR, CD55, CALCRL, CSF3, GPR132, IL4R, NLRP3, IL15RA, ADORA2B, GCH1, OLR1, PTGER2, CSF3R, MYC, RELA, TNFAIP6, IL7R, IL18, GABBR1, CD82, TNFSF9, NMUR1, IL2RB, TLR1, LPAR1, IRAK2, RIPK2, MMP14, P2RX7, SLC11A2, SELL, P2RY2, ABCA1, FFAR2, PROK2, GNAI3, TACR1, SLC7A1, CDKN1A, CYBB, TIMP1, HBEGF, SCARF1, EBI3, NFKBIA, SRI, SLC7A2, CCL17, TLR3, APLNR, OSMR, IL10RA, PSEN1, GPR183, ATP2B1, TNFRSF1B, BEST1, GPC3, SCN1B, ACVR1B, HPN, SEMA4D, KLF6, CD48, CXCR6, SLC1A2, GP1BA, TAPBP, RGS16, SLAMF1, LCK, HIF1A, AHR, NMI, RHOG, TPBG, NPFFR2, IFNAR1, ICOSLG, RASGRP1, IFITM1, KCNJ2, LY6E, IL18R1, IL10, KCNA3, HAS2, DCBLD2, LAMP3, VIP, CD70, RGS1, SLC31A1, ADRM1, KCNMB2, SERPINE1, MXD1, AXL, MEFV, PVR, CCL24, PDE4B, LCP2, PDPN, IRF7, MET, ATP2A2, SLC31A2, FZD5, ITGA5, SGMS2, MARCO, CD14, EIF2AK2, ROS1, ATP2C1, NDP, BTG2, MSR1, PTPRE, RNF144B, PCDH7, SPHK1, IL18RAP, RTP4, RAF1, CHST2, ITGB3, KIF1B, SELE, NOD2, C5AR1, EMP3, CLEC5A, TACR3, SLC4A4, MEP1A, SELENOS, LTA, PIK3R5, STAB1, IRF1, ICAM4, P2RX4, ABI1, CX3CL1, SLC28A2
OXIDATIVE_PHOSPHORYLATION	metabolic	oxidative phosphorylation and citric acid cycle	200	NDUFS3, UQCRB, NDUFS2, SDHA, UQCRC1, NDUFA9, NDUFS4, NDUFS1, NDUFA2, NDUFS8, SDHB, NNT, ATP5PO, ATP5MC3, NDUFS7, ATP5F1A, NDUFV1, COX5B, UQCRH, NDUFA1, ATP5F1C, ATP5F1B, COX7B, SDHD, CYCS, NDUFA6, NDUFAB1, COX8A, ACO2, ATP5MC1, CYC1, NDUFB6, ATP5F1E, COX5A, UQCRC2, COX6A1, ATP5F1D, COX6C, ATP5PF, NDUFB3, IDH3B, OGDH, NDUFB8, SURF1, COX6B1, NDUFB5, NDUFA4, NDUFB1, COX4I1, COX7C, UQCRCF1, SDHC, ATP6V1F, COX7A2, SUCLG1, NDUFS6, NDUFA7, FH, NDUFV2, OXA1L, NDUFC1, UQCR11, NDUFA5, CS, ATP6V1G1, ATP5PB, HCCS, HADHB, ATP5PD, PDHA1, NDUFA8, DLD, OPA1, SLC25A11, ATP5ME, PDHB, ATP5MF, NDUFB7, IDH2, MTX2, VDAC3, MDH1, ATP5MC2, IMMT, MDH2, SLC25A3, ATP6V1D, VDAC2, ACADM, COX7A2L, TIMM17A, ATP6V1E1, NDUFA3, SLC25A6, IDH3G, ACADVL, ETFA, TIMM9, IDH3A, TIMM8B, ATP6AP1, TIMM13, UQCRCQ, ABCB7, VDAC1, ATP5MG, PHB2, DECR1, SUCLA2, GOT2, DLAT, ATP6V1H, NDUFB2, FDX1, HADHA, ATP6V1C1, MAOB, NDUFB4, UQCR10, ETFDH, GPX4, PDHX, MFN2, AIFM1, ACAA2, ETFB, COX11, ECHS1, PMPCA, ATP6V0B, SLC25A5, DLST, COX15, CYB5A, ALAS1, SLC25A4, CPT1A, SLC25A20, MTRR, COX17, CYB5R3, TOMM22, ACAT1, MRPS11, ATP6V0C, PDK4, TIMM10, LDHA, ECI1, MRPL11, FXN, MRPS12, COX10, RHOT1, ACAA1, ACADSB, LDHB, MRPS30, ATP1B1, BDH2, SLC25A12, TIMM50, MRPL34, ISCA1, MRPL35, IDH1, HSPA9, MRPL15, MRPS15, TOMM70, TCIRG1, ISCU, POLR2F, NQO2, NDUFC2, MRPS22, POR, ATP6V0E1, PHYH, MPC1, GPI, AFG3L2, HSD17B10, CASP7, PRDX3, MGST3, HTRA2, BCKDHA, LRPPRC, RETSAT, ECH1, RHOT2, BAX, MTRF1, GLUD1, SUPV3L1, GRPEL1, PDP1, ALDH6A1, OAT

HYPOXIA	path way	response to hypoxia; HIF1A targets	200	PGK1, PDK1, GBE1, PFKL, ALDOA, ENO2, PGM1, NDRG1, HK2, ALDOC, GPI, MXI1, SLC2A1, P4HA1, ADM, P4HA2, ENO1, PFKP, AK4, FAM162A, PFKFB3, VEGFA, BNIP3L, TPI1, ERO1A, KDM3A, CCNG2, LDHA, GYS1, GAPDH, BHLHE40, ANGPTL4, JUN, SERPINE1, LOX, GCK, PPFA4, MAFF, DDIT4, SLC2A3, IGFBP3, NFIL3, FOS, RBPJ, HK1, CITED2, ISG20, GALK1, WSB1, PYGM, STC1, ZNF292, BTG1, PLIN2, CSRP2, VLDLR, JMJD6, EXT1, F3, PDK3, ANKZF1, UGP2, ALDOB, STC2, ERFF1, ENO3, PNRC1, HMOX1, PGF, GAPDHS, CHST2, TMEM45A, BCAN, ATF3, CAV1, AMPD3, GPC3, NDST1, IRS2, SAP30, GAA, SDC4, STBD1, IER3, PKLR, IGFBP1, PLAUR, CAVIN3, CCN5, LARGE1, NOCT, S100A4, RRAGD, ZFP36, EGFR, EDN2, IDS, CDKN1A, RORA, DUSP1, MIF, PPP1R3C, DPYSL4, KDELR3, DTNA, ADORA2B, HS3ST1, CAVIN1, NR3C1, KLF6, GPC4, CCN1, TNFAIP3, CA12, HEXA, BGN, PPP1R15A, PGM2, PIM1, PRDX5, NAGK, CDKN1B, BRS3, TKT1L, MT1E, ATP7A, MT2A, SDC3, TIPARP, PKP1, ANXA2, PGAM2, DDIT3, PRKCA, SLC37A4, CXCR4, EFNA3, CP, KLF7, CCN2, CHST3, TPD52, LXN, B4GALNT2, PPARGC1A, BCL2, GCNT2, HAS1, KLHL24, SCARB1, SLC25A1, SDC2, CASP6, VHL, FOXO3, PDGFB, B3GALT6, SLC2A5, SRPX, EFNA1, GLRX, ACKR3, PAM, TGFB1, DCN, SIAH2, PLAC8, FBP1, TPST2, PHKG1, MYH9, CDKN1C, GRHPR, PCK1, INHA, HSPA5, NDST2, NEDD4L, TPBG, XPNPEP1, IL6, SLC6A6, MAP3K1, LDHC, AKAP12, TES, KIF5A, LALBA, COL5A1, GPC1, HDLBP, ILVBL, NCAN, TGM2, ETS1, HOXB9, SELENBP1, FOSL2, SULT2B1, TGFB3
REACTIVE_OXYGEN_SPECIES_PATHWAY	path way	reactive oxygen species pathway	49	GSR, PRDX2, TXNRD1, SOD1, GCLC, CAT, GPX4, MPO, PRDX1, PRDX6, GCLM, TXN, SOD2, PRDX4, SELENOS, PDLIM1, TXNRD2, LAMTOR5, G6PD, MSRA, MBP, SRXN1, NQO1, OXSR1, GLRX2, HMOX2, FES, PFKP, NDUFB4, GPX3, SCAF4, CDKN2D, MGST1, ABCC1, FTL, ATOX1, STK25, EGLN2, ERCC2, SBNO2, JUNB, PTPA, LSP1, NDUFA6, HHEX, GLRX, NDUFS2, PRNP, IPCEF1
P53_PATHWAY	proliferation	p53 pathway	200	CDKN1A, BTG2, MDM2, CCNG1, FAS, TOB1, GADD45A, PHLDA3, TAP1, CDKN2B, SFN, ZMAT3, DDB2, EI24, PERP, DDIT4, ATF3, BAX, SESN1, FDXR, PIDD1, SAT1, CDKN2A, AEN, PPM1D, FOXO3, BTG1, TXNIP, SLC19A2, IER3, TP53, NOTCH1, RRAD, DCXR, NINJ1, FOS, S100A10, FBXW7, PLK3, XPC, AK1, TRIAP1, BAK1, CCND2, APAF1, PDGFA, NDRG1, RALGDS, SERPINB5, DGKA, CYFIP2, KLF4, IP6K2, ADA, TNFSF9, KLK8, PRKAB1, STOM, SOCS1, PLK2, CASP1, RCHY1, PCNA, RPS27L, RB1, PPP1R15A, POLH, RAB40C, ERCC5, CDH13, DDIT3, TGFB1, FUCA1, H2AW, TP63, HSPA4L, EPHX1, ABHD4, H2AJ, TRAF4, CTSF, IER5, TAX1BP3, TSC22D1, RGS16, HRAS, PVT1, ZFP36L1, SDC1, WRAP73, RAP2B, COQ8A, PLXNB2, HEXIM1, PROCR, SPHK1, NOL8, DEF6, SP1, JAG2, CCP110, DRAM1, RPL18, CEBPA, KIF13B, MXD1, TRAFD1, OSGIN1, ANKRA2, HBEGF, RAD51C, ITGB4, TRIB3, INHBB, VAMP8, VWA5A, ABAT, CTSD, PTPRE, HINT1, ALOX15B, VDR, ELP1, WWP1, NUPR1, TCN2, CDKN2AIP, POM121, ZNF365, EPHA2, JUN, MAPKAPK3, SLC7A11, SERTAD3, IRAK1, ABCC5, UPP1, CD81, LIF, RPL36, FAM162A, RNF19B, CDK5R1, STEAP3, PITPNC1, SLC35D1, TPRKB, RRP8, IL1A, PMM1, TPD52L1, IFI30, GM2A, RPS12, EPS8L2, TM4SF1, BLCAP, MKNK2, CD82, RACK1, ST14, TCHH, HDAC3, CCNK, RHBDF2, NUDT15, TGFA, ISCU, LDHB, TNNI1, FGF13, RXRA, APP, F2R, CLCA2, CGRRF1, CSRN2, ACVR1B, BMP2, GPX2, KRT17, TM7SF3, ZBTB16, PTPN14, TSPYL2, SLC3A2, S100A4, GLS2, CCND3, PRMT2, NHLH2, BAIAP2, RETSAT, IRAG2, H1-2, DNTTIP2, MXD4, SEC61A1, HMOX1, RAD9A
IL2_STAT5_SIGNALING	signaling	IL2 STAT5 signaling	199	SOCS2, CISH, PIM1, IL2RA, TNFRSF4, SOCS1, TNFRSF9, XBP1, RRAGD, HK2, PHLDA1, IL2RB, CTLA4, NFIL3, CD83, IKZF2, IL10, TNFRSF18, DHRS3, ECM1, ADAM19, SLC2A3, HIPK2, BATF3, BHLHE40, PTGER2, DENND5A, ITIH5, PHTF2, GADD45B, NRP1, NCOA3, CD79B, AHR, TNFRSF1B, NDRG1, BCL2L1, GABARAPL1, LIF, TIAM1, BMPR2, MAP3K8, RHOB, MYC, S100A1, ETFBKMT, CAPG, ST3GAL4, PENK, IRF4, CST7, WLS, TLR7, IKZF4, GBP4, RGS16, SPP1, IL13, SLC29A2, NFKBIZ, IL4R, MXD1, CSF2, FAH, CTSZ, ITGAE, MUC1, MAPKAPK2, TNFRSF21, NT5E,

				FLT3LG, CCND2, TRAF1, LCLAT1, IL3RA, CYFIP1, BCL2, FGL2, PRNP, EEF1AKMT1, PUS1, ITGAV, NCS1, DCPS, AMACR, FAM126B, PTH1R, ODC1, IGF1R, PTCH1, ENO3, CD81, MAFF, EMP1, CDKN1C, CAPN3, IL1R2, SYT11, TTC39B, ANXA4, BATF, P4HA1, GPR65, SLC1A5, IGF2R, CKAP4, CCR4, CD44, P2RX4, GATA1, KLF6, ARL4A, HOPX, GPR83, ITGA6, CD48, DRC1, SELP, GLIPR2, SMPDL3A, PLSCR1, FURIN, SERPINB6, TNFSF11, GPX4, LRRC8C, CCNE1, CASP3, SH3BGRL2, SNX9, PLEC, BMP2, ICOS, ALCAM, LTB, ENPP1, IL1RL1, MYO1C, IFNGR1, PLIN2, IL18R1, AHNK, PRKCH, TNFRSF8, SYNGR2, GALM, POU2F1, EOMES, NOP2, PTRH2, RHOH, CDC6, MYO1E, CXCL10, SNX14, IRF6, IL10RA, MAP6, TNFSF10, SPRED2, SELL, SERPINC1, CDCP1, RORA, COCH, CSF1, F2RL2, UCK2, CA2, IFITM3, UMPS, HUWE1, COL6A1, ABCB1, RNH1, IRF8, GUCY1B1, AH CY, PRAF2, GSTO1, TWSG1, CDC42SE2, PLAGL1, APLP1, PLPP1, SPRY4, SCN9A, SHE, PDCD2L, CCND3, LRIG1, SWAP70, SLC39A8, RABGAP1L, TGM2, PNP, AGER, ETV4, CD86
KRAS_SIGN ALING_UP	signa ling	KRAS signaling, upregulated genes	200	ANGPTL4, ITGA2, SPRY2, HBEGF, RBP4, HSD11B1, ETV4, GLRX, DUSP6, SCG5, ETV5, ITGB2, AKT2, PPBP, GOS2, GABRA3, IRF8, BIRC3, FGF9, DCBLD2, INHBA, TFPI, TSPAN1, ADAM8, SLPI, PRKG2, MMP11, MMP10, TMEM158, TNFAIP3, PRDM1, GALNT3, ETS1, MMP9, WNT7A, IGFBP3, SPP1, ETV1, CLEC4A, CCND2, TSPAN7, ITGBL1, EMP1, CDADC1, KIF5C, TRIB2, SDCCAG8, PCP4, CFHR2, ALDH1A2, NROB2, ALDH1A3, AMMECR1, SATB1, GUCY1A1, CSF2, APOD, TOR1AIP2, CMKLR1, TMEM176B, ADGRA2, LAPTM5, CD37, CAB39L, CIDEA, ZNF639, IL1B, GYPC, LY96, FLT4, SPON1, BMP2, PLEK2, IGF2, NR1H4, SNAP25, ACE, PRRX1, C3AR1, TRAF1, TLR8, ID2, TMEM100, PLAUR, GADD45G, CBX8, SCN1B, PTBP2, NAP1L2, AKAP12, PLAT, SCG3, ANO1, IL1RL2, CXCL10, ATG10, YRDC, HDAC9, PEG3, SEMA3B, TNNT2, LIF, CFB, BTC, PPP1R15A, PTPRR, CCL20, ARG1, RETN, KLF4, MMD, PDCD1LG2, H2BC3, HOXD11, TRIB1, F2RL1, ANXA10, TSPAN13, MTMR10, CFH, LAT2, ERO1A, RELN, KCNN4, TMEM176A, MAP4K1, PTGS2, IL33, MAFB, LCP1, NGF, CA2, SERPINA3, RGS16, CTSS, USP12, CPE, SPARCL1, ABCB1, USH1C, CSF2RA, BTBD3, IL2RG, DNMBP, IL10RA, EREG, PRELID3B, EPHB2, FBXO4, CROT, MPZL2, ANKH, CBR4, DOCK2, GPRC5B, RABGAP1L, MALL, STRN, ST6GAL1, PIGR, VWASA, PSMB8, F13A1, NRP1, SOX9, JUP, ADGRL4, ZNF277, EPB41L3, PCSK1N, FUCA1, PLVAP, ADAM17, AVL9, ADAMDEC1, HKDC1, MAP7, IL7R, RBM4, BPGM, ENG, GFPT2, PLAUI, GNG11, PTC2, MAP3K1, CBL, CXCR4, NIN, IKZF1, WDR33, MYCN, FCER1G, PECAM1, CCSER2, SNAP91, EVI5, TNFRSF1B, GPNMB, TPH1
MTORC1_S IGNALING	signa ling	mTORC1 signaling	200	FADS1, DDIT4, CALR, HK2, PGK1, SLC7A5, CTSC, ACSL3, SLC1A5, M6PR, TFRC, DDIT3, TMEM97, IFRD1, PLOD2, TUBA4A, PSAT1, CORO1A, LDHA, MTHFD2, FADS2, VLDLR, WARS1, SCD, P4HA1, ACTR2, IDH1, SLC2A1, GBE1, SERPINH1, NUPR1, PSMG1, PSPH, NAMPT, CDKN1A, BHLHE40, HSPA9, HSPA5, EGLN3, LGMN, PNP, XBP1, SLA, DDX39A, HSPE1, ACLY, SLC7A11, SSR1, GLA, SQSTM1, PDK1, PSMC2, PRDX1, SERP1, TRIB3, NFIL3, HMGC1, GOT1, TPI1, ELOVL6, ASNS, PSMD14, PSMA4, PPA1, HPRT1, AURKA, HMGC1, GAPDH, DHFR, DHCR7, IMMT, UCHL5, YKT6, INSIG1, SQLE, IGFBP5, IFI30, CYP51A1, FGL2, ENO1, IDI1, CYB5B, SHMT2, TXNRD1, G6PD, SLC9A3R1, RAB1A, EBP, PNO1, PIK3R3, ACTR3, LDLR, SLC2A3, UBE2D3, ELOVL5, CACYBP, EDEM1, ATP6V1D, TES, TM7SF2, PSMA3, ITGB2, AK4, SLC1A4, TOMM40, SLC6A6, PPIA, ADD3, ME1, CCNF, SLC37A4, ALDOA, BTG2, UFM1, CCNG1, STC1, NMT1, PSMC6, FDXR, RRM2, DHCR24, PSMC4, CTH, PSME3, CFP, POLR3G, ACACA, QDPR, MCM2, PSMD12, SC5D, CANX, RPN1, HSPA4, NIBAN1, TBK1, SEC11A, BCAT1, PSMB5, PSMD13, PGM1, PLK1, GLRX, COPS5, ETF1, GSK3B, NUP205, SORD, PHGDH, GMPS, RRP9, EEF1E1, LTA4H, SDF2L1, FKBP2, RDH11, CXCR4, MLLT11, GCLC, TCEA1, MAP2K3, HSPD1, SYTL2, MCM4, PPP1R15A, USO1, NFKBIB, UNG, GTF2H1, RPA1, HSP90B1, ERO1A, GSR, PITPNB, EPRS1, SRD5A1, TUBG1, MTHFD2L, ADIPOR2, NUFIP1, CDC25A,

				PDAP1, STARD4, BUB1, ARPC5L, GPI, EIF2S2, CD9, ATP2A2, GGA2, HMBS, RIT1, SKAP2, STIP1, DAPP1, ABCF2, NFYC, ATP5MC1, PFKL, CCT6A
NOTCH_SIGNALING	signaling	Notch signaling	32	JAG1, NOTCH3, NOTCH2, APH1A, HES1, CCND1, FZD1, PSEN2, FZD7, DTX1, DLL1, FZD5, MAML2, NOTCH1, PSENEN, WNT5A, CUL1, WNT2, DTX4, SAP30, PPARD, KAT2A, HEYL, SKP1, RBX1, TCF7L2, ARRB1, LFNG, PRKCA, DTX2, ST3GAL6, FBXW11
PI3K_AKT_MTOR_SIGNALING	signaling	PI3K signaling via AKT to mTORC1	105	MAPK8, PIK3R3, GRB2, NFKBIB, MAP2K6, MAPK9, AKT1, MAPK1, PLCG1, TRIB3, GSK3B, MAP2K3, CDKN1A, RAC1, RIPK1, AKT1S1, ACTR2, PRKAR2A, YWHAB, HRAS, PDK1, PIKFYVE, TBK1, ACTR3, E2F1, MYD88, ITPR2, SQSTM1, RPS6KA1, PTPN11, MAPKAP1, PLCB1, RAF1, CAMK4, RPTOR, CFL1, CDK4, TRAF2, GNGT1, UBE2N, ADCY2, CDKN1B, VAV3, FGF6, ECSIT, RALB, ARF1, MKNK1, CDK1, PTEN, ARHGDI, GRK2, FGF17, DDIT3, IRAK4, TIAM1, CDK2, SFN, PRKCB, GNA14, EIF4E, CLTC, TSC2, FGF22, PPP1CA, DUSP3, HSP90B1, IL4, STAT2, SLA, EGFR, PLA2G12A, MAPK10, CALR, THEM4, RIT1, MKNK2, PPP2R1B, CAB39L, ARPC3, PITX2, NCK1, IL2RG, PFN1, FASLG, NOD1, DAPP1, UBE2D3, CAB39, AP2M1, MAP3K7, PRKAG1, CSNK2B, PRKAA2, ATF1, SLC2A1, PIN1, TNFRSF1A, LCK, RPS6KA3, NGF, CXCR4, ACACA, SMAD2, PAK4
HEDGEHOG_SIGNALING	signaling	Hedgehog signaling	36	SHH, PTCH1, NRCAM, NRP1, SCG2, AMOT, UNC5C, ADGRG1, HEY1, GLI1, THY1, SLIT1, CDK6, HEY2, NRP2, TLE3, TLE1, L1CAM, PLG, NKX6-1, NF1, RASA1, ETS2, RTN1, CRMP1, MYH9, VEGFA, CELSR1, CNTFR, ACHE, PML, CDK5R1, VLDLR, OPHN1, LDB1, DPYSL2
TGF_BETA_SIGNALING	signaling	TGF beta signaling	54	TGFBF1, SMAD7, TGFB1, SMURF2, SMURF1, BMPR2, SKIL, SKI, ACVR1, PMEPA1, NCOR2, SERPINE1, JUNB, SMAD1, SMAD6, PPP1R15A, TGIF1, FURIN, SMAD3, FKBP1A, MAP3K7, BMPR1A, CTNBN1, HIPK2, KLF10, BMP2, ENG, APC, PPM1A, XIAP, CDH1, ID1, LEFTY2, CDKN1C, TRIM33, RAB31, TJP1, SLC20A1, CDK9, ID3, NOG, ARID4B, IFNGR2, ID2, PPP1CA, SPTBN1, WWTR1, BCAR3, THBS1, FNTA, HDAC1, UBE2D3, LTBP2, RHOA
TNFA_SIGNALING_VIA_NFKB	signaling	TNFA signaling via NFkB	200	JUNB, CXCL2, ATF3, NFKBIA, TNFAIP3, PTGS2, CXCL1, IER3, CD83, CCL20, CXCL3, MAFF, NFKB2, TNFAIP2, HBEGF, KLF6, BIRC3, PLAUR, ZFP36, ICAM1, JUN, EGR3, IL1B, BCL2A1, PPP1R15A, ZC3H12A, SOD2, NR4A2, IL1A, RELB, TRAF1, BTG2, DUSP1, MAP3K8, ETS2, F3, SDC4, EGR1, IL6, TNF, KDM6B, NFKB1, LIF, PTX3, FOSL1, NR4A1, JAG1, CCL4, GCH1, CCL2, RCAN1, DUSP2, EHD1, IER2, REL, CFLAR, RIPK2, NFKBIE, NR4A3, PHLDA1, IER5, TNFSF9, GEM, GADD45A, CXCL10, PLK2, BHLHE40, EGR2, SOCS3, SLC2A6, PTGER4, DUSP5, SERPINB2, NFIL3, SERPINE1, TRIB1, TIPARP, RELA, BIRC2, CXCL6, LITAF, TNFAIP6, CD44, INHBA, PLAUI, MYC, TNFRSF9, SGK1, TNIP1, NAMPT, FOSL2, PNRC1, ID2, CD69, IL7R, EFNA1, PHLDA2, PFKFB3, CCL5, YRDC, IFNGR2, SQSTM1, BTG3, GADD45B, KYNU, GOS2, BTG1, MCL1, VEGFA, MAP2K3, CDKN1A, CCN1, TANK, IFIT2, IL18, TUBB2A, IRF1, FOS, OLR1, RHOB, AREG, NINJ1, ZBTB10, PLPP3, KLF4, CXCL11, SAT1, CSF1, GPR183, PMEPA1, PTPRE, TLR2, ACKR3, KLF10, MARCKS, LAMB3, CEBPB, TRIP10, F2RL1, KLF9, LDLR, TGIF1, RNF19B, DRAM1, B4GALT1, DNAJB4, CSF2, PDE4B, SNN, PLEK, STAT5A, DENND5A, CCND1, DDX58, SPHK1, CD80, TNFAIP8, CCN1, FUT4, CCRL2, SPSB1, TSC22D1, B4GALT5, SIK1, CLCF1, NFE2L2, FOSB, PER1, NFAT5, ATP2B1, IL12B, IL6ST, SLC16A6, ABCA1, HES1, BCL6, IRS2, SLC2A3, CEBPD, IL23A, SMAD3, TAP1, MSC, IFIH1, IL15RA, TNIP2, BCL3, PANX1, FJX1, EDN1, EIF1, BMP2, DUSP4, PDLIM5, ICOSLG, GFPT2, KLF2, TNC, SERPINB8, MXD1
WNT_BETA_CATENIN_SIGNALING	signaling	canonical beta catenin pathway	42	MYC, CTNBN1, JAG2, NOTCH1, DLL1, AXIN2, PSEN2, FZD1, NOTCH4, LEF1, AXIN1, NKD1, WNT5B, CUL1, JAG1, MAML1, KAT2A, GNAI1, WNT6, PTCH1, NCOR2, DKK4, HDAC2, DKK1, TCF7, WNT1, NUMB, ADAM17, DVL2, PPARD, NCSTN, HDAC5, CCND2, FRAT1, CSNK1E, RBPJ, FZD8, TP53, SKP2, HEY2, HEY1, HDAC11

282 This table is part of the Hallmark gene sets table from Molecular Signatures Database (MSigDB) release version 7.4 as previously described in [24] (Liberzon *et*
283 *al.* The Molecular Signatures Database (MSigDB) hallmark gene set collection. Cell Syst. 2015 Dec 23;1(6):417-425).

284 **Table E2:** A stepwise multiple logistic regression model of having atopic dermatitis diagnosis.

<i>Atopic dermatitis diagnosis</i>							
Characteristic [#]	n [†]	OR	SE	95% CI	Overall <i>P</i> -value [‡]	<i>P</i> -value	<i>q</i> -value
Taxa-driven clusters[¶]					8.76 x 10⁻³		
• Cluster 2	87/239	3.89	0.411	1.76, 8.85		9.42 x 10⁻⁴	0.008
• Cluster 3	21/239	1.79	0.571	0.59, 5.65		0.308	0.308
• Cluster 4	81/239	2.18	0.394	1.01, 4.78		0.047	0.107
Ethnicity (White Caucasian)	192/239	0.46	0.420	0.19, 1.02		0.068	0.123
Season of inclusion*					0.063		
• Spring	53/239	0.53	0.441	0.22, 1.25		0.146	0.187
• Summer	60/239	0.57	0.420	0.25, 1.29		0.178	0.200
• Winter	54/239	0.32	0.433	0.13, 0.74		0.009	0.026
Library size	239	1.00	0.000	1.00, 1.00		0.102	0.153
Plate ID (Plate 2)	84/239	2.60	0.348	1.34, 5.26		0.006	0.026
McFadden's R ² = 0.103 , Nagelkerke R ² = 0.170, AIC = 292.2							

285 AIC: Akaike information criterion, CI: confidence interval, SE: standard error, and OR: odds ratio. [†] n=2/241 patients
286 with missing atopic dermatitis diagnosis were excluded from the regression analysis. [#] Variables in the model were
287 selected according to a stepwise process. [¶] Cluster 1 (n=50/239, with the lowest % of atopy diagnosis) was the
288 reference group for comparison in the stepwise process. * Fall season (n=72/239) was randomly selected as a
289 reference group for comparison in the stepwise process. [‡] The overall *P*-values were computed for variables with
290 >2 categories, in which all the variable's categories were taken into account (without a reference group selection).
291 The microbiota clusters with the statistically significant *q*-values after adjusting for covariates are highlighted in
292 bold-face. *q*-value < 0.05 is considered statistically significant.

Table E3: A stepwise multiple linear regression model of FEV₁ post-salbutamol % predicted.

<i>FEV₁ % predicted post-salbutamol</i>							
Characteristic [#]	n [†]	β	SE	95% CI	Overall P-value [‡]	P-value	q-value
Taxa-driven clusters[¶]					0.030		
• Cluster 1	29/143	6.3	3.76	-1.1, 14		0.094	0.148
• Cluster 3	10/143	15	5.51	4.3, 26		0.007	0.037
• Cluster 4	45/143	1.6	3.17	-4.7, 7.8		0.622	0.665
BMI z-score	143	2.1	1.10	-0.07, 4.3		0.058	0.118
Centre of Inclusion[*]					0.028		
• Centre B	11/143	2.5	5.66	-8.7, 14		0.665	0.665
• Centre D	4/143	-16	8.45	-33, 0.78		0.061	0.118
• Centre E	35/143	-11	3.89	-19, -3.3		0.005	0.037
• Centre F	30/143	-7.7	4.15	-16, 0.47		0.064	0.118
• Centre G	24/143	-3.9	4.41	-13, 4.9		0.383	0.469
OCS	27/143	-5.5	3.70	-13, 1.8		0.137	0.188
NCS	17/143	10	4.22	1.8, 19		0.017	0.064
R ² = 0.180; adjusted R ² = 0.112, AIC = 1209.8, overall P-value = 0.005							

β: beta regression co-efficient, AIC: Akaike information criterion, BMI: body mass index, CI: confidence interval, NCS: nasal corticosteroids, OCS: oral corticosteroids, and SE: standard error. † Only older children with available spirometry data (n=143/241) were included in the regression analysis. # Variables in the model were selected according to a stepwise process. ¶ Cluster 2 (n=59/143, with the lowest FEV₁ post-salbutamol % predicted median value) was the reference group for comparison in the stepwise process. *Inclusion center C (n=39/143) was randomly selected as a reference group in the stepwise process. ‡ The overall P-values were computed for variables with >2 categories, in which all the variable's categories were taken into account (without a reference group selection). The microbiota clusters with the statistically significant q-values after adjusting for covariates are highlighted in bold-face.

Table E4: A stepwise multiple logistic regression model of grass pollen sensitization.

<i>Grass pollen sensitization</i>							
Characteristic [#]	n [†]	OR	SE	95% CI	Overall <i>P</i> -value [‡]	<i>P</i> -value	<i>q</i> -value
Taxa-driven clusters[¶]					0.101		
• Cluster 2	81/219	3.14	0.470	1.27, 8.10		0.015	0.038
• Cluster 3	18/219	2.07	0.691	0.53, 8.15		0.292	0.292
• Cluster 4	74/219	2.07	0.481	0.82, 5.46		0.131	0.176
Age	219	1.28	0.038	1.19, 1.38		7.6 x10 ⁻¹¹	<0.001
Sex (female)	86/219	0.60	0.352	0.30, 1.19		0.147	0.176
Ethnicity (White Caucasian)	176/219	0.39	0.398	0.18, 0.85		0.019	0.038
McFadden's R ² = 0.233, Nagelkerke R ² = 0.366, AIC = 243.9							

AIC: Akaike information criterion, CI: confidence interval, SE: standard error, and OR: odds ratio. [†] only participants with grass pollen atopy sensitization (n=219/241), by either a skin prick test and/or an allergen-specific IgE, were included in the regression analysis. [#] Variables in the model were selected according to a stepwise process. [¶] Cluster 1 (n=46/219, with the lowest % of grass atopy diagnosis) was the reference group for comparison in the stepwise process. [‡] The overall *P*-value was computed for taxa-driven clusters, in which all clusters were taken into account (without a reference group selection). The microbiota clusters with the statistically significant *q*-values after adjusting for covariates are highlighted in bold-face. *q*-value < 0.05 is considered statistically significant.

312 **Table E5:** Stepwise multiple linear regression models of the statistically significant hallmark pathways.

<i>Transcriptomic pathways</i>							
<i>Wnt/β-Catenin signaling</i>							
Characteristic [#]	n [†]	β	SE	95% CI	Overall P-value [‡]	P-value	q-value
Taxa-driven clusters[¶]					4.12 x 10⁻⁰⁵		
• Cluster 2	69/188	0.08	0.033	0.01, 0.14		0.024	0.112
• Cluster 3	15/188	0.07	0.050	-0.03, 0.17		0.168	0.235
• Cluster 4	64/188	0.16	0.034	0.10, 0.23		2.95 x 10⁻⁰⁶	<0.001
Age	188	0.01	0.003	0.01, 0.02		3.41 x 10 ⁻⁰⁵	<0.001
Ethnicity (White Caucasian)	150/188	0.06	0.031	-0.01, 0.12		0.072	0.203
BMI z-score	188	0.02	0.011	0.00, 0.04		0.070	0.203
Centre of Inclusion[*]					0.070		
• Centre A	16/188	0.08	0.052	-0.02, 0.18		0.129	0.226
• Centre E	50/188	0.02	0.038	-0.06, 0.09		0.643	0.643
• Centre B	17/188	0.04	0.050	-0.06, 0.13		0.477	0.513
• Centre D	3/188	-0.13	0.099	-0.32, 0.07		0.197	0.251
• Centre F	33/188	-0.05	0.041	-0.13, 0.03		0.259	0.302
• Centre G	32/188	-0.06	0.040	-0.14, 0.01		0.111	0.226
NCS	12/188	-0.08	0.050	-0.18, 0.02		0.119	0.226
Plate ID (Plate 2)	69/188	-0.04	0.027	-0.09, 0.01		0.151	0.235
R ² = 0.245; adjusted R ² = 0.184, AIC = -137.5, overall P-value = 5.5 x 10 ⁻⁶							
<i>TGF-β signaling</i>							
Characteristic [#]	n [†]	β	SE	95% CI	Overall P-value [‡]	p-value	q-value
Taxa-driven clusters[¶]					0.002		
• Cluster 2	69/188	0.13	0.032	0.06, 0.19		1 x 10⁻⁴	<0.001
• Cluster 3	15/188	0.08	0.049	-0.02, 0.18		0.101	0.161
• Cluster 4	64/188	0.07	0.033	0.01, 0.14		0.027	0.072
Age	188	0.01	0.003	0.00, 0.01		0.008	0.032
Season of inclusion **					0.097		

• Spring	47/188	-0.06	0.033	-0.13, 0.00		0.069	0.139
• Summer	37/188	-0.03	0.035	-0.10, 0.04		0.345	0.394
• Winter	47/188	0.02	0.032	-0.04, 0.09		0.464	0.464
Library size	188	1×10^{-6}	7×10^{-6}	0.00, 0.00		0.145	0.193
$R^2 = 0.135$; adjusted $R^2 = 0.096$, AIC = -146.0, overall P -value = 9.3×10^{-4}							

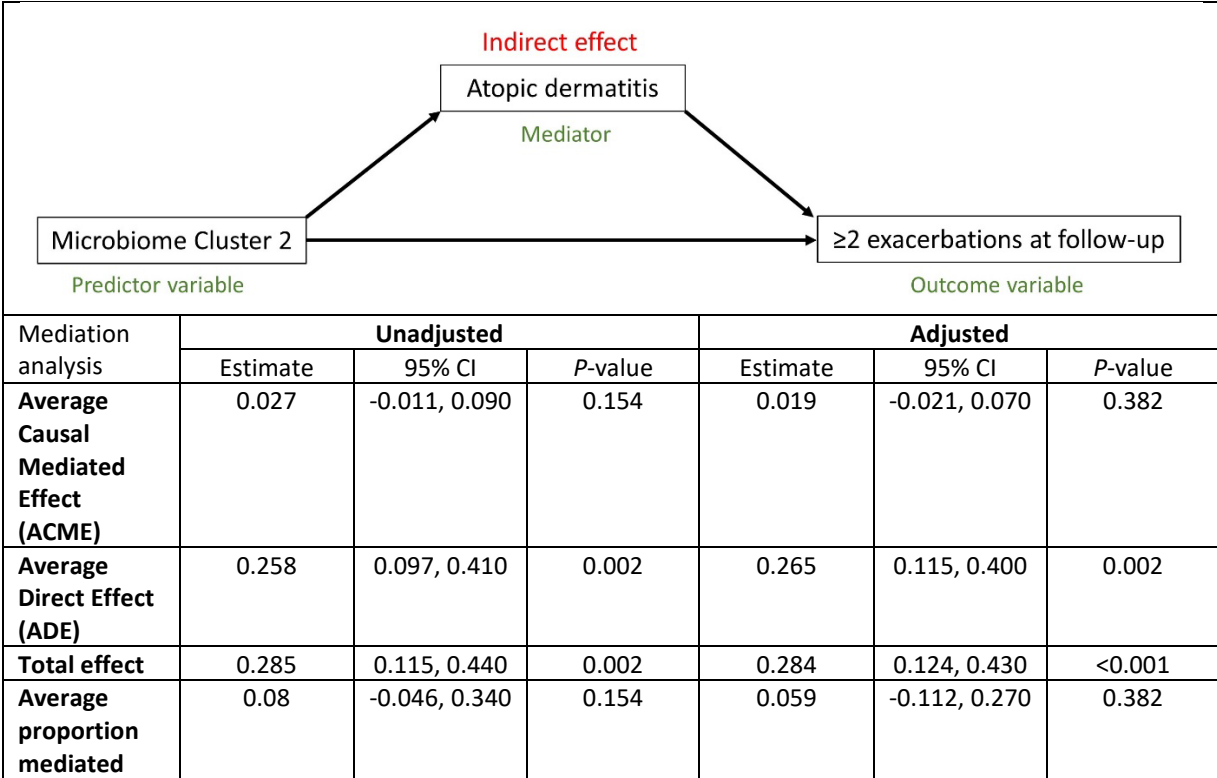
313 β : beta regression co-efficient, AIC: Akaike information criterion CI: confidence interval, NCS: nasal corticosteroids,
 314 SE: standard error, and TGF- β : transforming growth factor β . † Only children with available blood transcriptome
 315 data (n=188) were included in the regression analysis. # Variables in the model were selected according to a
 316 stepwise process. ¶ Cluster 1 (n=40/188, with the lowest enrichment scores median value) was the reference group
 317 for comparison in the stepwise process. * Inclusion center C (n=37/188) was randomly selected as a reference
 318 group for comparison in the stepwise process. ** Fall season (n=57/188) was randomly selected as a reference
 319 group for comparison in the stepwise process. ‡ The overall P -values were computed for taxa-driven clusters, in
 320 which all clusters were taken into account (without a reference group selection). The microbiota clusters with the
 321 statistically significant q -values after adjusting for covariates are highlighted in bold-face. q -value < 0.05 is
 322 considered statistically significant.

Table E6: A stepwise multiple logistic regression model of having ≥ 2 exacerbations/year during follow-up.

<i>≥ 2 exacerbations/year during follow-up</i>							
Characteristic [#]	n [†]	OR	SE	95% CI	Overall P-value [‡]	P-value	q-value
Taxa-driven clusters[¶]					1.92 x 10⁻⁴		
• Cluster 1	24/124	0.63	0.667	0.17, 2.33		0.481	0.569
• Cluster 3	11/124	0.06	1.06	0.01, 0.43		0.009	0.030
• Cluster 4	41/124	0.11	0.623	0.03, 0.34		3.6 x 10⁻⁴	0.005
Age	124	1.10	0.054	0.99, 1.23		0.077	0.144
Atopic dermatitis diagnosis	84/124	6.42	0.612	2.05, 23.1		0.002	0.016
Centre of Inclusion*					0.003		
• Centre A	10/124	0.23	1.24	0.01, 2.06		0.242	0.314
• Centre B	11/124	38.4	1.44	3.05, 1,169		0.012	0.030
• Centre D	3/124	0.48	1.48	0.02, 8.43		0.616	0.668
• Centre E	25/124	4.17	0.781	0.96, 21.0		0.068	0.144
• Centre F	27/124	0.93	0.775	0.20, 4.33		0.925	0.925
• Centre G	20/124	3.78	0.811	0.80, 19.8		0.101	0.150
Antibiotic prescription	39/124	5.52	0.622	1.72, 20.2		0.006	0.026
Sequencing run (run 2)	40/124	2.60	0.587	0.85, 8.69		0.104	0.150
McFadden's R ² = 0.341, Nagelkerke R ² = 0.503, AIC = 141.2							

AIC: Akaike information criterion, CI: confidence interval, SE: standard error, and OR: odds ratio. [†] Only children with severe asthma or severe wheezing were followed-up and have future exacerbation data (n=125/241), with n=1/125 patient with missing atopic dermatitis diagnosis was excluded from the regression analysis. [#] Variables in the model were selected according to a stepwise process. [¶] Cluster 2 (n = 48/124, with the highest % of ≥ 2 exacerbations/year during follow-up) was the reference group for comparison in the stepwise process. * Inclusion center C (n=28/124) was randomly selected as a reference group for comparison in the stepwise process. [‡] The overall P-values were computed for variables with >2 categories, in which all the variable's categories were taken into account (without a reference group selection). The microbiota clusters with the statistically significant q-values after adjusting for covariates are highlighted in bold-face. q-value < 0.05 is considered statistically significant.

Table E7: Mediation analysis investigating whether atopic dermatitis is mediating the association between microbiota Cluster 2 and follow-up exacerbations.



95% CI: 95% confidence interval. 95% CIs were computed by Quasi-Bayesian approximation (1000 simulations).

Supplementary Figures Legends:

Figure E1: The flow diagram of the inclusion numbers of the U-BIOPRED pediatric cohort, for which the oropharyngeal microbiota were characterized.

Figure E2: The general data analysis overview performed in this study.

Figure E3: Directed acyclic graph (DAG) to define the covariates (potential confounders) that may influence the microbiome clusters and the clinical asthma characteristics of interest.

Figure E4: Analysis of the negative and positive (mock) control samples with respect to the participants' oropharyngeal swabs. A; Distribution of the sample microbiome read counts across the control samples and oropharyngeal swabs. B; A box-whisker plot showing that negative extraction control samples had statistically significant lower Shannon α -diversity measure compared with the participants' oropharyngeal swab samples, in which the P-value was generated by a Mann-Whitney U test. C; Mean relative abundances of most abundant bacterial genera stratified by sample type, in which negative extraction controls mainly showed presence of *Corynebacterium_1*, *Pelomonas*, *Acidibacter* bacterial genera that were not found in oropharyngeal swab samples. D; The positive (mock community) control sample accurately represented all 17 different bacterial genera that were present in a mixture as described in the reference standard (Genomic DNA from Microbial Mock Community B (Even, Low Concentration), v5.1L, for 16S rRNA Gene Sequencing, HM-782D; BEI Resources, NIAID, NIH as part of the Human Microbiome Project).

Figure E5: Mean relative abundances of most abundant oropharyngeal bacterial genera across all samples (n=241).

Figure E6: Optimum number of hierarchical clusters based on multiple statistical indices calculated using the Bray-Curtis dissimilarity microbiome measure. Four was the suggested number of clusters based on the majority vote (3 out of 4 tested indices).

Figure E7: A; Topological data analysis (TDA) network based on the multi-dimensional scaling (MDS) lenses 1 and 2, wherein nodes were colored in accordance with spatial analysis of functional enrichment (SAFE) scores of hierarchical clustering assignments of participants. Four distinct regions (clusters) were observed in the TDA graph showing concordance of the TDA network with the hierarchical clusters assignments. **B;** TDA graph based on the principal co-ordinate analysis (PCoA) lenses 1 and 2, wherein nodes were colored in accordance with SAFE scores of hierarchical clustering assignments of participants.

Figure E8: Non-metric multi-dimensional scaling (NMDS) and principal co-ordinate analysis (PCoA) two-dimensional (first 2 dimensions) plots were depicted based on the Bray-Curtis dissimilarity microbiome measure, and nodes were colored according to the hierarchical clustering assignments. 95% confidence interval ellipses were added to the participants' nodes representing each cluster.

Figure E9: Violin box-whisker plot of Shannon α -diversity measure between the taxa-driven Clusters. The median diversity was highest for Cluster 4, followed by Cluster 2, and Cluster3, and was lowest in

Cluster1. Overall *P*-value was generated by the Kruskal-Wallis H test and pairwise *P*-values were generated by Dunn's post-hoc test.

Figure E10: Mean relative abundances of most abundant oropharyngeal bacterial stratified by the clusters.

Figure E11: A; Phylum-level relative abundances for each sample, grouped by the clusters. **B;** Genus-level relative abundances for each sample, grouped by the clusters. Only the most abundant bacterial taxa ($\geq 1\%$ and $\geq 5\%$ relative abundances for the phylum and genus levels, respectively) are shown.

Figure E12: Topological data analysis (TDA) network based on the multi-dimensional scaling (MDS) lenses 1 and 2, wherein nodes were colored according to the relative abundance of most abundant and differential amplicon sequence variants (ASVs); *Streptococcus* (A), *Veillonella* (B), *Rothia* (C), and *Haemophilus* (D). TDA regions showing the highest relative abundances of respective bacterial taxa are concordant with the clustering assignments regions shown in Figure E7A.

Figure E13: Topological data analysis (TDA) network based on the principal coordinate analysis (PCoA) lenses 1 and 2, wherein nodes were colored according to the relative abundance of most abundant and differential amplicon sequence variants (ASVs); *Streptococcus* (A), *Veillonella* (B), *Rothia* (C), and *Haemophilus* (D). TDA regions showing the highest relative abundances of respective bacterial taxa are concordant with the clustering assignments regions shown in Figure E7B.

Figure E14: Decision tree computed from a training data set ($\approx 75\%$ random participants) showed that the relative abundance of only 3 main bacterial genera could stratify participants into corresponding clusters. The performance of the decision tree was tested on a left-out validation set ($\approx 25\%$ random participants) exhibiting an accuracy of correct cluster classification = 0.86 (95% CI: 0.75-0.94, *P*-value = 8.24×10^{-15}).

Figure E15: Violin box-and-whisker plots showing the forced expiratory volume in 1 second (FEV₁) % predicted values pre- and post-salbutamol between the taxa-driven clusters. Overall *P*-values were generated by the Kruskal-Wallis H test and pairwise *P*-values were generated by Dunn's post-hoc test.

Figure E16: Violin box-and-whisker plots showing the number of aeroallergens sensitization between the taxa-driven clusters. Overall *P*-value was generated by the Kruskal-Wallis H test and pairwise *P*-values were generated by Dunn's post-hoc test.

Figure E17: Summary overview of clinical features associated with the taxa-driven clusters.

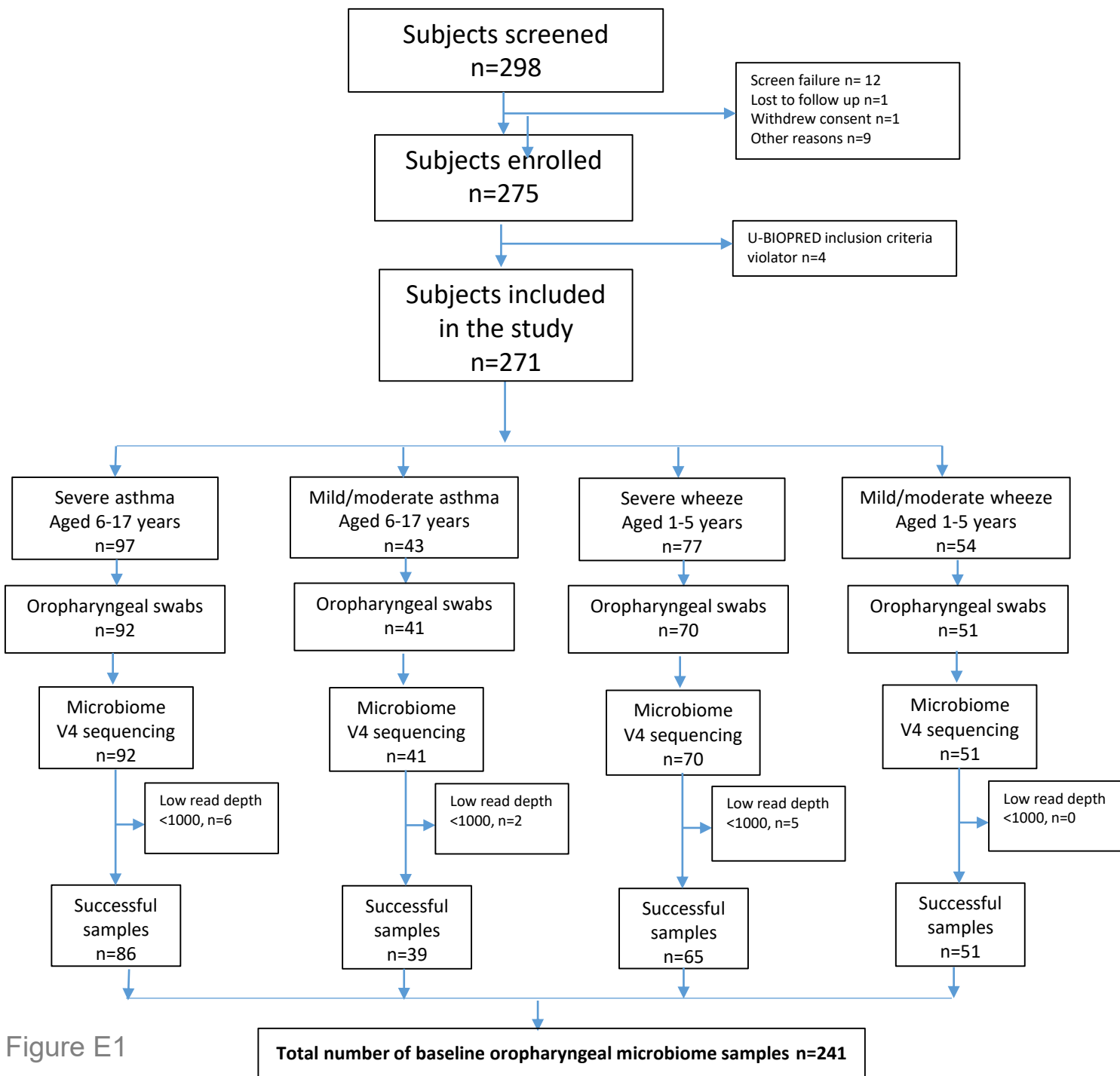


Figure E1

Figure E2

Unsupervised approach

Children with
asthma/wheezing

↓
Throat
swabs

↓
V4 16S rRNA
sequencing

↓
 β -diversity

↓
Clustering with
estimating optimum
number of clusters

↓ Clustering
validation

Obtained baseline
clusters and
phenotype discovery

Aim (1)
Check clusters differences
**In what clinical and microbiota
aspects do these clusters differ?**

Baseline peripheral
blood
transcriptome

↓

Hallmark pathways

Aim (2)
Check differential underlying biological pathways
**Are the baseline clusters associated with distinct underlying
transcriptomic pathways?**

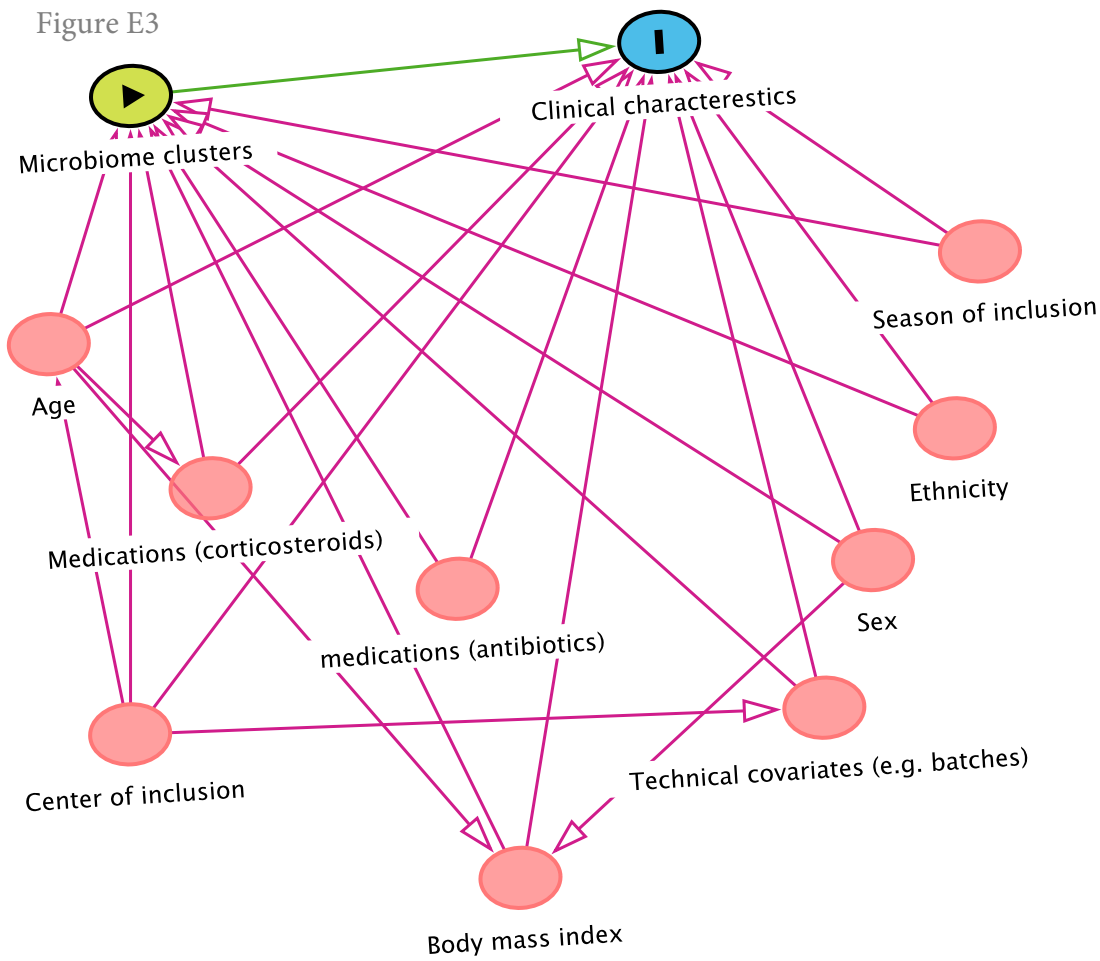
Follow-up of children with
severe asthma/wheezing
for 12-18 months

↓

Frequency of future
exacerbations/year

Aim (3)
Check future exacerbations
**Are the baseline clusters associated with the
risk of exacerbations?**

Figure E3



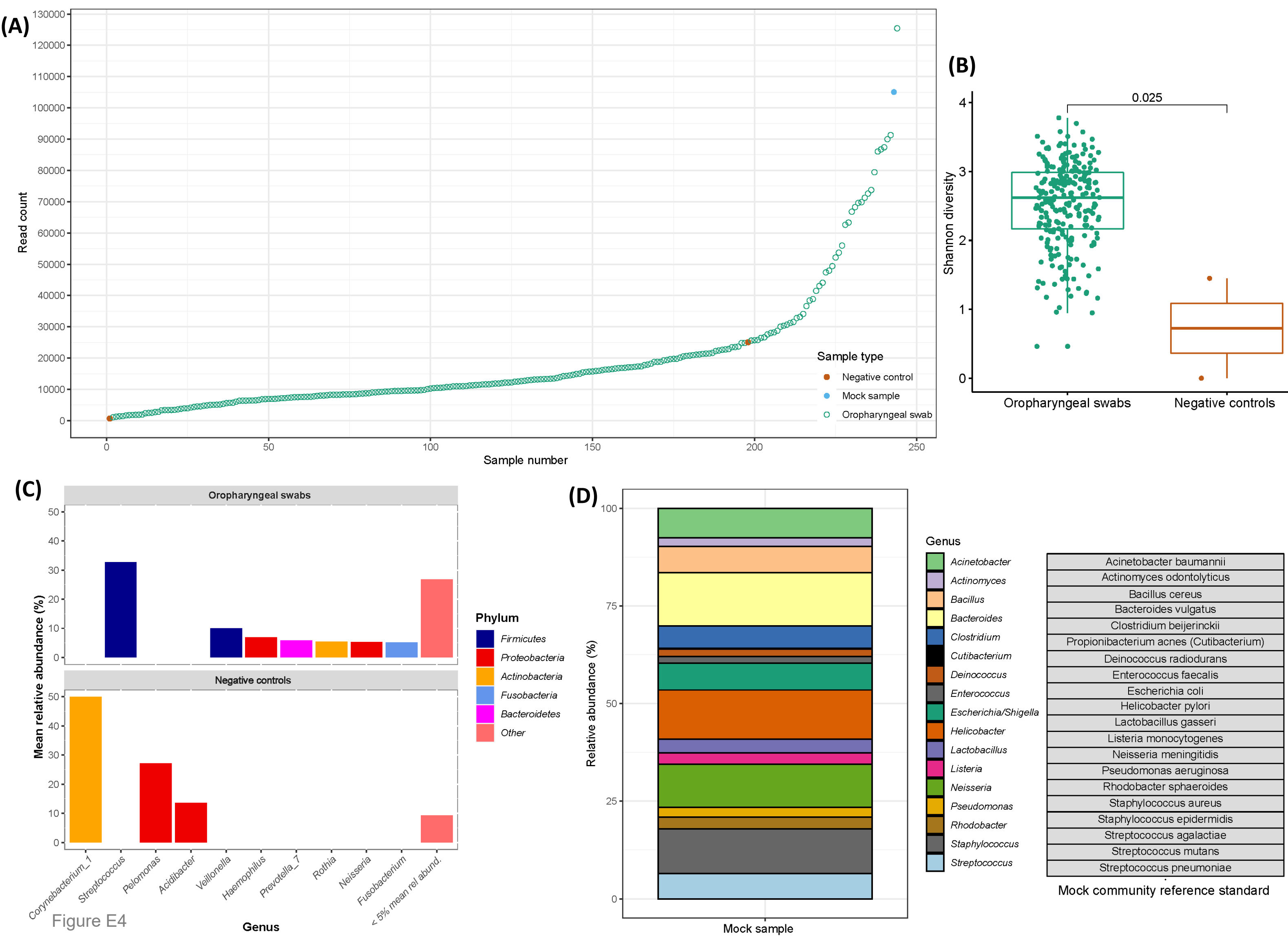


Figure E4

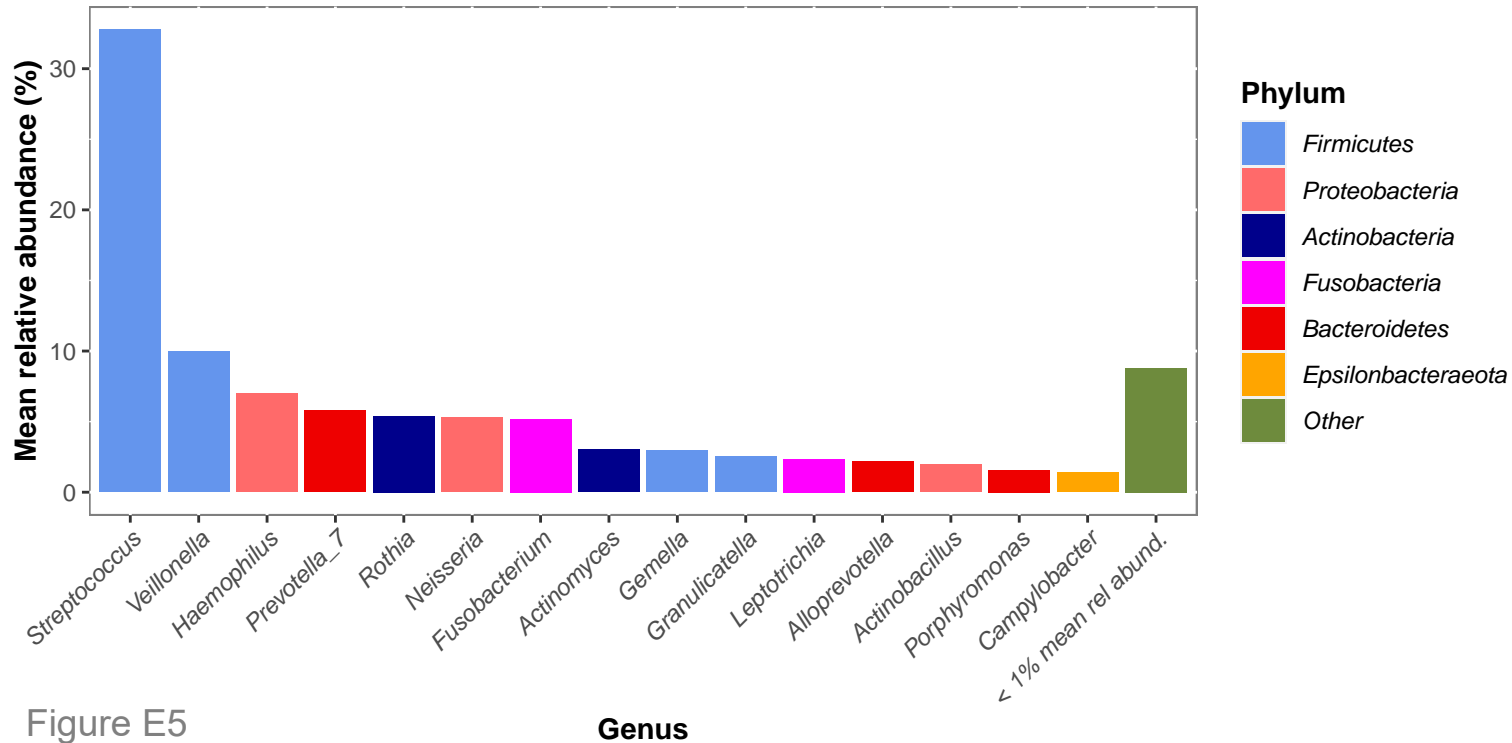


Figure E5

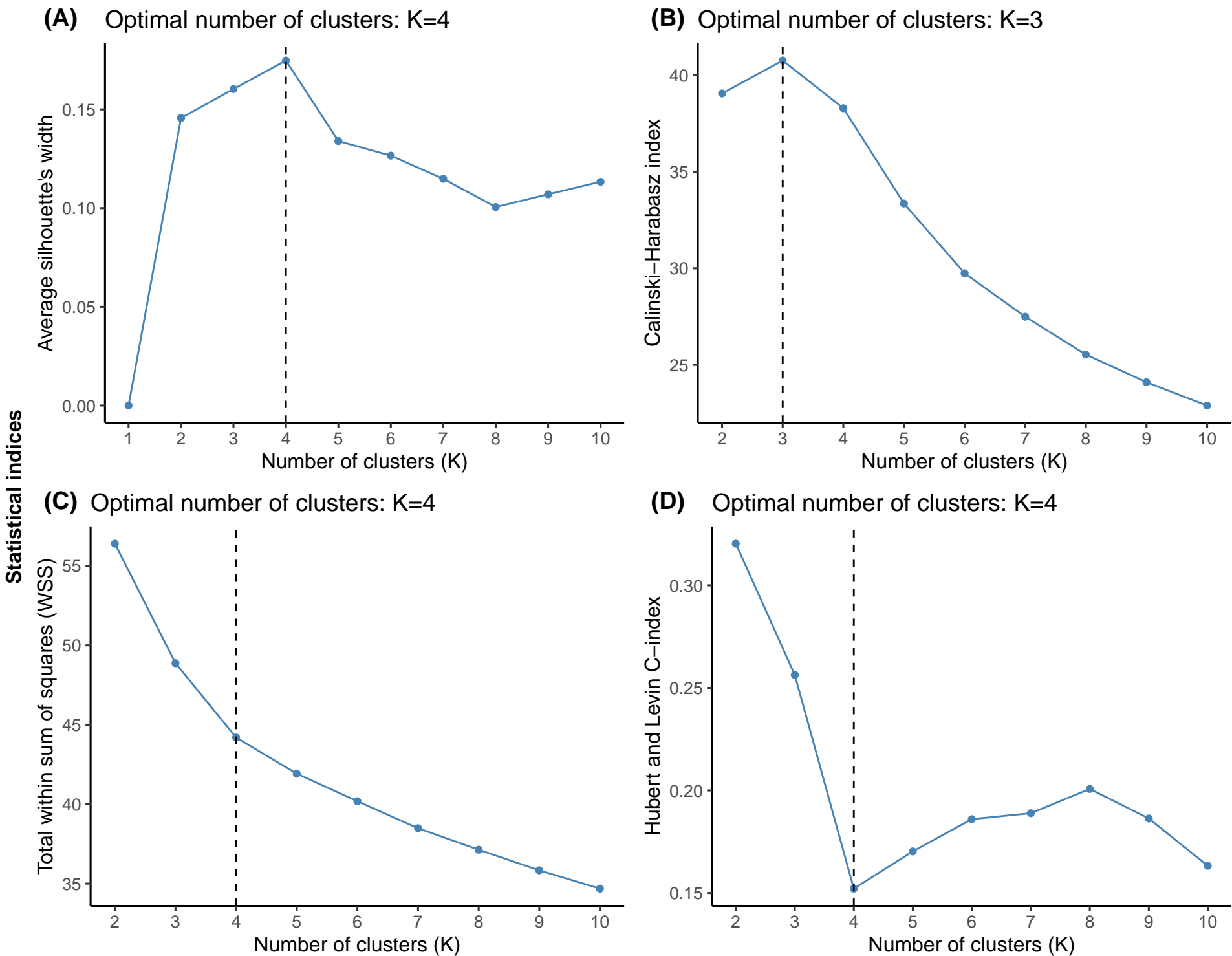


Figure E6

Optimum number of clusters

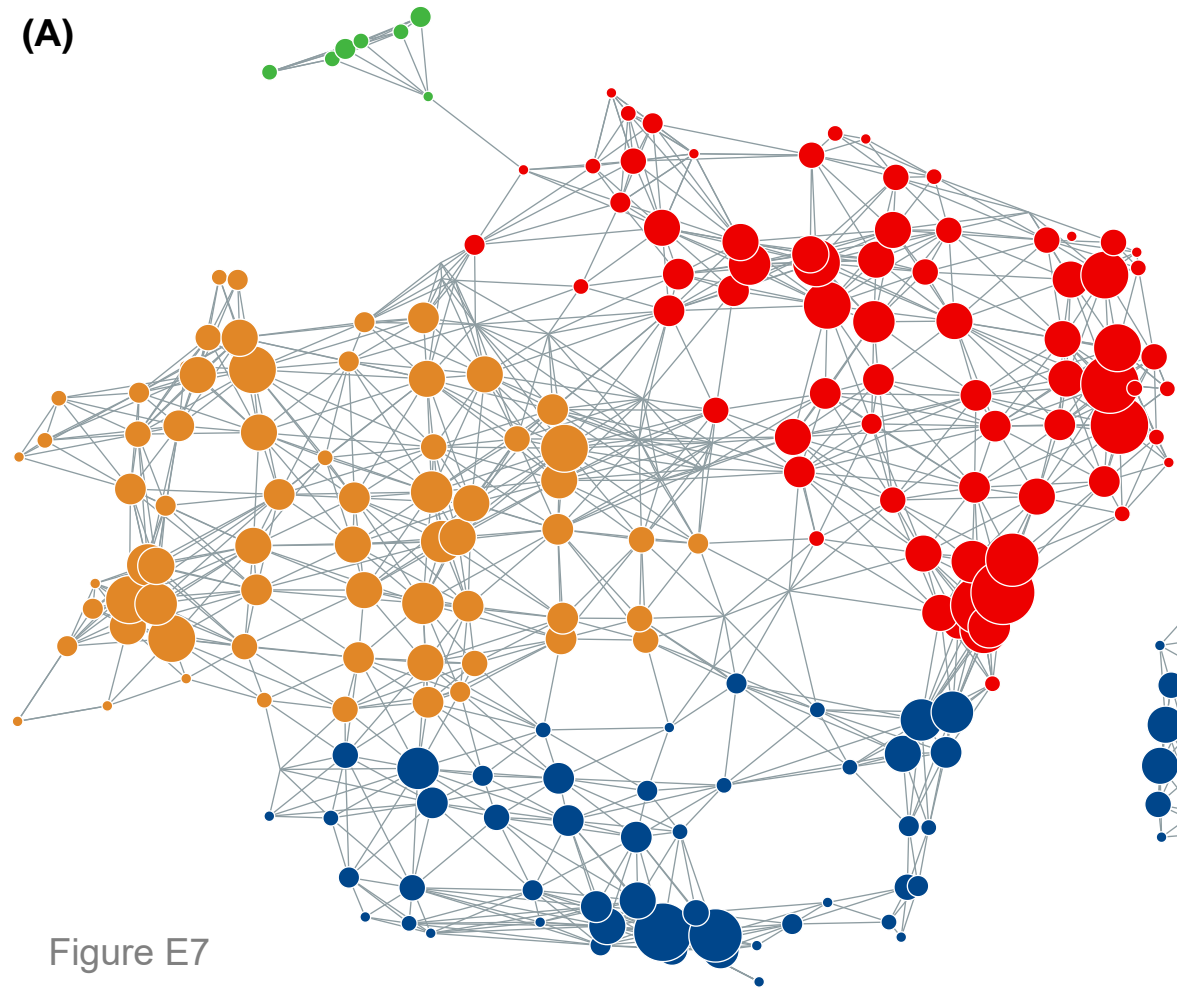
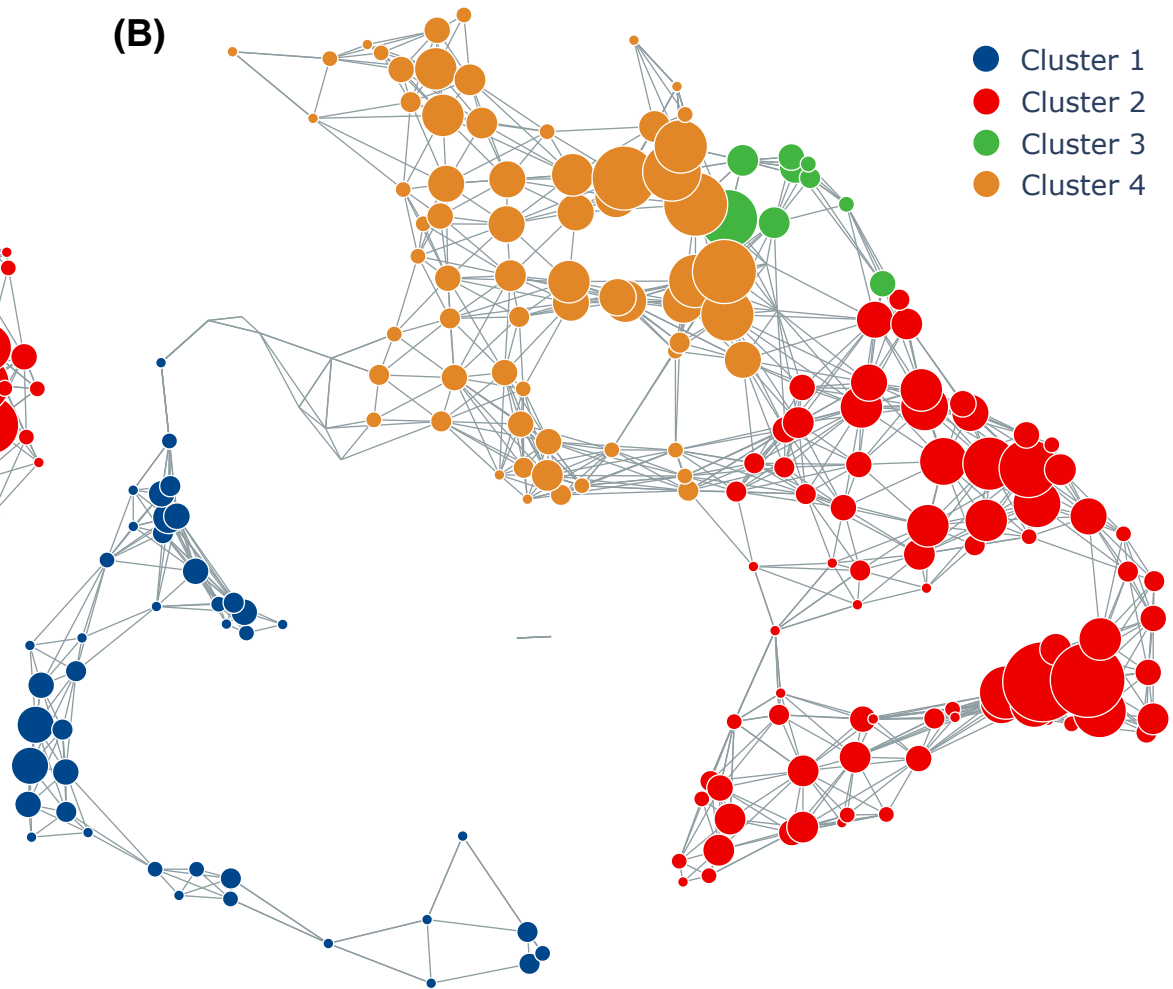
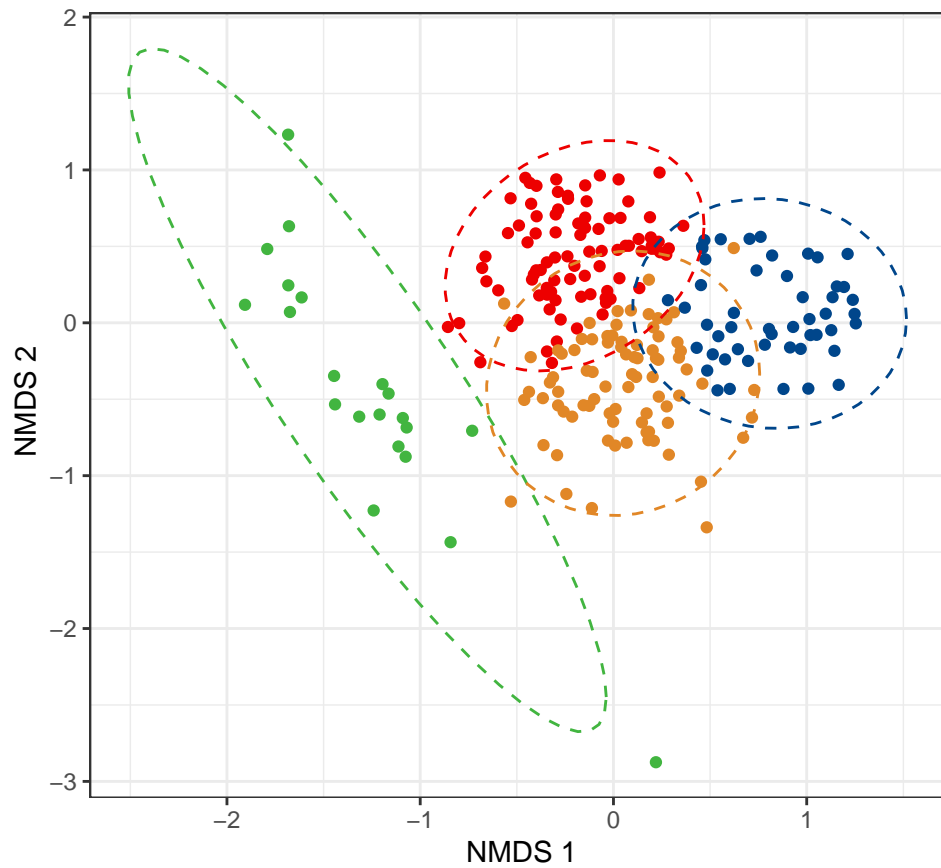
(A)**(B)**

Figure E7

Figure E8

Clusters Cluster 1 Cluster 2 Cluster 3 Cluster 4



Clusters  Cluster 1  Cluster 2  Cluster 3  Cluster 4

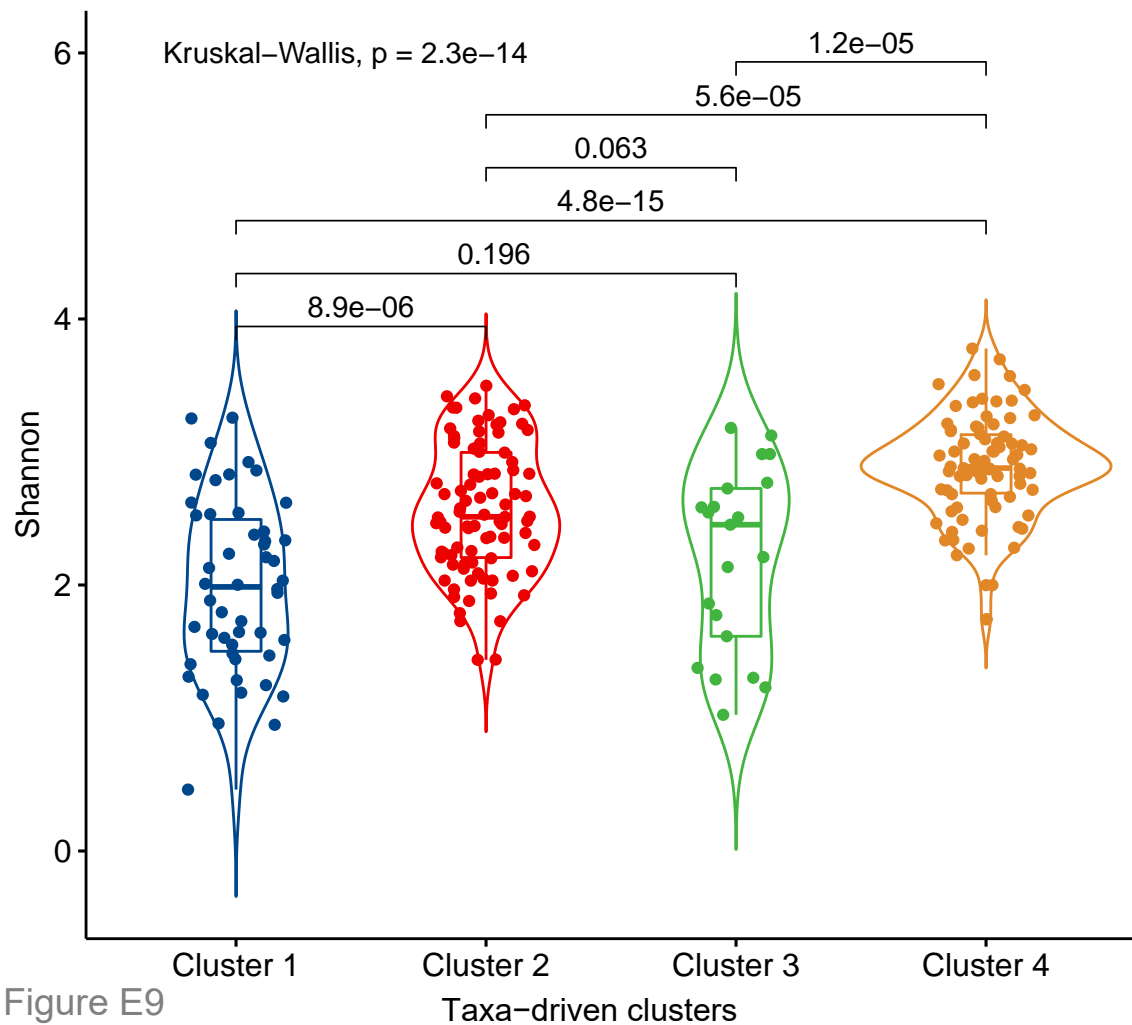
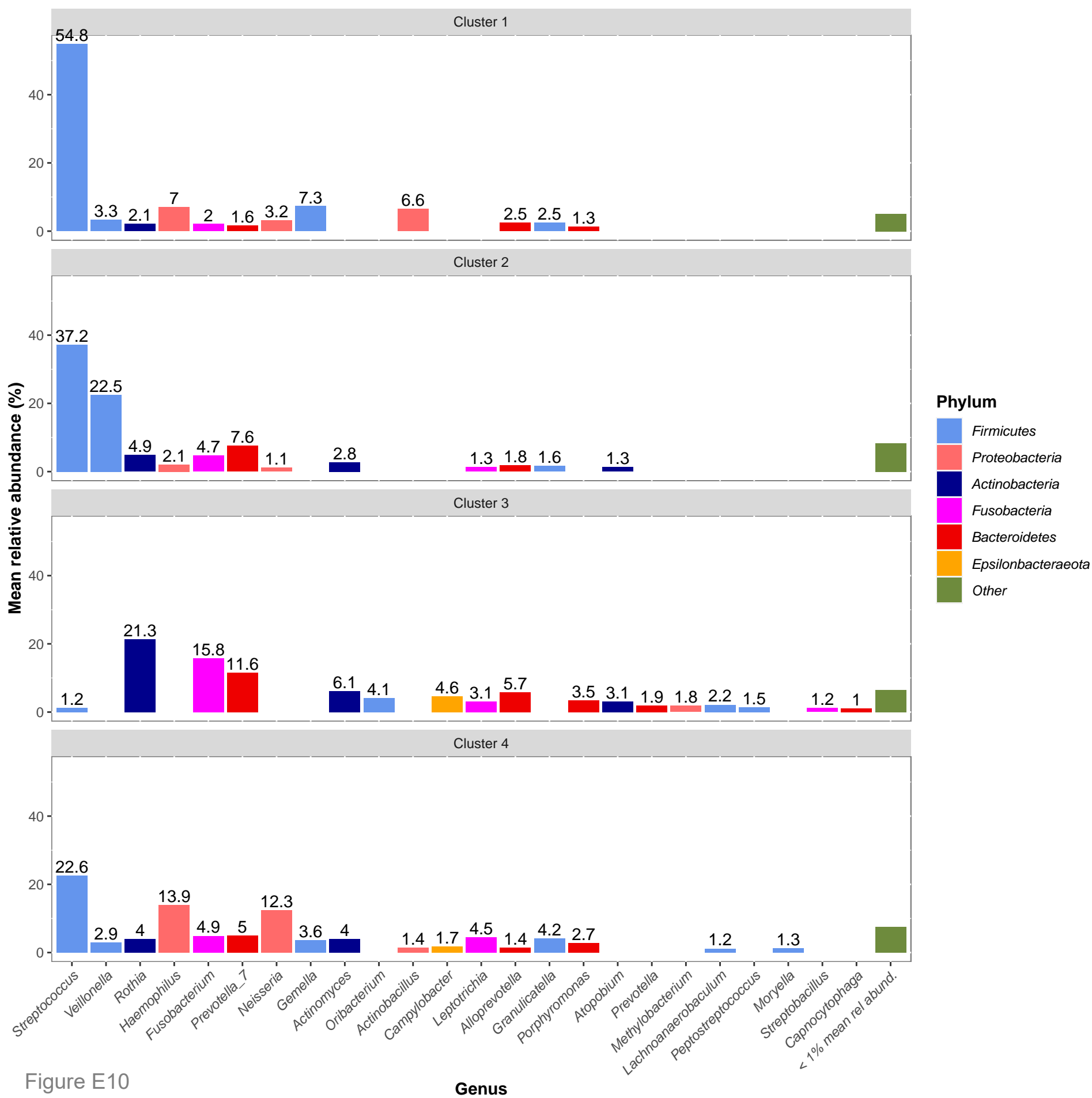


Figure E9



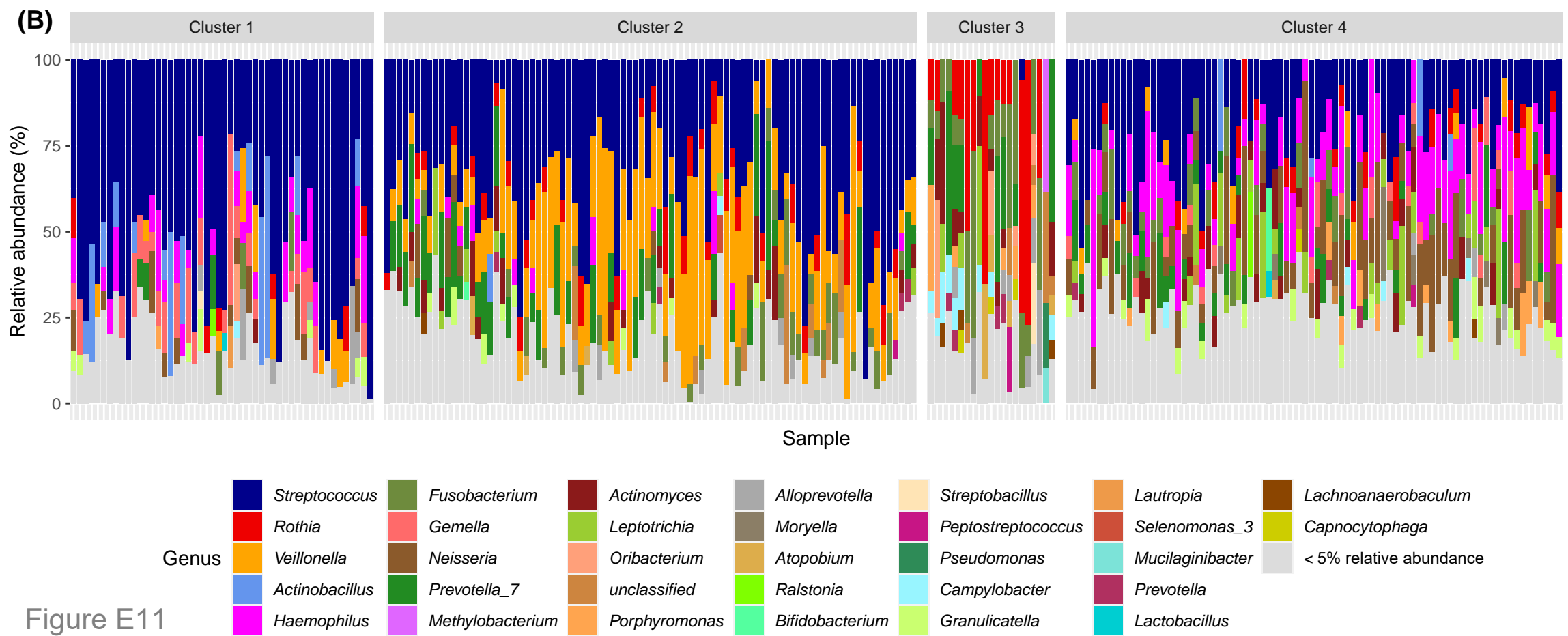
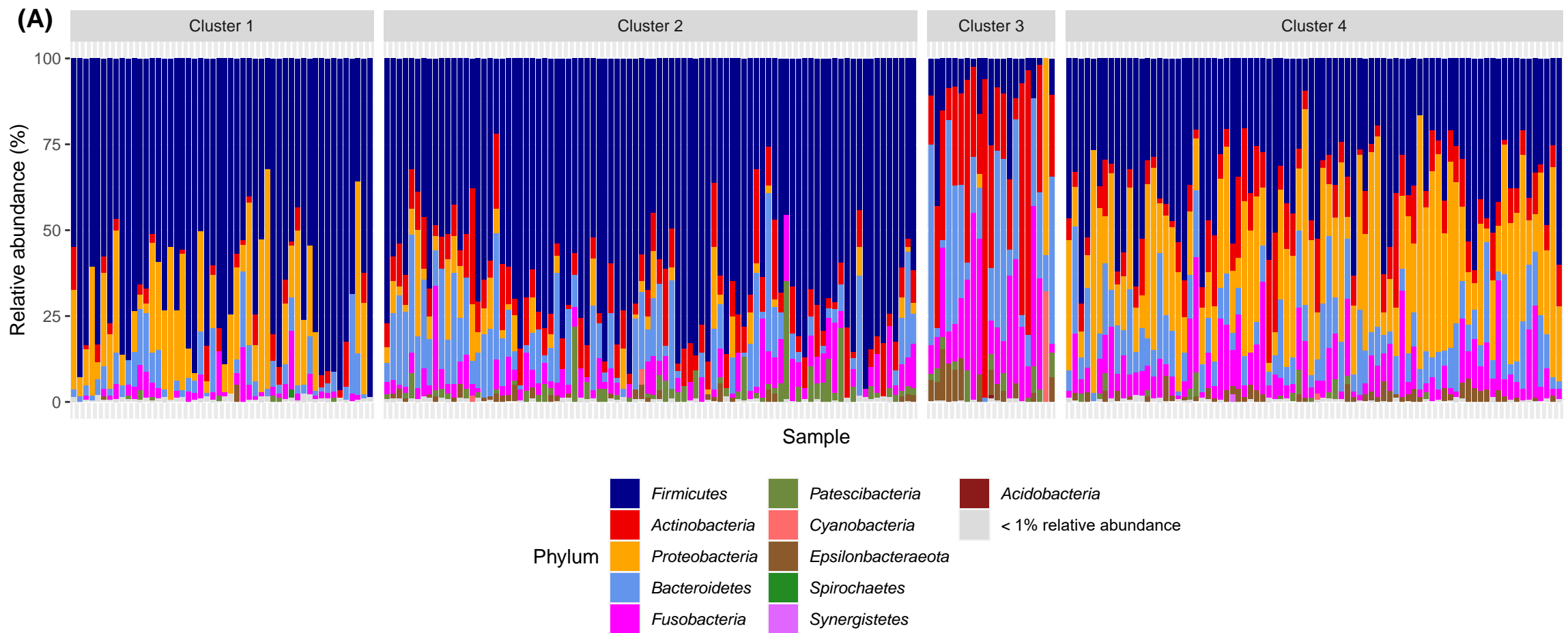
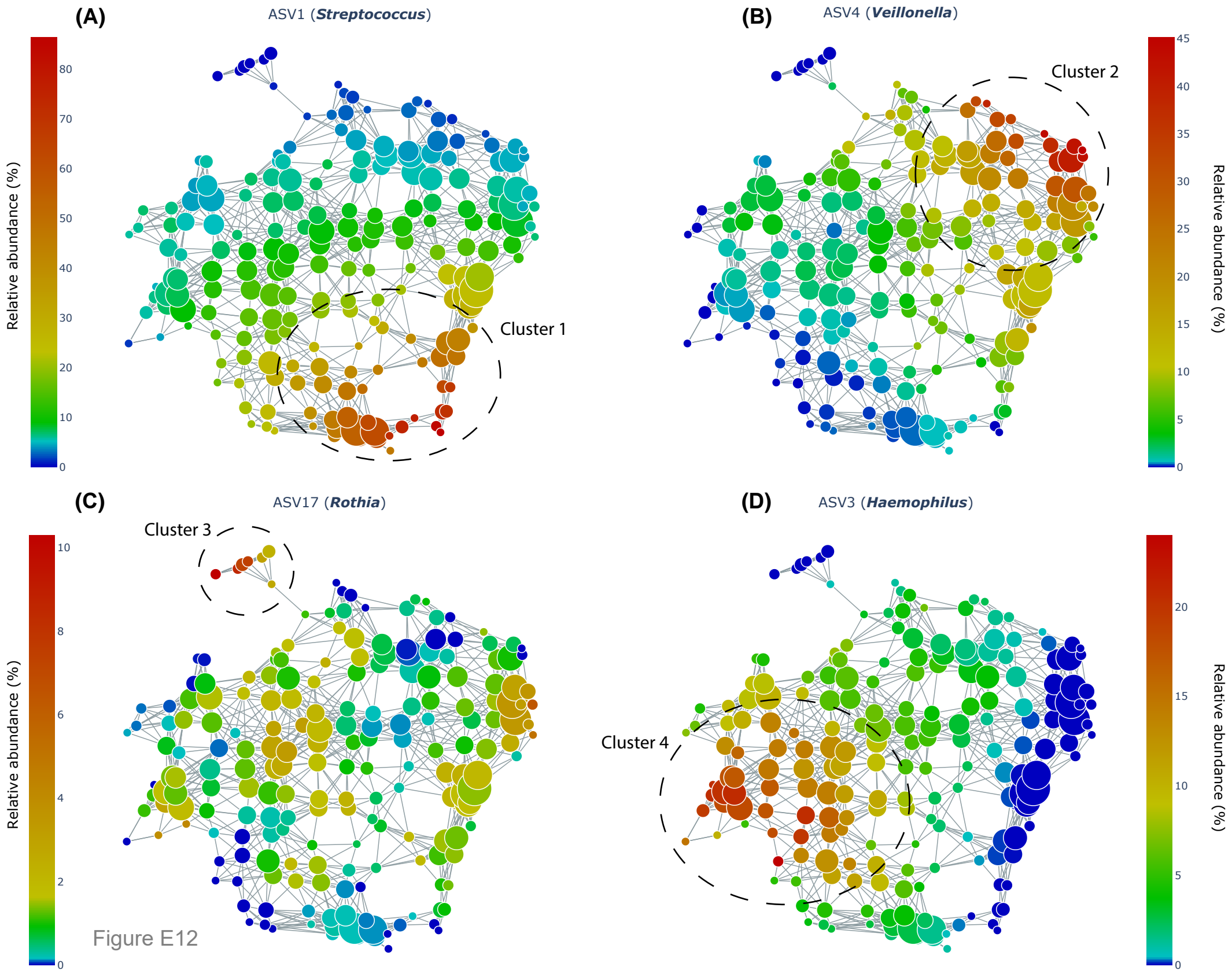


Figure E11



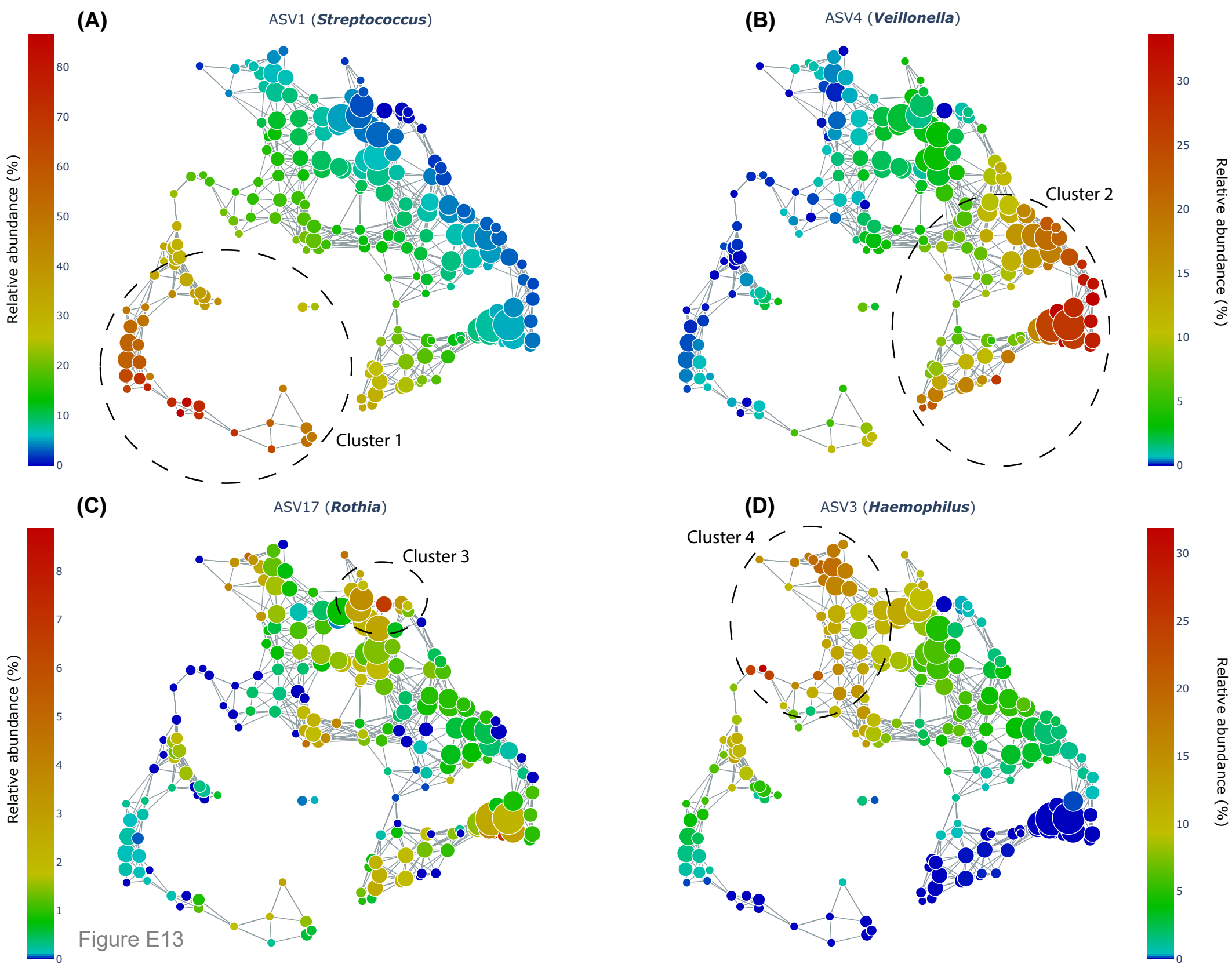
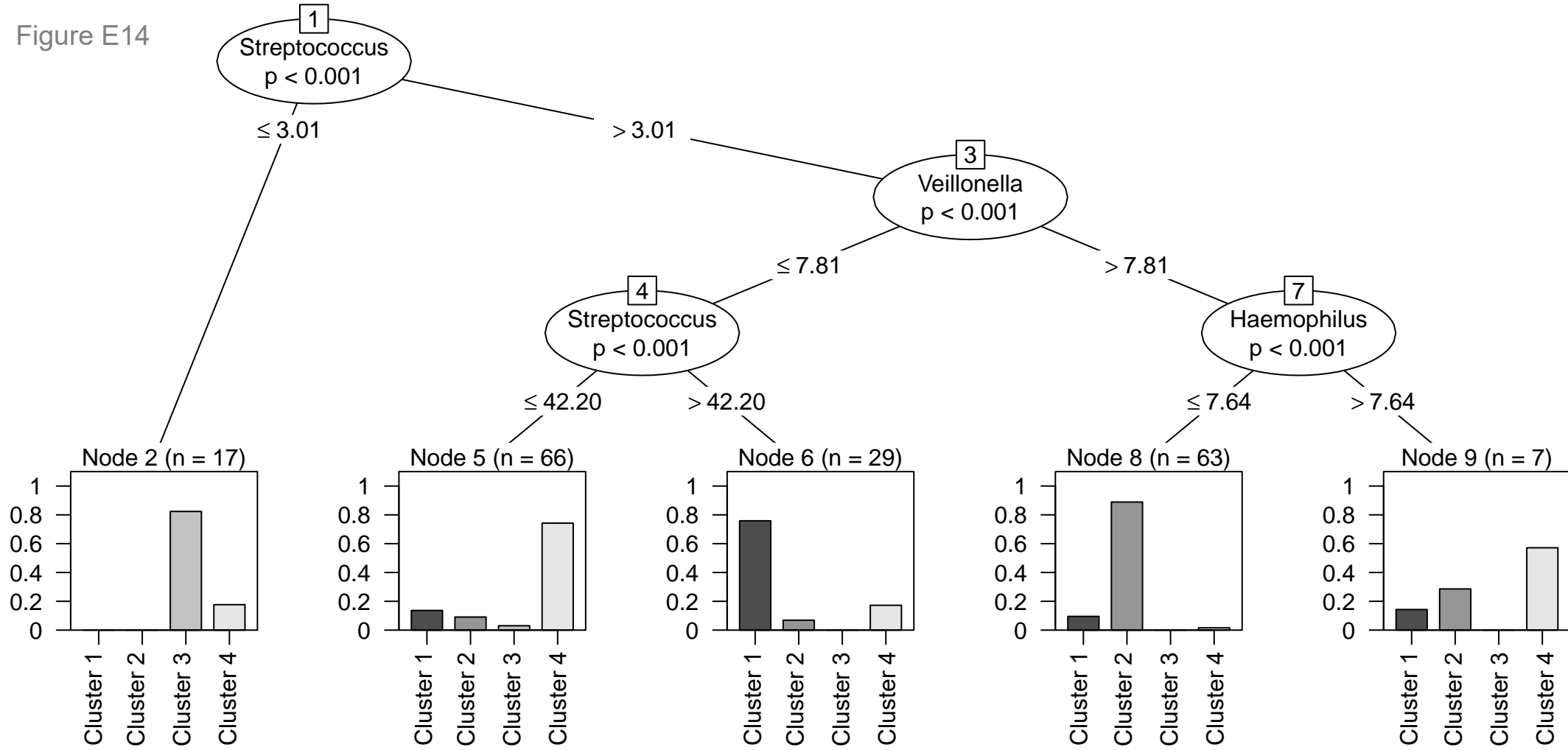


Figure E14



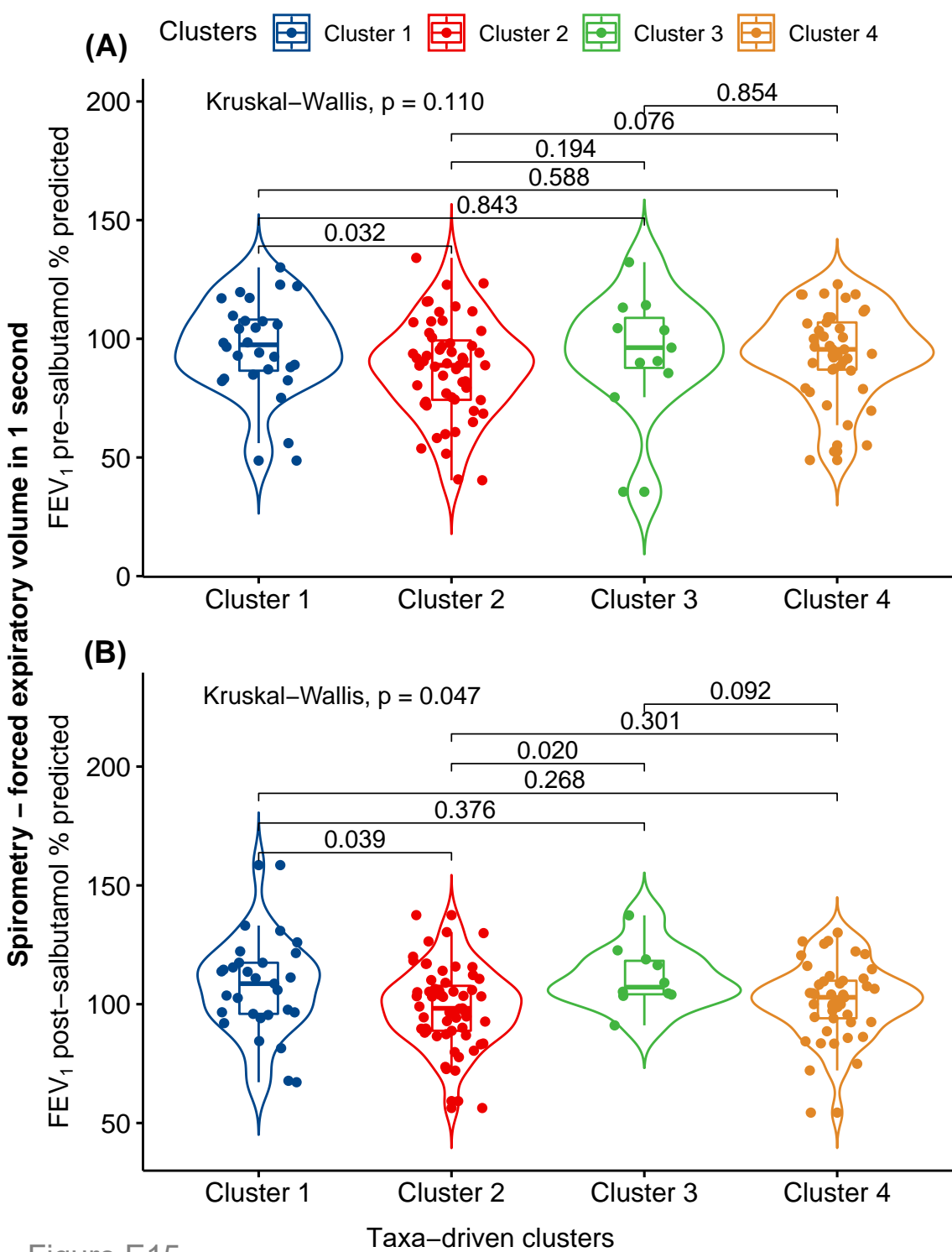
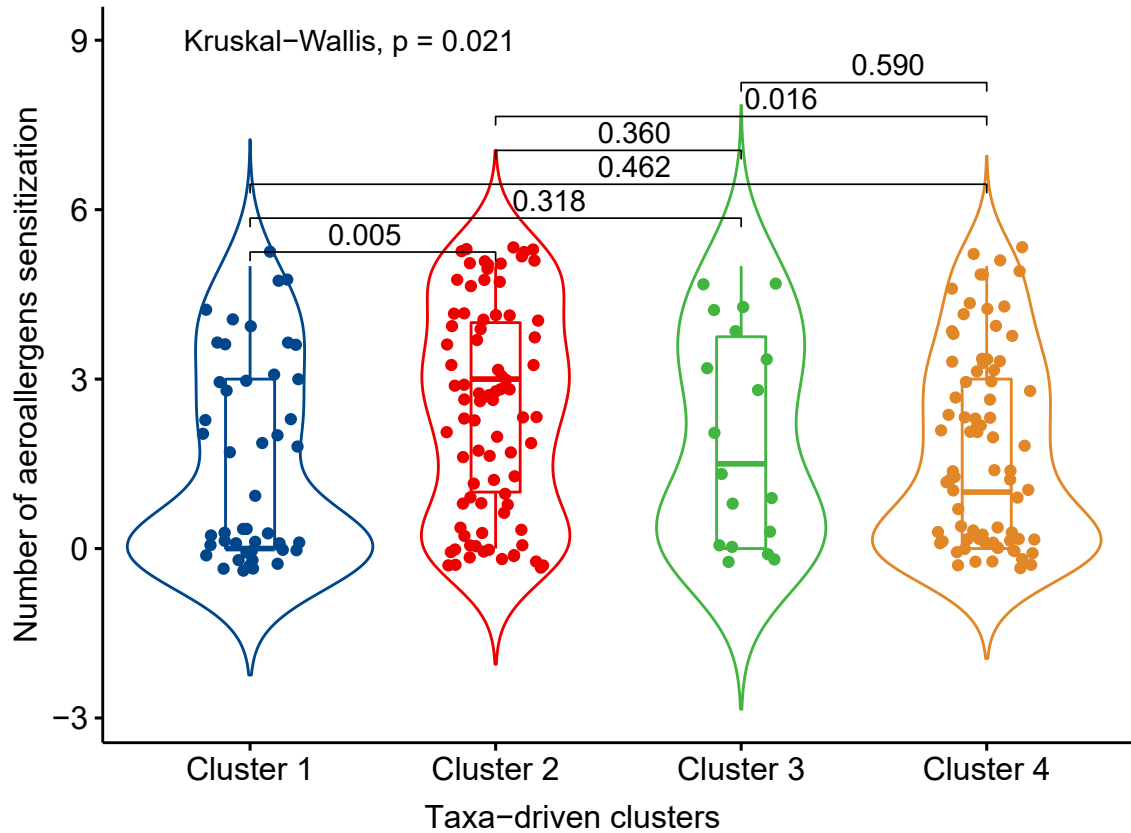
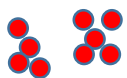


Figure E15

Figure E16

Clusters  Cluster 1  Cluster 2  Cluster 3  Cluster 4





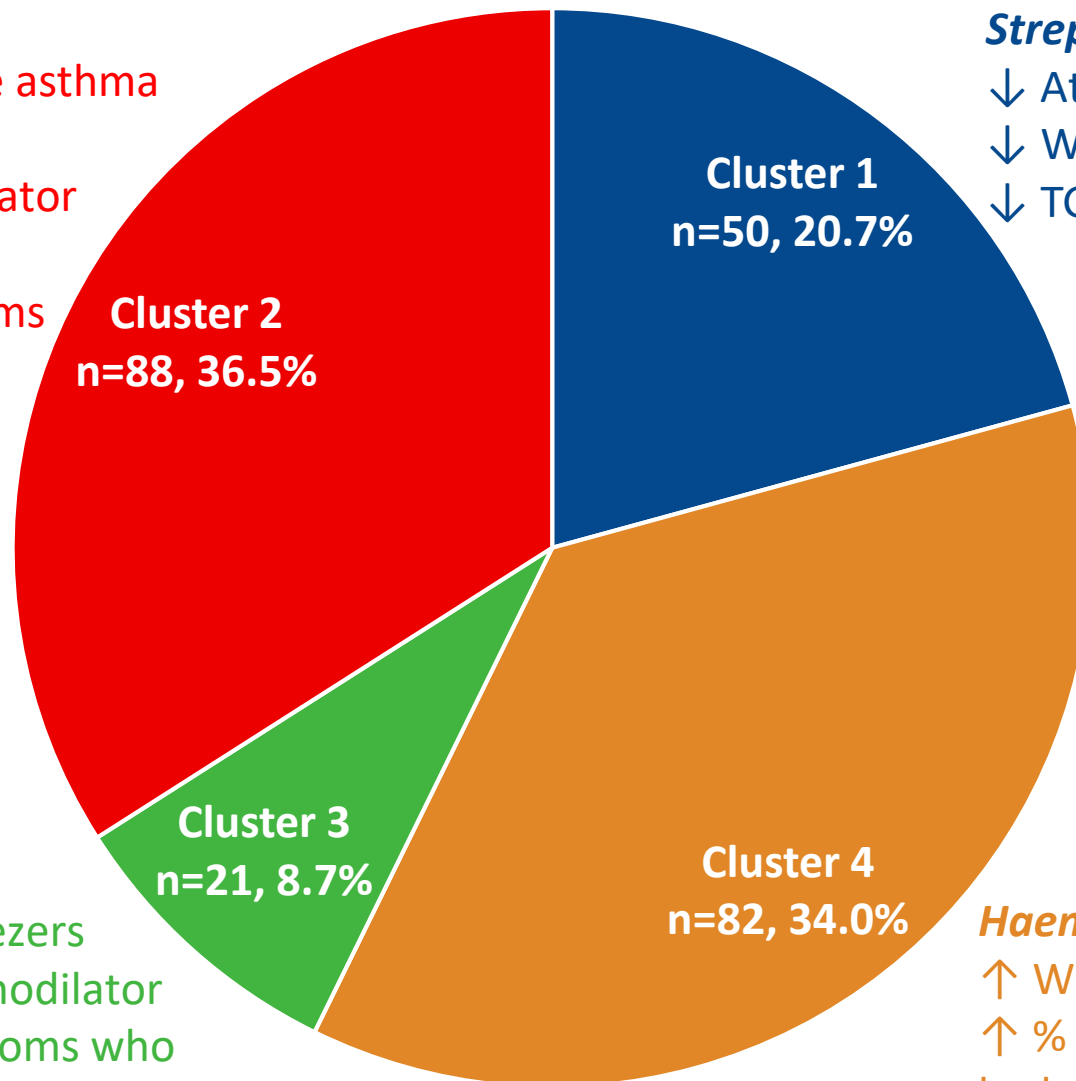
Veillonella-dominant

↑ % children with severe school-age asthma
↑ Atopic dermatitis, and ↑ Atopy
↓ FEV₁ % predicted post-bronchodilator
↑ TGF- β transcriptomic pathway
↑ % of children with severe symptoms who had ≥ 2 future exacerbations



Streptococcus-dominant

↓ Atopic dermatitis, and ↓ Atopy
↓ Wnt/ β -Catenin transcriptomic pathway
↓ TGF- β transcriptomic pathway



Rothia-dominant

↑ % severe preschool-age wheezers
↑ FEV₁ % predicted post-bronchodilator
↑ % children with severe symptoms who did not experience future exacerbations



Haemophilus/Neisseria-dominant

↑ Wnt/ β -Catenin transcriptomic pathway
↑ % children with severe symptoms who had one future exacerbation

Figure E17



U-BIOPRED

The U-BIOPRED consortium wishes to acknowledge the help and expertise of the following individuals and groups without whom, the study would not have been possible:

Definition for the U-BIOPRED Study Group Supplementary authors

 Clinical site research leads
 Platform leads
 Data cleaning team
 Data analysis team
 Scientific Board and Management Board members
 Core project management staff

Definition for the U-BIOPRED Study Group Contributors list

Significant involvement in the clinical study

Use of list:

This list is to be used for all non-core clinical papers.

Instructions

Follow up clinical papers should re-use the baseline cohort description paper lists, in order to recognize the clinical staff involved in the study.

U-BIOPRED Supplementary authors	
Name	Affiliation
Abdel-Aziz MI	Department of Respiratory Medicine, Amsterdam UMC, University of Amsterdam, Amsterdam, The Netherlands
Adcock I M	National Heart and Lung Institute, Imperial College, London, UK;
Andersson LI	Department of Respiratory Medicine, Karolinska University Hospital, Stockholm, Sweden
Auffray C	European Institute for Systems Biology and Medicine, CNRS-ENS-UCBL-INSERM, Lyon, France;
Badi YE,	National Heart and Lung Institute, Imperial College, London, UK;
Bakke P	Department of Clinical Science, University of Bergen, Bergen, Norway;
Bansal A T	Acclarogen Ltd, St. John's Innovation Centre, Cambridge, UK;
Baribaud F	Janssen R&D, LLC, Spring House, PA, USA
Bates S	Respiratory Therapeutic Unit, GSK, London, UK;
Bel E H	Academic Medical Centre, University of Amsterdam, Amsterdam, The Netherlands;
Bigler J	<i>Previously Amgen Inc</i>
Billing B	Department of Respiratory Medicine, Karolinska University Hospital, Stockholm, Sweden
Bisgaard H	COPSAC, Copenhagen Prospective Studies on Asthma in Childhood, Herlev and Gentofte Hospital, University of Copenhagen, Copenhagen, Denmark
Boedigheimer M J	Amgen Inc.; Thousand Oaks, USA
Bønnelykke K	COPSAC, Copenhagen Prospective Studies on Asthma in Childhood, Herlev and Gentofte Hospital, University of Copenhagen, Copenhagen, Denmark;
Brandsma J	University of Southampton, Southampton, UK
Brinkman P	Academic Medical Centre, University of Amsterdam, Amsterdam, The Netherlands;
Bucchioni E	Chiesi Pharmaceuticals SPA, Parma, Italy
Burg D	Centre for Proteomic Research, Institute for Life Sciences, University of Southampton, Southampton, UK



Bush A	National Heart and Lung Institute, Imperial College, London, UK; Royal Brompton and Harefield NHS trust, UK
Caruso M	Dept. Biomedical and Biotechnological Sciences, University of Catania, Catania, Italy;
Chalekis R	Institute of Environmental Medicine, Centre for Allergy Research, Karolinska Institutet, Stockholm, Sweden
Chanez P	Assistance publique des Hôpitaux de Marseille - Clinique des bronches, allergies et sommeil, Aix Marseille Université, Marseille, France
Chung F K	National Heart and Lung Institute, Imperial College, London, UK;
Checa T	Institute of Environmental Medicine, Centre for Allergy Research, Karolinska Institutet, Stockholm, Sweden
Compton C H	Respiratory Therapeutic Unit, GSK, London, UK
Corfield J	Areteva R&D, Nottingham, UK;
Cunoosamy D	Sanofi, Cambridge, USA
D'Amico A	University of Rome 'Tor Vergata', Rome Italy;
Dahlén B	Department of Respiratory Medicine, Karolinska University Hospital & Centre for Allergy Research, Karolinska Institutet, Stockholm, Sweden
Dahlén S E	Institute of Environmental Medicine, Centre for Allergy Research, Karolinska Institutet, and Department of Respiratory Medicine, Karolinska University Hospital, Stockholm, Sweden
De Meulder B	European Institute for Systems Biology and Medicine, CNRS-ENS-UCBL-INSERM, Lyon, France;
Djukanovic R	NIHR Southampton Respiratory Biomedical Research Unit and Clinical and Experimental Sciences, Southampton, UK;
Erpenbeck V J	Translational Medicine, Respiratory Profiling, Novartis Institutes for Biomedical Research, Basel, Switzerland;
Erzen D	Boehringer Ingelheim Pharma GmbH & Co. KG; Biberach, Germany
Fichtner K	Boehringer Ingelheim Pharma GmbH & Co. KG; Biberach, Germany
Fleming L J	National Heart and Lung Institute, Imperial College, London, UK; Royal Brompton and Harefield NHS trust, UK
Formaggio E	<i>Previously CROMSOURCE, Verona Italy</i>
Fowler S J	Division of infection, immunity and respiratory medicine, School of biological sciences, University of Manchester, Manchester University NHS Foundation Trust, Manchester Academic Health Science Centre, Manchester, United Kingdom
Frey U	University Children's Hospital, Basel, Switzerland;
Gahlemann M	Boehringer Ingelheim (Schweiz) GmbH, Basel, Switzerland;
Geiser T	Department of Respiratory Medicine, University Hospital Bern, Switzerland;
Goss V	NIHR Respiratory Biomedical Research Unit, University Hospital Southampton NHS Foundation Trust, Integrative Physiology and Critical Illness Group, Clinical and Experimental Sciences, Sir Henry Wellcome Laboratories, Faculty of Medicine, University of Southampton, Southampton, UK;
Guo Y	Data Science Institute, Imperial College, London, UK;
Hashimoto S	Academic Medical Centre, University of Amsterdam, Amsterdam, The Netherlands;
Haughney J	International Primary Care Respiratory Group, Aberdeen, Scotland;
Hedlin G	Dept. Women's and Children's Health & Centre for Allergy Research, Karolinska Institutet, Stockholm, Sweden;
Hekking P W	Academic Medical Centre, University of Amsterdam, Amsterdam, The Netherlands;
Higenbottam T	Allergy Therapeutics, West Sussex, UK;



Hohlfeld J M	Fraunhofer Institute for Toxicology and Experimental Medicine, Hannover, Germany
Holweg C	Respiratory and Allergy Diseases, Genentech, San Francisco, USA
Horváth I	Department of Pulmonology and Department of Public Health, Semmelweis University, Budapest, Hungary.
Howarth P	NIHR Southampton Respiratory Biomedical Research Unit, Clinical and Experimental Sciences and Human Development and Health, Southampton, UK
James A J	Institute of Environmental Medicine, Centre for Allergy Research, Karolinska Institutet, Stockholm, Sweden;
Knowles RG	Knowles Consulting Ltd, Stevenage, UK;
Kolmert J	Institute of Environmental Medicine, Centre for Allergy Research, Karolinska Institutet, Stockholm, Sweden
Konradsen J	Dept. Women's and Children's Health & Centre for Allergy Research, Karolinska Institutet, Stockholm, Sweden
Krug N	Fraunhofer Institute for Toxicology and Experimental Medicine, Hannover, Germany;
Lazarinis N	Department of Respiratory Medicine, Karolinska University Hospital & Centre for Allergy Research, Karolinska Institutet, Stockholm, Sweden
Li C-X	Department of Medicine Solna, Karolinska Institutet, Stockholm, Sweden
Loza M J	Janssen R&D, LLC, Spring House, PA, USA
Lutter R	Academic Medical Centre, University of Amsterdam, Amsterdam, The Netherlands;
Manta A	Roche Diagnostics GmbH, Mannheim, Germany
Masefield S	European Lung Foundation, Sheffield, UK;
Maitland-van der Zee Anke-Hilse	Department of Respiratory Medicine, Amsterdam UMC, University of Amsterdam, Amsterdam, The Netherlands;
Matthews J G	Respiratory and Allergy Diseases, Genentech, San Francisco, USA;
Mazein A	European Institute for Systems Biology and Medicine, CNRS-ENS-UCBL-INSERM, Lyon, France
Middelveld R J M	Centre for Allergy Research, Karolinska Institutet, Stockholm, Sweden
Miralpeix M	Almirall, Barcelona, Spain;
Montuschi P	Università Cattolica del Sacro Cuore, Milan, Italy;
Murray C S	Division of infection, immunity and respiratory medicine, School of biological sciences, University of Manchester, Manchester University NHS Foundation Trust, and Manchester Academic Health Science Centre, Manchester, United Kingdom
Musial J	Dept. of Medicine, Jagiellonian University Medical College, Krakow, Poland
Mumby, S	National Heart and Lung Institute, Imperial College, London, UK
Myles D	Respiratory Therapeutic Unit, GSK, London, UK;
Nordlund B	Dept. Women's and Children's Health & Centre for Allergy Research, Karolinska Institutet, Stockholm, Sweden
Pandis I	Data Science Institute, Imperial College, London, UK
Pavlidis S	National Heart and Lung Institute, Imperial College, London, UK
Postle A	University of Southampton, UK
Powel P	European Lung Foundation, Sheffield, UK;
Praticò G	CROMSOURCE, Verona, Italy
Puig Valls M	CROMSOURCE, Barcelona, Spain
Rao N	Janssen R&D, LLC, Spring House, PA, USA
Reinke S	Institute of Environmental Medicine, Karolinska Institutet, Stockholm, Sweden
Riley J	Respiratory Therapeutic Unit, GSK, London, UK;
Roberts A	Asthma UK, London, UK;



Roberts G	NIHR Southampton Respiratory Biomedical Research Unit, Clinical and Experimental Sciences and Human Development and Health, Southampton, UK;
Rowe A	Janssen R&D, UK;
Sandström T	Dept of Public Health and Clinical Medicine, Umeå University, Umeå, Sweden;
Schofield JPR	Centre for Proteomic Research, Institute for Life Sciences, University of Southampton, Southampton, UK
Seibold W	Boehringer Ingelheim Pharma GmbH, Biberach, Germany
Shaw D E	Respiratory Research Unit, University of Nottingham, UK;
Sigmund R	Boehringer Ingelheim Pharma GmbH & Co. KG; Biberach, Germany
Singer F	Pediatric Respiratory Medicine, Department of Pediatrics, Inselspital, Bern University Hospital, University of Bern, Bern, Switzerland.
Skipp P J	Centre for Proteomic Research, Institute for Life Sciences, University of Southampton, Southampton, UK
Smicker M	Sanofi, Cambridge, USA
Sousa A R	Respiratory Therapeutic Unit, GSK, London, UK;
Sparreman-Mikus M	Department of Medicine Huddinge, Karolinska Institutet, and Department of Respiratory Medicine, Karolinska University Hospital, Stockholm, Sweden
Sterk P J	Academic Medical Centre, University of Amsterdam, Amsterdam, The Netherlands;
Ström M	Department of Medicine Solna, Karolinska Institutet, Stockholm, Sweden
Sun K	Data Science Institute, Imperial College, London, UK
Thornton B	MSD, USA
Uddin M	AstraZeneca BioPharmaceuticals R&D, Gothenburg, Sweden
Versi A	National Heart and Lung Institute, Imperial College, London, UK
Vestbo J	Centre for Respiratory Medicine and Allergy, Institute of Inflammation and Repair, University of Manchester and University Hospital of South Manchester, Manchester Academic Health Sciences Centre, Manchester, United Kingdom
Vissing N H	COPSAC, Copenhagen Prospective Studies on Asthma in Childhood, Herlev and Gentofte Hospital, University of Copenhagen, Copenhagen, Denmark;
Wagers S S	BioSci Consulting, Maasmechelen, Belgium
Wheelock A M	Respiratory Medicine Unit, Department of Medicine Solna and Center for Molecular Medicine, Karolinska Institutet, Stockholm, Sweden; and Department of Respiratory Medicine and Allergy, Karolinska University Hospital Solna, Stockholm, Sweden;
Wheelock C E	Institute of Environmental Medicine, Centre for Allergy Research, Karolinska Institutet, Stockholm, Sweden;
Wilson S J	Histochemistry Research Unit, Faculty of Medicine, University of Southampton, Southampton, UK;
Yasinska V	Department of Medicine Huddinge, Karolinska Institutet, and Department of Respiratory Medicine, Karolinska University Hospital, Stockholm, Sweden
Zounemat Kermani, N	Data Science Institute, Imperial College, London, UK

Contributors

Ahmed H, European Institute for Systems Biology and Medicine, CNRS-ENS-UCBL-INSERM, Lyon, France;

Aliprantis Antonios, Merck Research Laboratories, Boston, USA;



Allen David, North West Severe Asthma Network, Pennine Acute Hospital NHS Trust, UK
Alving Kjell, Dept Women's & Children's Health, Uppsala University, Uppsala, Sweden
Badorrek P, Fraunhofer ITEM; Hannover, Germany
Balgoma David, Centre for Allergy Research, Karolinska Institutet, Stockholm, Sweden
Ballereau S, European institute for Systems Biology and Medicine, University of Lyon, France
Barber Clair, NIHR Southampton Respiratory Biomedical Research Unit and Clinical and Experimental Sciences, Southampton, UK;
Batuwitage Manohara Kanangana, Data Science Institute, Imperial College, London, UK
Bautmans An, MSD, Brussels, Belgium
Bedding A, Roche Diagnostics GmbH, Mannheim, Germany
Behndig AF, Umeå University, Umea, Sweden
Beleta Jorge, Almirall S.A., Barcelona, Spain;
Berglind A, MSD, Brussels, Belgium
Bochenek Grazyna, II Department of Internal Medicine, Jagiellonian University Medical College, Krakow, Poland;
Braun Armin, Fraunhofer Institute for Toxicology and Experimental Medicine, Hannover, Germany;
Campagna D, Department of Clinical and Experimental Medicine, University of Catania, Catania, Italy;
<i>Carayannopoulos Leon, Previously at: MSD, USA;</i>
Casaulta C, University Children's Hospital of Bern, Switzerland
Chaiboonchoe A, European Institute for Systems Biology and Medicine, CNRS-ENS-UCBL-INSERM, Lyon, France;
Chaleckis Romanas, Centre of Allergy Research, Karolinska Institutet, Stockholm, Sweden
Davison Timothy Janssen R&D, LLC, Spring House, PA, USA
De Alba Jorge, Almirall S.A., Barcelona, Spain;
De Lepeleire Inge, MSD, Brussels, BE
Dekker Tamara, Academic Medical Centre, University of Amsterdam, Amsterdam, The Netherlands;
Delin Ingrid, Centre for Allergy Research, Karolinska Institutet, Stockholm, Sweden
Dennison P, NIHR Southampton Respiratory Biomedical Research Unit, Clinical and Experimental Sciences, NIHR-Wellcome Trust Clinical Research Facility, Faculty of Medicine, University of Southampton, Southampton, UK;
Dijkhuis Annemiek, Academic Medical Centre, University of Amsterdam, Amsterdam, The Netherlands;
Dodson Paul, AstraZeneca BioPharmaceuticals R&D, Gothenburg, Sweden
Draper Aleksandra, BioSci Consulting, Maasmechelen, Belgium;
Dyson K, CROMSOURCE; Stirling, UK
Edwards Jessica, Asthma UK, London, UK;
El Hadjam L, European Institute for Systems Biology and Medicine, University of Lyon
Emma Rosalia, Department of Biomedical and Biotechnological Sciences, University of Catania, Catania, Italy;
Ericsson Magnus, Karolinska University Hospital, Stockholm, Sweden



Faulenbach C, Fraunhofer ITEM; Hannover, Germany
Flood Breda, European Federation of Allergy and Airways Diseases Patient's Associations, Brussels, Belgium
Galfy G, Semmelweis University, Budapest, Hungary;
Gallart Hector, Centre for Allergy Research, Karolinska Institutet, Stockholm, Sweden
Garissi D, Global Head Clinical Research Division, CROMSOURCE, Italy
Gent J, Royal Brompton and Harefield NHS Foundation Trust, London, UK;
Gerhardsson de Verdier M, AstraZeneca BioPharmaceuticals R&D, Gothenburg, Sweden
Gibeon D, National Heart and Lung Institute, Imperial College, London, UK;
Gomez Cristina, Centre for Allergy Research, Karolinska Institutet, Stockholm, Sweden
Gove Kerry, NIHR Southampton Respiratory Biomedical Research Unit and Clinical and Experimental Sciences, Southampton, UK;
Gozzard Neil, UCB, Slough, UK;
Guilmant-Farry E, Royal Brompton Hospital, London, UK
Henriksson E, Karolinska University Hospital & Karolinska Institutet, Stockholm, Sweden
Hewitt Lorraine, NIHR Southampton Respiratory Biomedical Research Unit, Southampton, UK
Hoda U, Imperial College, London, UK
Hu Richard, Amgen Inc. Thousand Oaks, USA
Hu Sile, National Heart and Lung Institute, Imperial College, London, UK;
Hu X, Amgen Inc.; Thousand Oaks, USA
Jeyasingham E, UK Clinical Operations, GSK, Stockley Park, UK
Johnson K, Centre for respiratory medicine and allergy, Institute of Inflammation and repair, University Hospital of South Manchester, NHS Foundation Trust, Manchester, UK
Jullian N, European Institute for Systems Biology and Medicine, University of Lyon
Kamphuis Juliette, Longfonds, Amersfoort, The Netherlands;
Kennington Erika J., Asthma UK, London, UK;
Kerry Dyson, CromSource, Stirling, UK;
Kerry G, Centre for respiratory medicine and allergy, Institute of Inflammation and repair, University Hospital of South Manchester, NHS Foundation Trust, Manchester, UK
Klüglich M, Boehringer Ingelheim Pharma GmbH & Co. KG; Biberach, Germany
Knobel Hugo, Philips Research Laboratories, Eindhoven, The Netherlands;
Knox Alan J, Respiratory Research Unit, University of Nottingham, Nottingham, UK;
Kolmert Johan, Centre for Allergy Research, Karolinska Institutet, Stockholm, Sweden
Konradsen J R, Dept. Women's and Children's Health & Centre for Allergy Research, Karolinska Institutet, Stockholm, Sweden
Kots Maxim, Chiesi Pharmaceuticals, SPA, Parma, Italy;
Kretsos Kosmas, UCB, Slough, UK
Krueger L, University Children's Hospital Bern, Switzerland
Kuo Scott, National Heart and Lung Institute, Imperial College, London, UK;
Kupczyk Maciej, Centre for Allergy Research, Karolinska Institutet, Stockholm, Sweden
Lambrecht Bart, University of Gent, Gent, Belgium;



Lantz A-S, Karolinska University Hospital & Centre for Allergy Research, Karolinska Institutet, Stockholm, Sweden
Larminie Christopher, GSK, London, UK
Larsson L X, AstraZeneca BioPharmaceuticals R&D, Gothenburg, Sweden
Latzin P, University Children's Hospital of Bern, Bern, Switzerland
Lazarinis N, Karolinska University Hospital & Karolinska Institutet, Stockholm, Sweden
Lefaudeux Diane, European Institute for Systems Biology and Medicine, CNRS-ENS-UCBL-INSERM, Lyon, France;
Lemonnier N, European Institute for Systems Biology and Medicine, CNRS-ENS-UCBL-INSERM, Lyon, France
Li Chuan-Xing, Respiratory Medicine Unit, Department of Medicine Solna and Center for Molecular Medicine, Karolinska Institutet, Stockholm, Sweden; and Department of Respiratory Medicine and Allergy, Karolinska University Hospital Solna, Stockholm, Sweden;
Lone-Latif Saeeda, Academic Medical Centre, University of Amsterdam, Amsterdam, The Netherlands;
Lowe L A, Centre for respiratory medicine and allergy, Institute of Inflammation and repair, University Hospital of South Manchester, NHS Foundation Trust, Manchester, UK
Manta Alexander, Roche Diagnostics GmbH, Mannheim, Germany
Marouzet Lisa, NIHR Southampton Respiratory Biomedical Research Unit, Southampton, UK
Martin Jane, NIHR Southampton Respiratory Biomedical Research Unit, Southampton, UK
Mathon Caroline, Centre of Allergy Research, Karolinska Institutet, Stockholm, Sweden
McEvoy L, University Hospital, Department of Pulmonary Medicine, Bern, Switzerland
Meah Sally, National Heart and Lung Institute, Imperial College, London, UK;
Menzies-Gow A, Royal Brompton and Harefield NHS Foundation Trust, London, UK;
<i>Metcalf Leanne, Previously at: Asthma UK, London, UK;</i>
Meiser Andrea, Data Science Institute, Imperial College, London, UK
Mikus Maria, Science for Life Laboratory & The Royal Institute of Technology, Stockholm, Sweden;
Monk Philip, Synairgen Research Ltd, Southampton, UK;
Mores N, Università Cattolica del Sacro Cuore, Milan, Italy;
Naz Shama, Centre for Allergy Research, Karolinska Institutet, Stockholm, Sweden
Nething K, Boehringer Ingelheim Pharma GmbH & Co. KG; Biberach, Germany
Nicholas Ben, University of Southampton, Southampton, UK
Nihlén U, <i>Previously</i> AstraZeneca BioPharmaceuticals R&D, Gothenburg, Sweden
Nilsson Peter, Science for Life Laboratory & The Royal Institute of Technology, Stockholm, Sweden;
Niven R, North West Severe Asthma Network, University Hospital South Manchester, UK
Nordlund B, Dept. Women's and Children's Health & Centre for Allergy Research, Karolinska Institutet, Stockholm, Sweden
Nsubuga S, Royal Brompton Hospital, London, UK
Pacino Antonio, Lega Italiano Anti Fumo, Catania, Italy;
Palkonen Susanna, European Federation of Allergy and Airways Diseases Patient's Associations, Brussels, Belgium.



Pahus L, Assistance publique des Hôpitaux de Marseille, Clinique des bronches, allergies et sommeil Espace Éthique Méditerranéen, Aix-Marseille Université, Marseille, France
Pellet J, European Institute for Systems Biology and Medicine, CNRS-ENS-UCBL-INSERM, Lyon, France
Pennazza Giorgio, Unit of Electronics for Sensor Systems, Department of Engineering, Campus Bio-Medico University of Rome, Rome, Italy
Petrén Anne, Centre for Allergy Research, Karolinska Institutet, Stockholm, Sweden
Pink Sandy, NIHR Southampton Respiratory Biomedical Research Unit, Southampton, UK
Pison C, European Institute for Systems Biology and Medicine, CNRS-ENS-UCBL-INSERM, Lyon, France
Rahman-Amin Malayka, Previously at: Asthma UK, London, UK;
Ravanetti Lara, Academic Medical Centre, University of Amsterdam, Amsterdam, The Netherlands;
Ray Emma, NIHR Southampton Respiratory Biomedical Research Unit, Southampton, UK
Reinke Stacey, Centre for Allergy Research, Karolinska Institutet, Stockholm, Sweden
<i>Reynolds Leanne, Previously at: Asthma UK, London, UK;</i>
Riemann K, Boehringer Ingelheim Pharma GmbH & Co. KG; Biberach, Germany
Robberechts Martine, MSD, Brussels, Belgium
Rocha J P, Royal Brompton and Harefield NHS Foundation Trust
Rossios C, National Heart and Lung Institute, Imperial College, London, UK;
Russell Kirsty, National Heart and Lung Institute, Imperial College, London, UK;
Rutgers Michael, Longfonds, Amersfoort, The Netherlands;
Santini G, Università Cattolica del Sacro Cuore, Milan, Italy;
Santonico Marco, Unit of Electronics for Sensor Systems, Department of Engineering, Campus Bio-Medico University of Rome, Rome, Italy
Saqi M, European Institute for Systems Biology and Medicine, CNRS-ENS-UCBL-INSERM, Lyon, France
Schoelch Corinna, Boehringer Ingelheim Pharma GmbH & Co. KG, Biberach, Germany
Scott S, North West Severe Asthma Network, Countess of Chester Hospital, UK
Sehgal N, North West Severe Asthma Network; Pennine Acute Hospital NHS Trust
Selby A, NIHR Southampton Respiratory Biomedical Research Unit, Clinical and Experimental Sciences and Human Development and Health, Southampton, UK;
Sjödin Marcus, Centre for Allergy Research, Karolinska Institutet, Stockholm, Sweden
Smids Barbara, Academic Medical Centre, University of Amsterdam, Amsterdam, The Netherlands;
Smith Caroline, NIHR Southampton Respiratory Biomedical Research Unit, Southampton, UK
Smith Jessica, Asthma UK, London, UK;
Smith Katherine M., University of Nottingham, UK;
Söderman P, Dept. Women's and Children's Health, Karolinska Institutet, Stockholm, Sweden
Sogbesan A, Royal Brompton and Harefield NHS Foundation Trust, London, UK;
Spycher F, University Hospital Department of Pulmonary Medicine, Bern, Switzerland
Staykova Doroteya, University of Southampton, Southampton, UK



Stephan S, Centre for respiratory medicine and allergy, Institute of Inflammation and repair, University Hospital of South Manchester, NHS Foundation Trust, Manchester, UK
Stokholm J, University of Copenhagen and Danish Pediatric Asthma Centre Denmark
Strandberg K, Karolinska University Hospital & Karolinska Institutet, Stockholm, Sweden
Sunther M, Centre for respiratory medicine and allergy, Institute of Inflammation and repair, University Hospital of South Manchester, NHS Foundation Trust, Manchester, UK
Szentkereszty M, Semmelweis University, Budapest, Hungary;
Tamasi L, Semmelweis University, Budapest, Hungary;
Tariq K, NIHR Southampton Respiratory Biomedical Research Unit, Clinical and Experimental Sciences, NIHR-Wellcome Trust Clinical Research Facility, Faculty of Medicine, University of Southampton, Southampton, UK;
Thörngren John-Olof, Karolinska University Hospital, Stockholm, Sweden
Thorsen Jonathan, COPSAC, Copenhagen Prospective Studies on Asthma in Childhood, Herlev and Gentofte Hospital, University of Copenhagen, Copenhagen, Denmark;
Valente S, Università Cattolica del Sacro Cuore, Milan, Italy;
van Aalderen W M, Academic Medical Centre, University of Amsterdam, Amsterdam, The Netherlands
van de Pol Marianne, Academic Medical Centre, University of Amsterdam, Amsterdam ,The Netherlands;
van Drunen C M, Academic Medical Centre, University of Amsterdam, Amsterdam, The Netherlands;
Van Eyll Jonathan, UCB, Slough, UK
Versnel Jenny, Previously at: Asthma UK, London, UK;
Vink Anton, Philips Research Laboratories, Eindhoven, The Netherlands;
von Garnier C, University Hospital Bern, Switzerland;
Vyas A, North west Severe Asthma Network, Lancashire Teaching Hospitals NHS Trust, UK
Wagener A H, Academic Medical Center Amsterdam, Amsterdam, The Netherlands
Wald Frans, Boehringer Ingelheim Pharma GmbH & Co. KG, Biberach, Germany
Walker Samantha, Asthma UK, London, UK;
Ward Jonathan, Histochemistry Research Unit, Faculty of Medicine, University of Southampton, Southampton, UK;
Wetzel Kristiane, Boehringer Ingelheim Pharma GmbH, Biberach, Germany
Wiegman Coen, National Heart and Lung Institute, Imperial College, London, UK;
Weiszhart Z, Semmelweis University, Budapest, Hungary
Williams Siân, International Primary Care Respiratory Group, Aberdeen, Scotland;
Yang Xian, Data Science Institute, Imperial College, London, UK
Yeyasingham Elizabeth, UK Clinical Operations, GSK, Stockley Park, UK;
Yu W, Amgen Inc., Thousand Oaks, USA
Zetterquist W, Dept. Women's and Children's Health & Centre for Allergy Research, Karolinska Institutet, Stockholm, Sweden
Zolkipli Z, NIHR Southampton Respiratory Biomedical Research Unit, Clinical and Experimental Sciences and Human Development and Health, Southampton, UK;



Zwinderman A H, Academic Medical Centre, University of Amsterdam, The Netherlands;

Partner organisations	
Novartis Pharma AG	University of Southampton, Southampton, UK
Academic Medical Centre, University of Amsterdam, Amsterdam, The Netherlands	Imperial College London, London, UK
University of Catania, Catania, Italy	University of Rome 'Tor Vergata', Rome, Italy
Hvidovre Hospital, Hvidovre, Denmark	Jagiellonian Univ. Medi.College, Krakow, Poland
University Hospital, Inselspital, Bern, Switzerland	Semmelweis University, Budapest, Hungary
University of Manchester, Manchester, UK	Université d'Aix-Marseille, Marseille, France
Fraunhofer Institute, Hannover, Germany	University Hospital, Umea, Sweden
Ghent University, Ghent, Belgium	Ctr. Nat. Recherche Scientifique, Lyon, France
Università Cattolica del Sacro Cuore, Rome, Italy	University Hospital, Copenhagen, Denmark
Karolinska Institutet, Stockholm, Sweden	Nottingham University Hospital, Nottingham, UK
University of Bergen, Bergen, Norway	Netherlands Asthma Foundation, Leusden, NL
European Lung Foundation, Sheffield, UK	Asthma UK, London, UK
European. Fed. of Allergy and Airways Diseases Patients' Associations, Brussels, Belgium	Lega Italiano Anti Fumo, Catania, Italy
International Primary Care Respiratory Group, Aberdeen, Scotland	Philips Research Laboratories, Eindhoven, NL
Synaigen Research Ltd, Southampton, UK	Aerocrine AB, Stockholm, Sweden
BioSci Consulting, Maasmechelen, Belgium	Almirall
AstraZeneca BioPharmaceuticals R&D	Boehringer Ingelheim
Chiesi	GlaxoSmithKline
Roche	UCB
Janssen Biologics BV	Amgen NV
Merck Sharp & Dome Corp	

MEMBERS OF THE ETHICS BOARD			
Name	Task	Affiliation	e-mail
Jan-Bas Prins	Biomedical research	LUMC/the Netherlands	J.B.Prins@lumc.nl
Martina Gahlemann	Clinical care	BI/Germany	Martina.Gahlemann@boehringer-ingelheim.com
Luigi Visintin	Legal affairs	LIAF/Italy	visintin@inrete.it
Hazel Evans	Paediatric care	Southampton/UK	hazel.evans@uhs.nhs.uk
Martine Puhl	Patient representation (co-chair)	NAF/ the Netherlands	martine@puhl.nl
Lina Buzermaniene	Patient representation	EFA/Lithuania	lina.buzermaniene@pavb.lt
Val Hudson	Patient representation	Asthma UK	hudsonval7@gmail.com
Laura Bond	Patient representation	Asthma UK	lvbond22@googlemail.com
Pim de Boer	Patient representation and pathobiology	IND	deboer.pim@hetnet.nl



Guy Widdershoven	Research ethics	VUMC/the Netherlands	g.widdershoven@vumc.nl
Ralf Sigmund	Research methodology and biostatistics	BI/Germany	ralf.sigmund@boehringer-ingelheim.com

THE PATIENT INPUT PLATFORM	
Name	Country
Amanda Roberts	UK
David Supple (chair)	UK
Dominique Hamerlijnck	The Netherlands
Jenny Negus	UK
Juliëtte Kamphuis	The Netherlands
Lehanne Sergison	UK
Luigi Visintin	Italy
Pim de Boer (co-chair)	The Netherlands
Susanne Onstein	The Netherlands

MEMBERS OF THE SAFETY MONITORING BOARD	
Name	Task
William MacNee	Clinical care
Renato Bernardini	Clinical pharmacology
Louis Bont	Paediatric care and infectious diseases
Per-Ake Wecksell	Patient representation
Pim de Boer	Patient representation and pathobiology (chair)
Martina Gahlemann	Patient safety advice and clinical care (co-chair)
Ralf Sigmund	Bio-informatician